Epithelial cell rearrangements during tubular organ formation

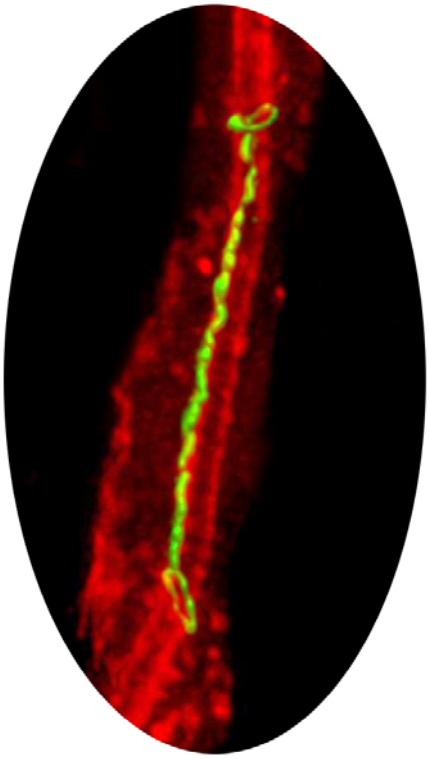

Inauguraldissertation

zur Erlangung der Würde eines Doktors der Philosophie
vorgelegt der
Philosophisch-Naturwissenschaftlichen Fakultät der Universität Basel
von

Marc Neumann
aus Deutschland

Ausgeführt unter der Aufsicht von Prof. Dr. Markus Affolter
Biozentrum der Universität Basel
Abteilung Zellbiologie

Basel, 2005

Genehmigt von der Philosophisch-Naturwissenschaftlichen Fakultät auf Antrag von:

Prof. Markus Affolter

Prof. Walter J. Gehring

Prof. Sylvia Arber

Basel, den 22.11.2005

Prof. Dr. Hans-Jakob Wirz
Dekan der Philosophisch-
Naturwissenschaftlichen Fakultät

Für Sabine und Eva

Index

Abstract

The tracheal system of *Drosophila* is a simple branched tubular organ that consists of different branches with distinct cellular architectures. We have analyzed how these branches are formed during embryonic development and how this process is controlled genetically. In particular we focused our analysis on the intercalation process that underlies the transition from thick, multicellular branches to finer branches, in which single cells reach around the lumen and seal it with autocellular AJs.

To study tracheal development at the cellular level, I developed a technique that allows for the visualization and manipulation of single tracheal cells *in vivo*. Using this technique we characterized the intercalation process during dorsal branch formation. Based on these findings we proposed a model of intercalation that involves four steps. We also found that intercalation is specifically blocked in the dorsal trunk by the expression of the transcription factor *spalt* (*sal*) and that *sal* is sufficient to block intercalation also in other branches. To mediate this function, *sal* expression is required in a group of cells.

In the following I tried to identify genes that are involved in this process using different approaches. In a candidate approach I tested a variety of genes that have been implicated in cell rearrangement and intercalation in other systems. Furthermore I tested several candidates with potentially interesting domains that show a trachea-specific expression pattern. I also searched for phenotypes that resemble the gain or loss of function phenotype of *sal* in a genetic screen using molecularly mapped deficiencies. Finally I initiated a screen using gene chips to identify *sal* target genes.

Using these different approaches I characterized the molecular basis of intercalation. On the one hand I ruled out that some obvious candidates contribute to the process. On the other hand I identified candidates that affect intercalation. In the deficiency screen I identified a deletion that shows ectopic intercalation. This deficiency also exhibits cargo-specific secretion defects. I am currently mapping the gene responsible for these defects by generating new deficiencies.

Finally I attempted to characterize the forces that drive intercalation. Investigating the role of the FGF pathway I identified a putative positive input of the FGF pathway on intercalation via the transcription factor *pointed*.

Preface

Aim of the thesis

The aim of this thesis is to characterize the cellular and molecular events that take place during the formation of a branched tubular organ that give rise to distinct branches of distinct cellular architecture. We use the *Drosophila* tracheal system as a model to study this process. On the one hand we analyze the morphological events underlying cellular rearrangements on the single cell level. On the other hand we analyze the genetic regulation of this process and try to identify novel components involved in it. Ultimately, we hope to gain a comprehensive understanding of branching morphogenesis, which may be extended to other, more complex situations.

Structure of the thesis

The thesis is divided into introduction, results and discussion. It is based on three papers: First, a general review that gives a broad overview over tracheal development, comparing it to other organs. This paper is attached to the introduction section. The second manuscript is a research paper that characterizes the intercalation process and its genetic regulation. This paper provides the basis for most of the unpublished work found in this thesis. Therefore it has been put to the beginning of the results section. The third paper is a "concept" paper that largely consists of a discussion of the current knowledge in a broader context and has therefore been attached to the discussion section. While we hope that with this organization the thread of the thesis can best be followed, we apologize for occasional redundancies that occur. These redundancies are due to the fact that each paper has its own introduction and due to the fact that we have to discuss some of the aspects that are discussed in the papers also in the light of our unpublished results.

Acknowledgments

First of all, I would like to thank Markus Affolter for giving me the chance to perform my thesis in his lab. With his extraordinary enthusiasm he encouraged me throughout my work, gave me guidance when I needed it and freedom when I wanted it. Thank you for everything!

I thank Carlos Ribeiro for a joyful and fruitful collaboration and all other present and past members of the lab for a stimulating environment and a good atmosphere. I thank Clemens Cabernard for various fly lines, Alain Jung, Li Lin and Helene Chanut for the EMS lines; Georgios Pyrowolakis for help with the generation of new deficiencies; Alain Jung for reading the thesis manuscript.

I would like to thank Greg Beitel for supplying the YFP balancer that made much of the work presented possible; Christian Dahmann for allowing us to screen the in situ collection and for willingly sharing fly lines; Maria Leptin for providing the EMS lines.

Many thanks go to Markus Dürrenberger for help with the confocal microscope, Hubertus Kohler for help with FACS sorting, Ursula Sauder for an introduction to electron microscopy, Karin Mauro, Bernadette Bruno and Gina Evora for supplying the fly-food.

I thank Prof. Walter Gehring and Prof. Silvia Arber for being in my thesis committee.

I would like to thank Georgios Pyrowolakis, Britta Hartmann and Carlos Ribeiro for drinks and discussion after work and Georgios Pyrowolakis, Heinz-Georg Belting and the soccer team for physical compensation.

Finally, I thank my family and my friends for granting me a happiness and fulfillment beyond science. Without that this thesis would not have been possible.

Introduction

Tubulogenesis

In most animals there are manifold examples of organs that are built from tubular epithelia. They are used to transport gases and fluids and in many cases are highly branched to maximize the surface available for gas and fluid exchange. This enlargement of the surface is one of the prerequisites for organisms to grow in size. Generally the cells

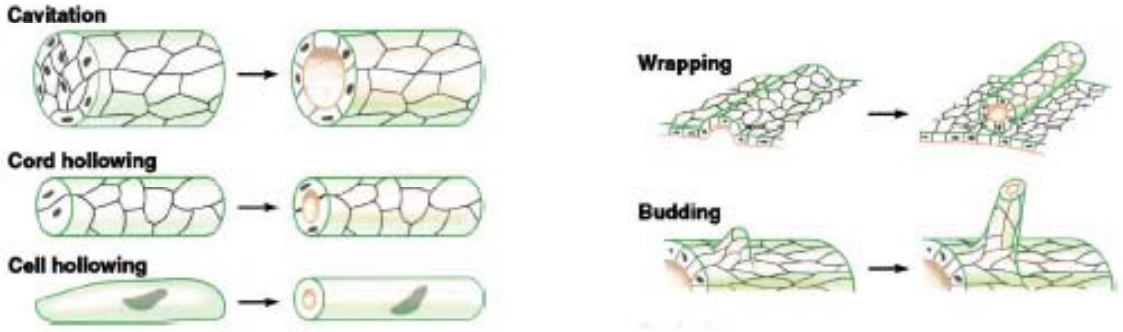

Figure 1 Different mechanisms of tubulogenesis.
Tubulogenesis via cavitation, cord hollowing or cell hollowing relies on the de novo formation of lumen. Wrapping and budding transform preexisting epithelia into tubes. From (Lubarsky and Krasnow, 2003)

in these epithelia are oriented with their apical surface facing the lumen. However, during development these tubes can arise via different mechanisms (reviewed in (Hogan and Kolodziej, 2002; Lubarsky and Krasnow, 2003)) (Fig.1).

They can arise via cavitation like during vertebrate salivary gland formation (Melnick and Jaskoll, 2000) or via cord hollowing like in the C. elegans gut (Leung et al., 1999) or via cell hollowing like for example in some *Drosophila* tracheal cells (Samakovlis et al., 1996) on which we will not further elaborate. All of these examples are likely to rely at least partially on the polarized deposition of vesicles carrying apical membrane components in the center of the developing tube. This assembly of apical membrane creates a lumen that may be opened up by liquid secretion (Manning and Krasnow, 1993). During all of these examples apico-basal polarity arises secondarily as the lumen forms.

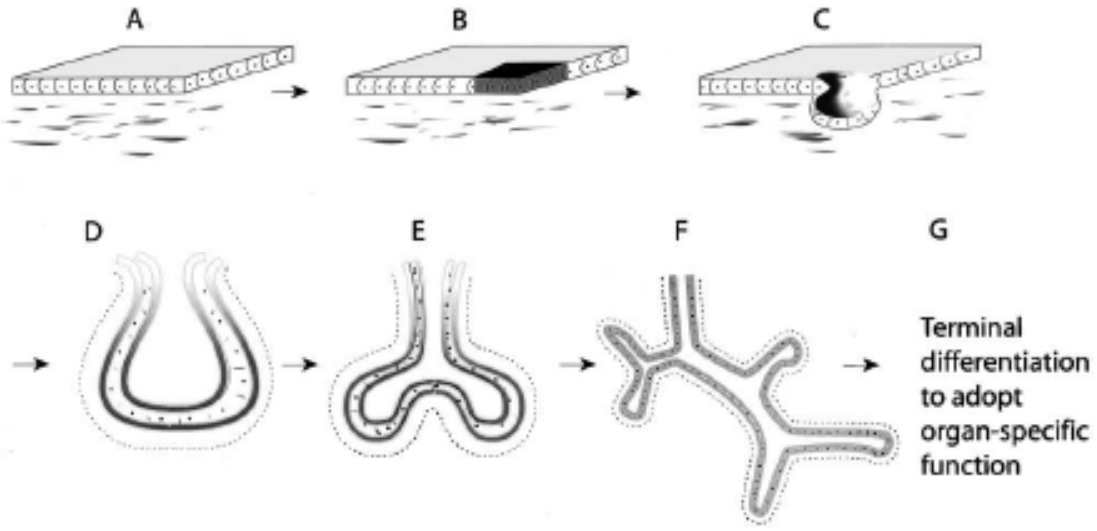

Figure 2 Mechanism of branching morphogenesis.
In a flat epithelium a set of cells is specified as precursors. These cells bud in and undergo reiterative budding events transforming the flat epithelium into a ramified network of branches. From (Affolter et al., 2003).

Other mechanisms to generate tubular structures start from existing epithelia. For example, the neural tube arises via wrapping in most vertebrates (Colas and Schoenwolf, 2001). Another widely used mechanism to generate tubes is the generation of new tubes via budding, in a process called branching morphogenesis. Amongst others branching morphogenesis underlies the formation of the vertebrate lung, the collective duct of the kidney, the mammary gland and also the *Drosophila* tracheal system (Affolter et al., 2003). During branching morphogenesis a set of cells are specified as a precursor. These cells then invaginate and form a sac-like tube that eventually grows and undergoes reiterative rounds of budding events, transforming an initially flat epithelium into a ramified network of branches. (Fig.2). In contrast to the examples that rely on the generation of apical surface tubes are largely formed by cell migration, cell rearrangement, cell shape changes and cell division during branching morphogenesis.

Organization of epithelial tissues in Drosophila

Many tubular organs in *Drosophila* are built from a preexisting, basic epithelium. A basic epithelium consists of a single layer of cells that have an apical domain and a basolateral membrane domain. The apical and the baso-lateral compartment have a distinct molecular composition and have distinct functions for the cell. While the apical domain is facing the lumen mediating the contact with the environment, the baso-lateral side is facing the inside of the organism. In this region epithelial cells are connected to each other and to the surrounding via various junctions (Tepass et al., 2001) (Fig.3). Hemiadherens junctions (or focal contacts) are integrin-based structures. They are found

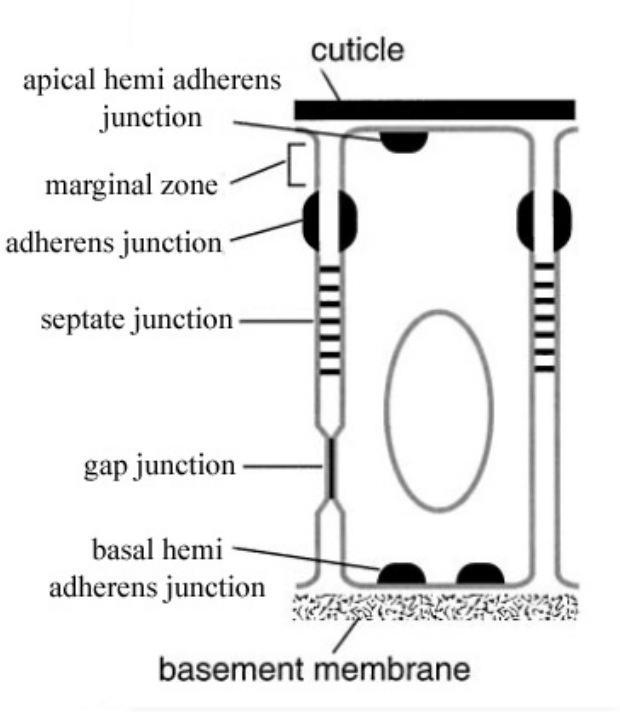

Figure 3 Characteristic structures of epithelial cells.
Epithelial cells are connected to each other and to the environment via various junctions. From (Tepass et al., 2001)

on the basal side where they mediate the attachment of the cells to the basement membrane (Brown et al., 2000). Also apical hemiadherens junctions that mediate the contact with the cuticle have been reported.

Another type of junctions, the septate junctions, are located at the lateral side of epithelial cells and act as a diffusion barrier (Tepass et al., 2001). They are the functional equivalent of the chordate tight junctions. Although they are different form these tight junctions and are found in a different position they have recently been shown to share

some crucial components in particular the claudins. Mutations in several claudin genes have been identified. (Behr et al., 2003; Wu et al., 2004). In all of these mutants the most obvious phenotype is seen in the trachea. The dorsal trunk is convoluted and shows dilations and constrictions. Though this phenotype is not completely understood it is clear that in all of these mutations the function of the septate junction as a diffusion barrier is impaired.

Gap junctions are also found on the lateral side of the cell. They consist of channels that connect the cytoplasm of neighboring cells. In *Drosophila* they are formed by innexins that -though unrelated in sequence- perform similar functions as the vertebrate connexins (Pauline Phelan, 2001).

Another characteristic structure of an epithelium is the adherens junction (AJ) that is located subapicallly. The key component of the AJ is E-cadherin, a transmembrane molecule that mediates homophilic adhesion among neighboring cells in a Ca^{2+}-dependent manner. E-cadherin is characterized by extracellular repeats called cadherin repeats. It furthermore shows a highly conserved intracellular domain which is characteristic for classical cadherins and which has been shown to interact with p120 catenin (p120ctn) and β-catenin. β-catenin in turn binds to α-catenin which links the AJ to the actin cytoskeleton. Together, E-cadherin and the three catenins constitute the core AJ protein complex (Tepass et al., 2001). In addition to these proteins a large variety of other factors has been shown to interact with the AJs in certain situations (Fig.4). These factors account for the wide range of possible functions that have been attributed to AJs. These functions range from the regulation of spindle orientation and the regulation of actin dynamics to an involvement in signaling (Perez-Moreno et al., 2003). Furthermore the AJs play a crucial role for the regulation of cell adhesion and cell rearrangement.

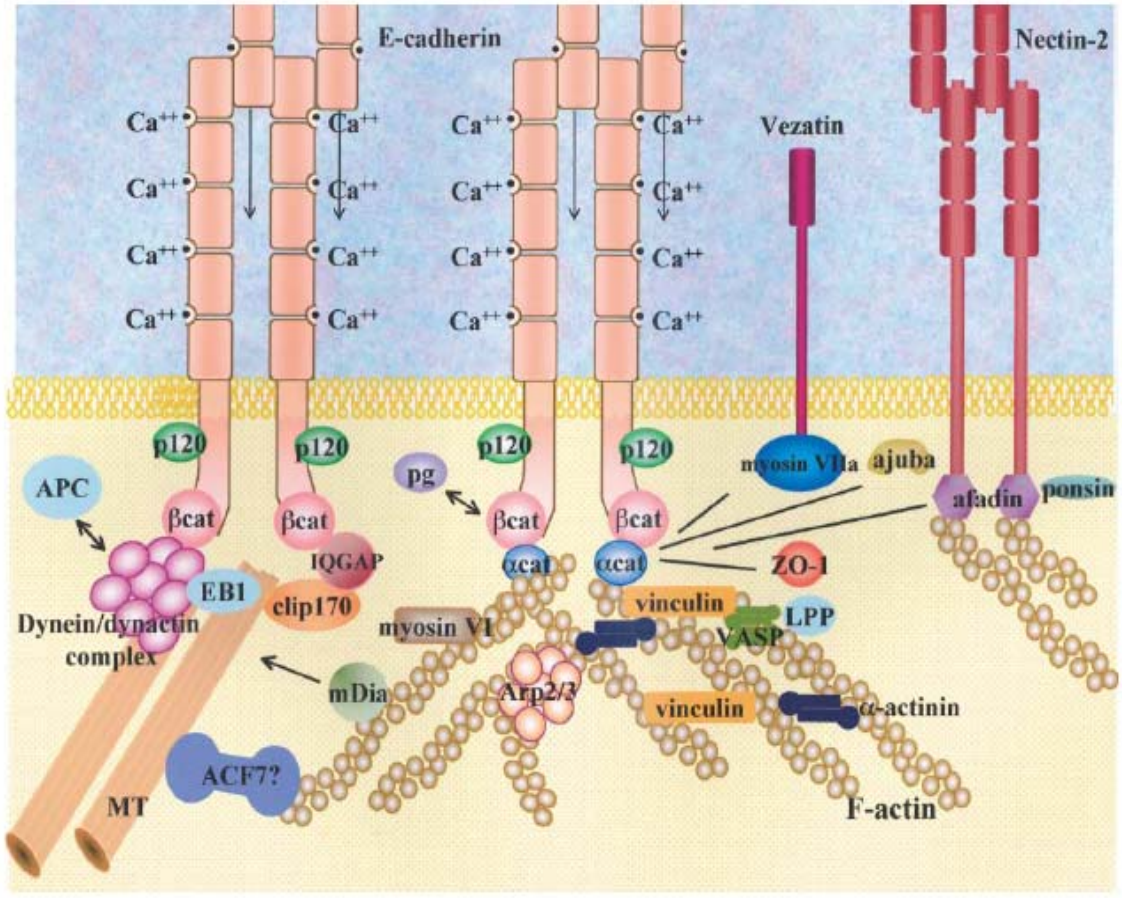

Figure 4 Molecules binding to adherens junctions
A large variety of molecules binds to the adherens junctions and the cadherin-catenin-complex. These molecules mediate and regulate the interaction with the cytoskeleton, and the dynamics of the cytoskeleton, the turnover and the stability of the complex and also participate in signaling. From (Perez-Moreno et al., 2003).

Mechanisms of cell rearrangement

Cell rearrangement is one of the fundamental processes underlying the shaping of multicellular organisms. A special form of cell rearrangement is cell intercalation, leading to convergent extension of a given tissue. During intercalation neighboring cells slip in between each other, converging at a certain point. This leads to an extension of the tissue perpendicular to the direction of convergence (Fig.5). Intercalation is involved in the development of many structures. It has been particularly well studied in the frog and

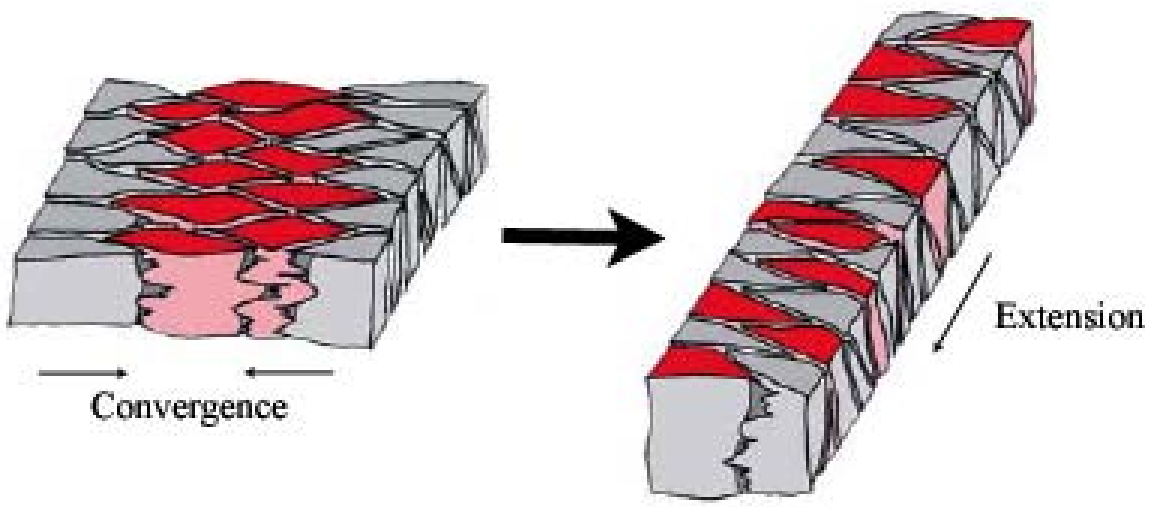

Figure 5 Principle of convergent extension.
Convergent extension relies on intercalation of cells that converge at a specific point. This leads to an extension of the tissue perpendicular to the axis of convergence. From (Keller, 2002).

the fish (Wallingford et al., 2002). In explants of the Xenopus neural epithelium convergent extension movements occur spontaneously without the application of an external force (Keller and Danilchik, 1988; Keller et al., 1992), showing that this process can be driven by forces generated inside the tissue. Yet, intercalation in epithelial cells of Xenopus can also be induced by the application of external forces (Beloussov et al., 2000).

Intercalation movements are not only observed in epithelial cells. Some of the best-studied examples are mesenchymal cells (Shih and Keller, 1992). Although it has not systematically been investigated, it seems clear that the mechanisms underlying epithelial and mesenchymal cell intercalation are not identical. The various junctions that connect epithelial cells need to be remodeled during cell rearrangement. It has been proposed that epithelial cell rearrangements are driven by baso-lateral protrusions that are successively filled via cortical flow (cortical tractor model, (Jacobson et al., 1986)). Such protrusions have been observed during cell rearrangements in the hypodermis of *C. elegans* (Williams-Masson et al., 1998), yet the molecular basis of the movement is not known.

Recently, two studies shed light on the molecular basis of epithelial cell intercalation during *Drosophila* germband extension (Bertet et al., 2004; Zallen and Wieschaus, 2004). During *Drosophila* gastrulation cell intercalation is used to elongate the body axis. It has now been shown that this intercalation depends on the differential localization of two molecules. Myosin II is localized in the vicinity of AJs oriented along the dorsal-ventral

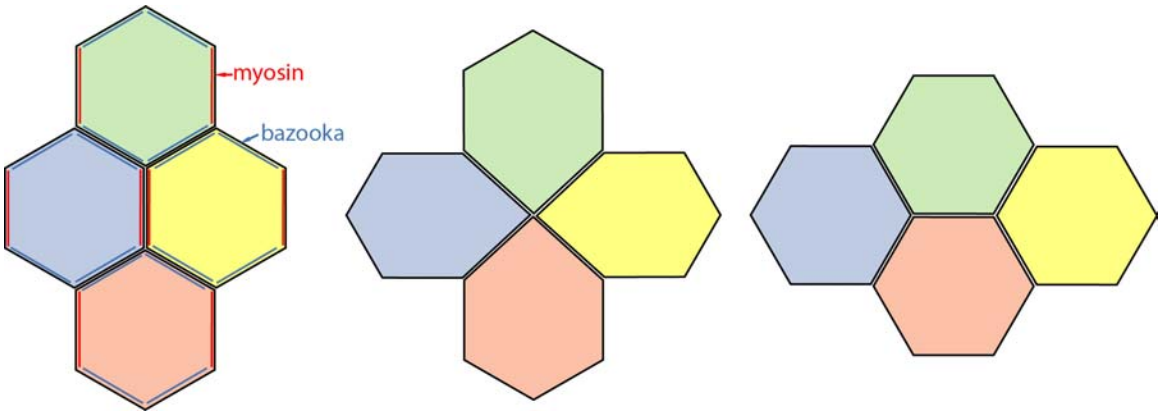

Figure 6 Cell intercalation during germband extension.
Non muscle myosin is localized to shrinking AJs during germband extension. Bazooka is localized complementarily. Efficient germband extension depends on the proper localization of these two molecules.

axis, while Bazooka is excluded form these junction but present on the junctions oriented along the anterior-posterior axis (Fig.6). It turns out that Myosin II and its activation by Rho kinase is required to destabilize and shorten the AJs oriented along the dorsal-ventral axis; in contrast, Bazooka might stabilize the other AJs. Although theses studies nicely demonstrate a requirement of the localization of these molecules the precise effect on the AJ and the cadherin catenin complex is not clear. This complex could contribute to cell rearrangements by many means.

During cell rearrangement, the cadherin-catenin complex is not only responsible for the adhesion among epithelial cells, but it can also directly mediate cell rearrangements. For example, interference with cadherin function leads to defective convergent extension movements during Xenopus gastrulation (Zhong et al., 1999). A classical example of how cadherins drive cell rearrangements and morphogenesis is cell sorting via the expression of different cadherins on different cells. During the formation of the neural

tube, cells of the neural epithelium expressing N-cadherin are separated from the epidermal cells which express E-cadherin (Detrick et al., 1990; Fujimori et al., 1990). These effects can also be mimicked in cultured cells (Nose et al., 1988). However, cell sorting cannot only be achieved via the expression of different cadherins but also via the expression of different levels of the same cadherin (Steinberg and Takeichi, 1994).

Even in cases where cadherin does not play an instructive role for cell rearrangements it is evident that it has to play a permissive role. In a static situation AJs keep the cells tightly attached to each other. During cell rearrangements in an epithelial sheet AJs need to be flexible allowing cell movements without the loss of adhesion. Therefore the adhesive properties of AJs have to be carefully tuned. Several mechanisms have been proposed that would allow for a regulation of cadherin-mediated adhesion (Gumbiner, 2005).

It is possible that the flexibility of the AJs relies on cadherin levels at the surface. The levels of E-cadherin determine the epithelial character of the cells. Loss of E-cadherin leads to an epithelial to mesenchymal transition (EMT) and to a more motile behavior of the cells. EMT has been observed in response to various stimuli and is found during regular development as well as during cancerogenesis and metastasis (Thiery, 2003). Although a full EMT is not compatible with epithelial cell rearrangements as the cells loose their epithelial character it is possible that a reduction of E-cadherin levels leads to a partial EMT allowing cell rearrangements.

A fast way to reduce E-cadherin levels is to degrade it. Degradation of E-cadherin can for example be induced by v-Src induced tyrosine phosphorylation of E-cadherin (Behrens et al., 1993). Such tyrosine phosphorylated E-cadherin is then specifically bound by the E3 ubiqutin ligase Hakai and targeted to the degradation pathway(Fujita et al., 2002).

While E-cadherin can be specifically degraded, it can also be specifically stabilized at the AJ. It seems like p120 catenin is responsible for this stabilization as E-cadherin is rapidly degraded upon arrival at the surface in cells lacking p120 catenin (Ireton et al., 2002). However, the precise role of p120 catenin in this context remains to be discovered.

It is also possible that rather than the mere levels of E-cadherin at the surface, the turnover of E-cadherin at the surface regulates cell rearrangements. Consistent with this idea a number of intracellular trafficking components have been found to be involved in

E-cadherin dependent adhesion (Bryant and Stow, 2004; D'Souza-Schorey, 2005). Additionally there is a constitutive turnover of E-cadherin at the surface involving recycling inside the cell. This recycling of E-cadherin is crucial for AJ assembly and the recycling process can be modulated depending on the status of the AJs (Le et al., 1999).
The flexibility of AJs can also be regulated via the regulation of the interaction with the actin cytoskeleton. There is evidence that the small GTPase Rac1 is involved in this regulation. Activation of Rac1 usually leads to increased adhesion(Braga et al., 1997). Similar results are obtained upon overexpression of Tiam1, a guanyl-exchange-factor (GEF) activating Rac. Interestingly, Tiam1 localizes to AJs suggesting a physical role in AJ remodeling (Hordijk et al., 1997). Usually small GTPases act via the modification of downstream effectors. In the context of adhesion, however, one role of Rac1 might solely be the binding of IQGAP thereby displacing β-catenin, that otherwise binds IQGAP. Only then β-catenin is able to interact with α-catenin and exert a function in the AJs (Fukata et al., 2001). Also other small GTPases, such as Rho, have been shown to affect adhesion (Bloor and Kiehart, 2002; Braga and Yap, 2005) but the exact roles of these proteins are still controversial. Interestingly, Rho has been found to directly bind to α-catenin and p120 catenin in *Drosophila* (Magie et al., 2002).

Embryonic tracheal development in Drosophila

To study epithelial cell rearrangements during the formation of branched tubular organs, we use the tracheal system of *Drosophila* as a model. The tracheal system of *Drosophila* consists of branches that are simple tubes consisting of an epithelial monolayer wrapped into a tube around a central lumen. It arises via branching morphogenesis. The development of the tracheal system is initiated in the early embryo upon the determination of 10 bilaterally symmetrical clusters of approximately 20 tracheal precursor cells (Manning and Krasnow, 1993). The determination depend on the localized expression of the transcription factors *trachealess* (Isaac and Andrew, 1996) and *ventral veinless* (Llimargas and Casanova, 1997). Upon invagination and two additional rounds of cell divisions, each of the tracheal sacs undergoes a similar sequence

of developmental events to generate one segment of the tracheal network. From the initial sac like invaginations branches bud out into different directions (Fig.7A) ultimately forming distinct branches (Fig.7B) (Movie1, see supplementary material). Some of these branches fuse with corresponding branches in neighboring segments to form an interconnected tubular network. Finally specialized terminal cells send out fine highly ramified protrusions throughout the embryo. The entire tracheal branching process takes place in the absence of further cell divisions or cell death. Therefore the cellular processes involved in branch formation are directional cell migration, cell rearrangements and cell shape changes.

Several signaling systems interplay to ensure the specification of the different branches and their outgrowth. The best understood signaling system is based on *breathless* (*btl*) and *branchless* (*bnl*). *btl* encodes an FGF receptor expressed in tracheal cells, but not in surrounding epithelial cells (Klambt et al., 1992; Reichman-Fried et al., 1994), while *bnl* encodes the FGF ligand and is expressed in individual cells or cell clusters surrounding the invaginating tracheal placode (Sutherland et al., 1996), prefiguring the directions of branch outgrowth (Fig.7C). The absence of either of these two gene products leads to a complete failure of branch outgrowth, despite proper determination of tracheal cells. Conversely, *bnl* expression in ectopic positions induces branch outgrowth towards such sites. Thus this signaling system is required and sufficient to determine the direction of branch outgrowth as well as outgrowth per se. Gain-of-function and loss-of-function studies combined with live imaging revealed that the Bnl ligand induces a migratory behavior by promoting fast cytoskeletal dynamics in a few cells at the tip of the tracheal branches (Ribeiro et al., 2002) (Fig.7E) (Movie2). The stalk cells appear to follow these tip cells passively.

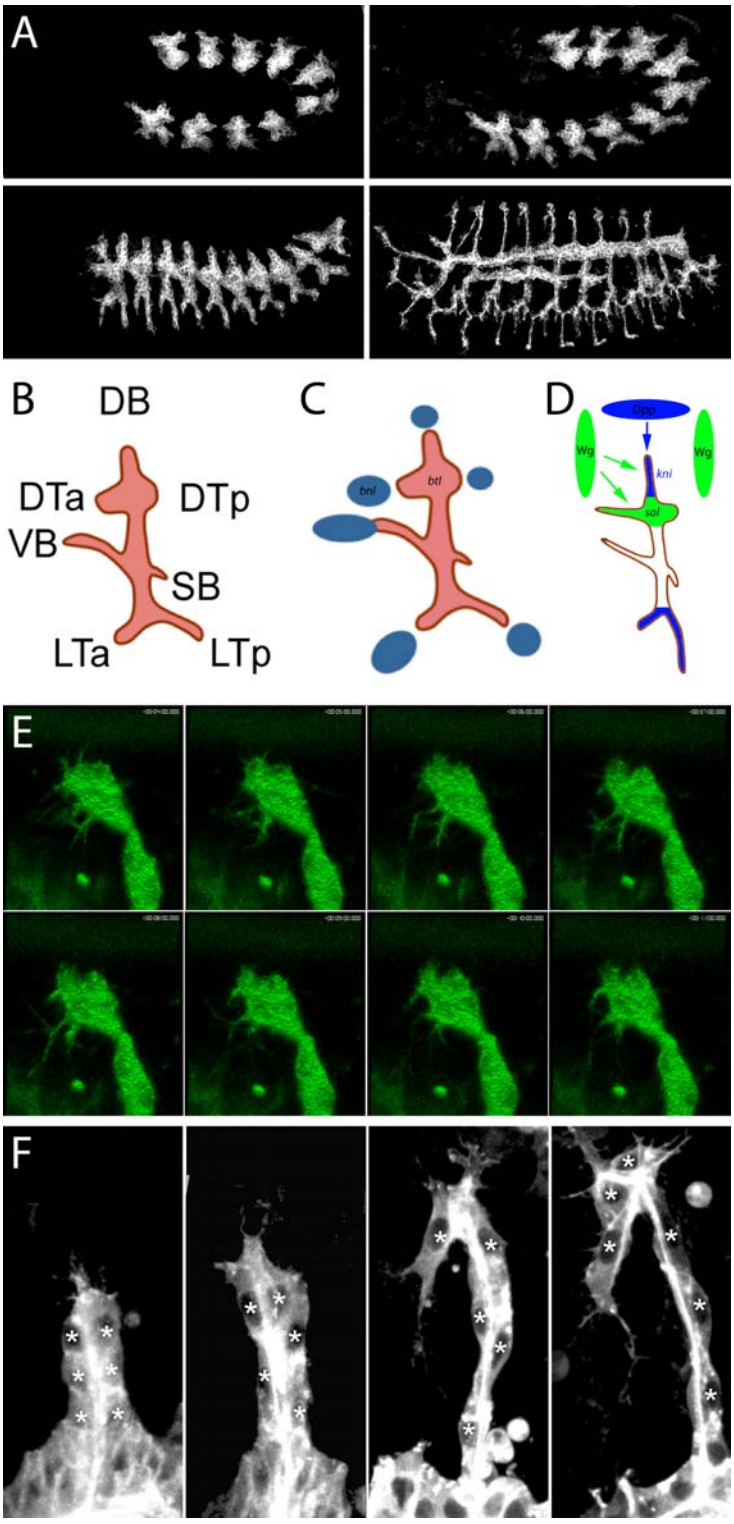

Figure 7 Embryonic tracheal development.
(A) Starting from a tracheal placode branches bud out into different directions. Some branches fuse to form an interconnected network of branches. (B) The tracheal system consists of different branches. (C) Bnl is expressed in distinct spots around the tracheal placode prefiguring the direction of branch outgrowth. (D) *wg* induces *sal* in the presumptive dorsal branches and in the dorsal trunk of the tracheal system. *dpp* induces *kni* in dorsal and ventral branches. *kni* represses *sal.* (E) Filopodial movements occur in a time frame of minutes. (F) During branch outgrowth cell are moved from a side-by-side to an end-to-end arrangement.
(A) Anti GFP antibody staining of embryos expressing GFPactin under the control of bt*l*-Gal4. (E,F) Live embryos expressing GFPactin under the control of *btl*-Gal4. (E) Still pictures from a time lapse analysis 1 frame / min. DB dorsal branch, DT dorsal trunk, VB visceral branch, LT lateral trunk, SB spiracular branch.

During branch formation, all tracheal cells maintain their epithelial character and remain attached to each other via their AJs. As the branches elongate the cells in some branches undergo obvious cell rearrangements. Starting in a side-by-side arrangement the cells of the dorsal branch successively move into an end-to-end configuration (Fig.7F) (Samakovlis et al., 1996). It has been proposed that cell rearrangements during tracheal development are regulated by Rac1. In this context Rac1 is thought to modulate the incorporation of newly synthesized E-cadherin into the AJs. (Chihara et al., 2003).

Despite the well-defined role of the *btl*/*bnl* signaling system it was shown that branch outgrowth is influenced by other signaling systems as well. Ectopic expression of the Drosophila BMP2/4 homologue Dpp (Decapentaplegic) is able to direct cells from migration along the anterior-posterior axis toward migration along the dorso-ventral axis (Vincent et al., 1997). In the absence of *dpp* signaling, prospective dorsal branch cells start to migrate dorsally, but ultimately reintegrate into the dorsal trunk and thus never form a definitive dorsal branch. However, the cytoskeletal dynamics induced by *bnl* are normal in this situation arguing that *dpp* does not affect the *bnl/btl* signaling system (Ribeiro et al., 2002). The effect of *dpp* is largely mediated by the transcription factors *knirps* (*kni*) and *knirps-related* (*knrl*) which are induced in dorsal and ventral tracheal branches by the *dpp* signal (Chen et al., 1998) (Fig.7D).

wingless (*wg*) signaling has been shown to be required for the migration along the anterior-posterior axis (Chihara and Hayashi, 2000; Llimargas, 2000). *wg* induces *spalt* (*sal*) and *spalt related* (*salr*) in the dorsal branch and the dorsal trunk. Here *sal* specifies a dorsal fate of the placode (Franch-Marro and Casanova, 2002). At stage 13-14 *sal* is repressed in the dorsal branch by *kni* (Fig.7D). At this stage *sal* in the dorsal trunk is required for the formation of this branch. In *sal* mutants all cells move in dorso-ventral directions and a dorsal trunk does not form (Kuhnlein and Schuh, 1996).

A specific failure in anterior-posterior migration of tracheal cells and in the formation of a dorsal trunk has also been reported for mutations in the EGF pathway (Llimargas and Casanova, 1999; Wappner et al., 1997) and in the transcription factor *ribbon*. (*rib*) (Bradley and Andrew, 2001; Shim et al., 2001). Yet, these defects seem to be unrelated to *wg* and *sal*. For none of these mutations the cellular basis of the defect is clear.

Cellular and molecular mechanisms involved in branching morphogenesis of the Drosophila tracheal system

Clemens Cabernard, Marc Neumann and Markus Affolter

Journal of Applied Physiology **97** pages 2347-2353, 2004

Results

Tools to visualize and manipulate single tracheal cells in vivo

As discussed above the central events during tracheal morphogenesis are cell migration, cell rearrangements and cell shape changes. While cell migration during tracheal development has been well characterized (Ribeiro et al., 2002; Sato and Kornberg, 2002) only little is known about cell rearrangements and cell shape changes. This is largely due to the fact that the outline of single cells cannot be identified, making conclusions about cell shape impossible. Similarly, conclusions about cell rearrangements have so far relied on crude markers, such as for example the position of the nuclei (Samakovlis et al., 1996). In order to circumvent these problems, we developed a tool that allows the visualization and manipulation of single tracheal cells *in vivo* making use of the FLP-FRT system (Basler and Struhl, 1994).

A fragment of the *btl* enhancer driving expression specifically in the developing trachea was cloned in front of the *Gal4* gene. To avoid constitutive expression of the transcriptional activator *Gal4* in the entire tracheal system, the *Gal4* coding sequence was separated from the *btl* enhancer by a flip-out cassette containing the *yellow* (*y*) gene (including transcriptional stop signals) flanked by FRT recombination sites (Fig.8A). Induction of the FLP recombinase with a mild heat shock results in the removal of the *y* cassette in individual cells, allowing for the transcription of the *Gal4* gene. Such cells can be visualized by monitoring the expression of a transgene driving a GFP fusion protein of choice under the control of the Upstream Activating Sequences (UAS). This allows the visualization of the behavior of single tracheal cells via immunohistochemisty (Fig.8B) or *in vivo* (Fig.8C) (Movie3). At the same time it allows a manipulation of the targeted cells by the simultaneous expression of another UAS construct. We have shown that the expression of dominant active *btl* receptor in single tracheal cells can trigger ectopic branch outgrowth (Fig.8D,E).

In the antibody stainings shown we visualized the entire tracheal system with the 2A12 antibody (Fig) allowing to assign the exact localization of the marked cells. In the *in vivo* example presented we lack such a possibility. Especially when few cells are marked this complicates the analysis. To locate single cells in the context of the entire tracheal system

in vivo, we also generated flies transgenic for an *mRFP1-GMA* construct (labeling filamentous actin) under the direct control of the *btl* enhancer; introduction of a chromosome containing this construct into the experimental background allows for the simultaneous visualization of single tracheal cells (in green) in the context of the entire tracheal system (red). To label the single cells any UAS-GFP line can be used. We have so far tested actin-GFP, tau-GFP and α-catenin-GFP (Fig.8F,G,H).

In the following we use this tool to characterize the AJ-remodeling events underlying cell intercalation during dorsal branch outgrowth.

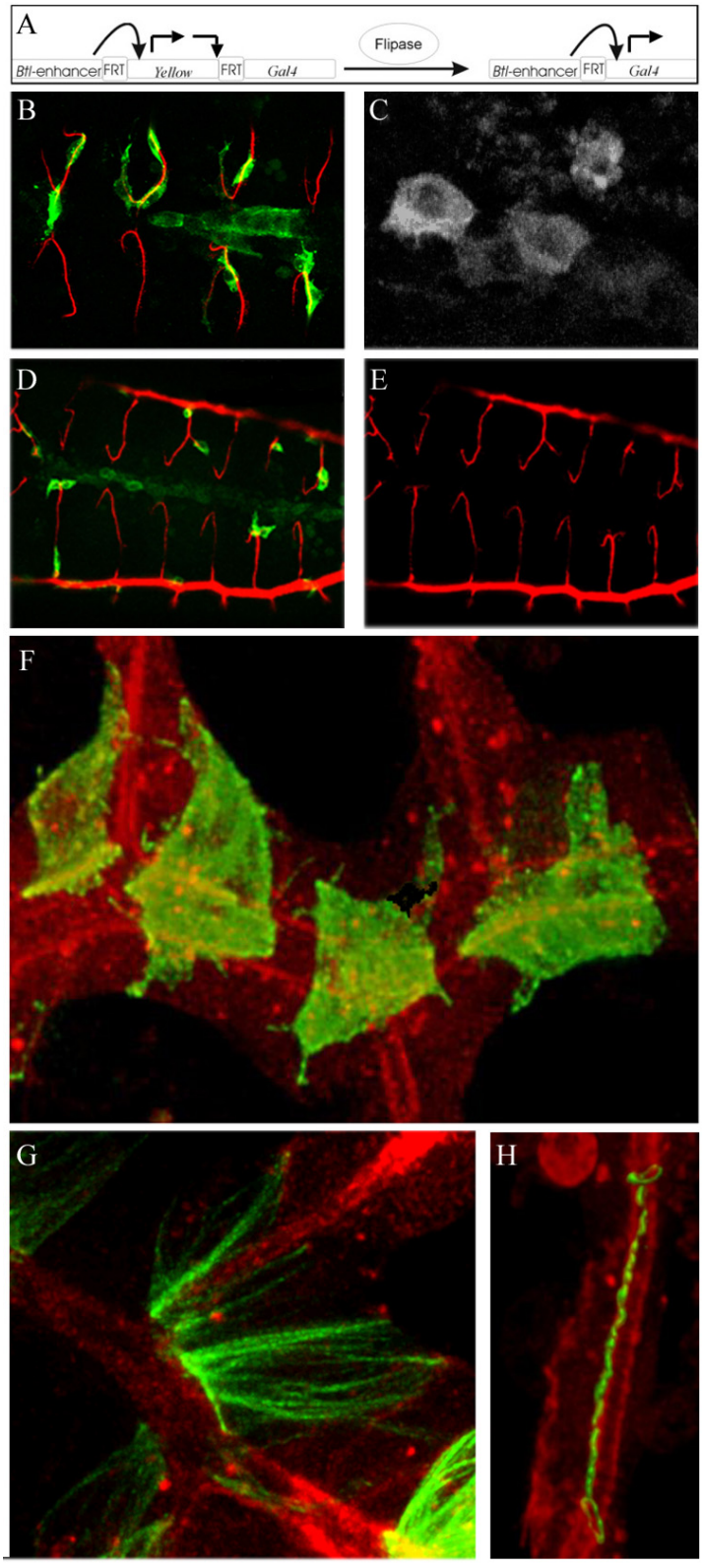

Figure 8 Labeling single tracheal cells.
(A) Single tracheal cells can be labeled by the generation of a tissue specific flipout construct either (B) *in vitro* or (C) *in vivo*. (D,E) Expression of dominant active *btl* in single tracheal cells triggers ectopic branch outgrowth. (F,G,H) Single tracheal cells can be labeled using various GFP-fusion proteins.
Antibody staining with anti-GFP and 2A12 antibody of embryos expressing (B) actinGFP or (D,E) actin GFP and dominant active *btl* in single tracheal cells. Live embryos expressing (C,F) GFPactin in single tracheal cells and (F) RFPmoe under the control of the btl-enhancer. Live embryos expressing RFPmoe under the control of the btl-enhancer and (G) tauGFP or (H) α-catenin-GFP in single tracheal cells.

Genetic control of cell intercalation during tracheal morphogenesis in Drosophila

Carlos Ribeiro, Marc Neumann and Markus Affolter

Current Biology **14,** pages 2197-2207, 2004

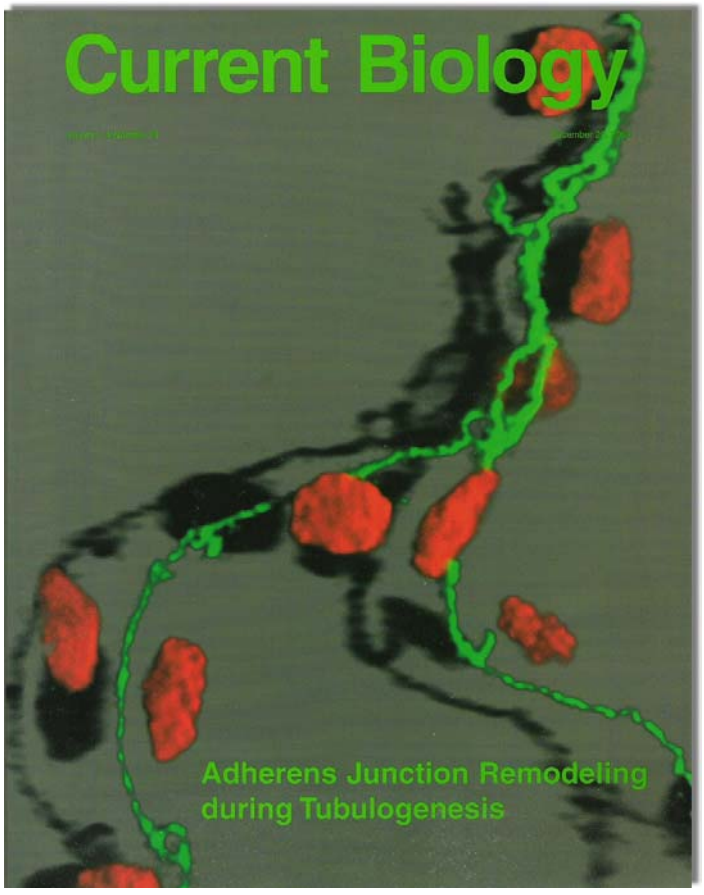

My contribution to this work was the development of the single cell labeling and the confirmation of the proposed model using this system shown in Figure 3. I also confirmed the requirement of a community effect for *sal* function as shown in figure 5. In a common effort we developed the model shown in figure 2.

Candidate approach to identify genes involved in tracheal cell rearrangements

In this section we test genes that due to various reasons are good candidates to affect AJ remodeling and intercalation. First we test genes which have been found previously to affect tracheal development and that have a phenotype that suggests an involvement in intercalation. Then we test genes that have been found to affect similar processes in other systems. Finally we test the available components of the AJ.

Tube size mutants

Tracheal cell rearrangements result in the transition of multicellular tubes with intercellular AJs to unicellular tubes with autocellular AJs. This transition is accompanied by a reduction of the tube diameter. In a genetic screen a set of mutations has been shown to affect tube size (Beitel and Krasnow, 2000). In these mutants all branches show tube size defects without showing defects in cell number. The most prominent phenotype is seen in the dorsal trunk, which is convoluted and displays a "sausage like" appearance with dilations and constrictions. For several of these mutations the corresponding genes have been cloned and shown to encode genes that are required for the formation of septate junctions (Wu and Beitel, 2004).

Currently it is not clear whether or how septate junctions are required for epithelial cell rearrangements. We wanted to know whether defective septate junctions interfere with cell intercalation and by this means result in tube size defects. We examined mutations in *sinuous*, *lachesin* and *megatrachea* with respect to their AJs. Although the described defects in the dorsal trunk are obvious (Fig.9A), all three show a normal AJ pattern. The AJs of the dorsal trunk are exclusively intercellular (Fig.9B) and the AJs of dorsal and ventral branches are mostly autocellular (Fig.9C). The dilations and constrictions of the dorsal trunk are not due changes in the AJ pattern. Thus intact septate junctions do not seem to be required for cell rearrangements during tracheal development.

Apart from the above-mentioned genes, other molecules are known to contribute to the correct assembly of septate junctions. Among them Gliotactin is particularly interesting with respect to the process we study. It specifically localizes to tricellular junctions

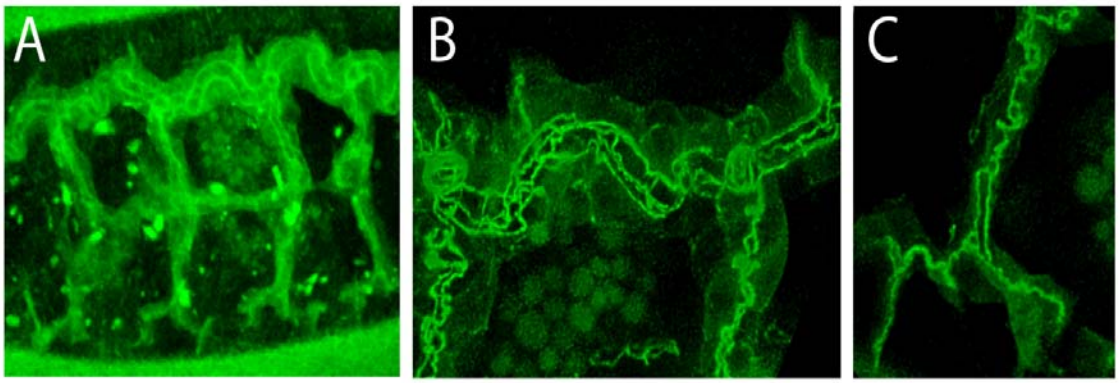

Figure 9 Intact septate junctions are not required for proper intercalation.
(A) *mega* embryos show a convoluted dorsal trunk. (B) The dorsal trunk in these embryos contains exclusively intercellular AJs. (C) The ganglionic branches in these embryos are made up of cells with autocellular AJs.
(A,B,C) Embryos mutant for *megatrachea* expressing α-catenin-GFP in the trachea.

(Schulte et al., 2003). As described above (Fig.2 in (Ribeiro et al., 2004)) the initial autocellular contact that is generated by the reaching around the lumen step results in a tricellular contact at this site. To check whether *gliotactin* fulfills a specific function at this site, we checked the loss of function phenotype. Although we clearly see the typical tracheal defects arising in the absence of septate junction components, we did not observe any defects in autocellular AJ formation (data not shown).

ribbon is required for cell intercalation

The most obvious tracheal phenotype in *sal* mutants is the lack of a dorsal trunk (Kuhnlein and Schuh, 1996). To identify other genes that -like *sal*- are involved in AJ remodeling we sought for mutations with a similar phenotype. Mutations in components of the EGF pathway as well as mutations in the transcription-factor *rib* specifically affect dorsal trunk development (Bradley and Andrew, 2001; Wappner et al., 1997).

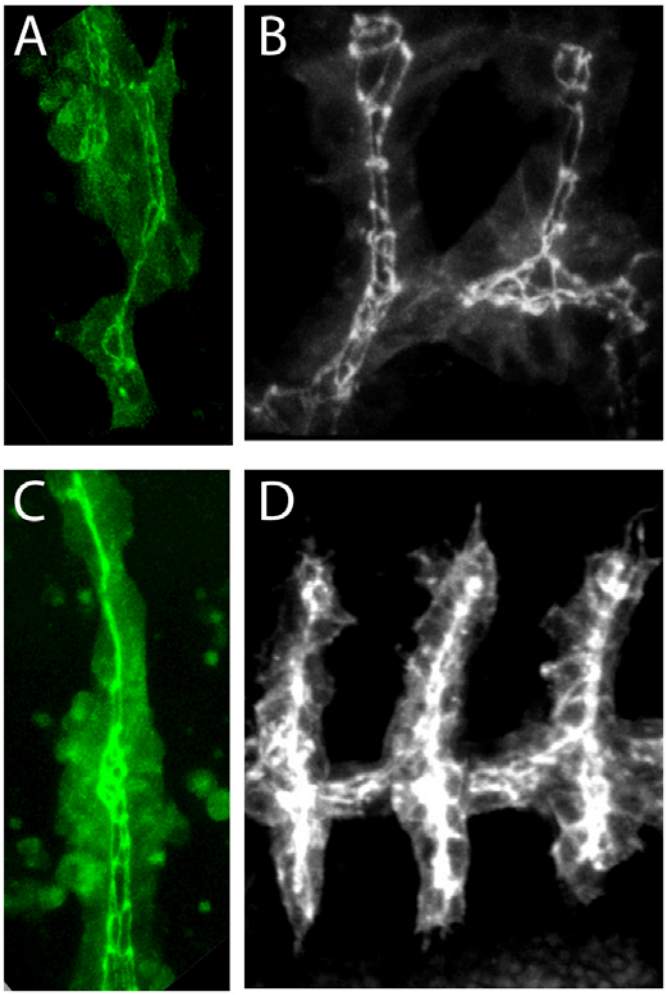

Figure 10 Genes affecting dorsal trunk development.
(A) A mutation in rhomboid does not affect intercalation. (B) In ribbon mutants intercalation is blocked except (C) in rare late embryos. (D) Filopodial dynamics are observed at the tip of growing branches in ribbon mutants.
(A) *rhomboid* or (B,C) *ribbon* mutants expressing α-catenin-GFP in the trachea. (D) *ribbon* mutant expressing GFPactin in the trachea.

All mutations in the EGF pathway were shown to exhibit similar effects on tracheal development. We studied mutations in *rhomboid* (*rho*) which is needed for the efficient signaling via the EGF-ligand Spitz (Bang and Kintner, 2000). Examining the tracheal AJ of *rho* mutants we did not find any ectopic autocellular AJ formation as in the *sal* mutant. We rather observe a slight shift towards intercellular AJ. Yet autocellular AJs can still be formed (Fig.10A). Thus the EGF pathway does not seem to affect cell intercalation.

Checking the AJ of *rib* mutant embryos we found to our surprise a phenotype that is opposite to the *sal* phenotype. Intercalation is blocked in *rib* mutant embryos and virtually no autocellular AJ are found (Fig.10B). This phenotype persists for a long time as shown by time-lapse analysis (Movie4). Only in late embryos when most severe tracheal defects were observed we occasionally find short stretches of autocellular AJ (Fig.10C). It was shown that *rib* does not interfere with FGF, EGF, *dpp* / *kni* or *wg* / *sal*

signals on the transcriptional level (Bradley and Andrew, 2001). Labeling the actin-cytoskeleton *in vivo* we find that also the cytoplasmic activity induced by FGF is not affected in *rib* mutants (Fig.10D) as it has already been proposed based on antibody stainings (Shim et al., 2001). Therefore we conclude that *rib* is specifically required to allow intercalation. Yet, it does not seem to be sufficient to induce cell intercalation as overexpression of *rib* does not cause any obvious effects (data not shown).

Small GTPases in tracheal development

Small GTPases have been shown to regulate a variety of cellular events. Especially small GTPases of the Rho family have been suggested in the regulation of epithelial adhesion (Braga and Yap, 2005). The best-characterized GTPases of this family are RhoA, Rac1 and CDC42. A Dominant negative RhoA has been shown to decrease adhesion in the *Drosophila* epidermis and to inhibit dorsal closure(Bloor and Kiehart, 2002). Using dominant active and dominant negative versions, Rac1 has been proposed to regulate cell rearrangements during tracheal development (Chihara et al., 2003). We wanted to find out whether we observe a specific effect on intercalation.

Dominant active Rac1 has been suggested to increase cell rearrangements. This interpretation is largely based on the fact that in later stages the trachea disintegrate and end up as cell clumps. This observation could be confirmed (Fig.11A) (see also thesis C. Dossenbach). Furthermore we see that in these cells α-catenin-localization is lost. However, checking the AJs earlier, when α-catenin is still localized to the AJs we do not see any ectopic autocellular AJ formation. Rather we find that as long as we detect localized α-catenin, no intercalation is observed (Fig.11B,C). These results are consistent with the observation that upon overexpression of Rac1V12 only few branch outgrowth is observed and that these branches eventually retract (Fig.11D) (Movie5) despite filopodial activity at the tip of the growing branch. Thus, in our hands activated Rac1 does not seem to enhance ordered cell rearrangements in the form of cell intercalation.

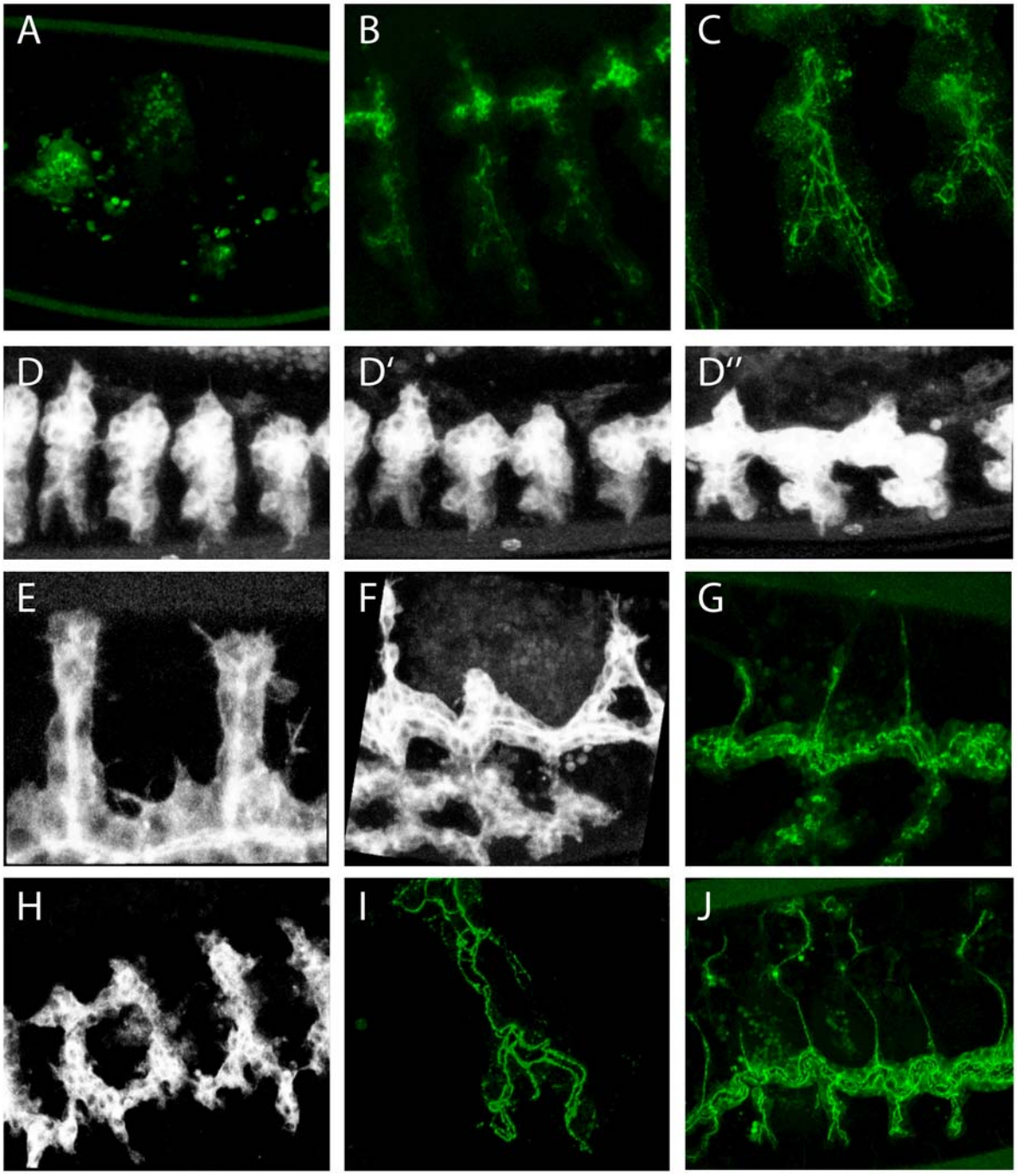
A
B
C
D
D′
D″
E
F
G
H
I
J

Figure 11 Small GTPases during tracheal development.
(A) Dominant active Rac causes disintegration of the trachea and loss of α-catenin-GFP localization in late stages. (B,C) No autocellular AJs are observed in earlier stages. (D) Branch outgrowth is initiated upon expression of dominant active Rac, but then stalls. (E) Dominant negative Rac cause lamellipodia-like cytoplasmic extensions (F) leading to a disintegration of the tracheal system. (G) It does not seem to affect the AJ pattern. (H) Rac mutant embryos show typical signs of a loss of E-cadherin mediated adhesion, but no lamillipodia. (I) Dominant active RhoA largely inhibits intercalation. (J) Dominant negative RhoA results in a convoluted dorsal trunk.
Embryos expressing (A,B,C,G,I,J) α-catenin-GFP or(D,E,F,H) GFPactin in tracheal cells together with (A,B,C,D) dominant active Rac, (E,F,G) dominant negative Rac, (I) dominant active RhoA or (J) dominant negative RhoA. (H) Rac mutant. (D) Still pictures of a time lapse analysis.

Dominant negative Rac1 has been proposed to block cell rearrangements (Chihara et al., 2003). Yet, in a time lapse analysis we see that branch outgrowth is initially normal. The most prominent effects are dramatic lamellipodia-like protrusions on all branches (Fig.11E) (Movie6). This cytoplasmic activity later leads to the disintegration of the trachea (Fig.11F) (Movie7), which like in the above-described scenario, end up as cell clumps (see thesis C. Dossenbach). Examining the AJs we find that also upon expression of dominant negative Rac1 α catenin localization is progressively lost (Fig.11G). As this loss starts before autocellular AJ formation takes place we have no means to faithfully determine whether intercalation is blocked or not.

It has been shown that the dominant negative phenotype does not always match the genetic loss of function phenotype (Ng et al., 2002). We therefore checked the phenotype of a double mutant of Rac1 and Rac2 that were shown to substitute for each other. In these mutants we did observe tracheal defects like dorsal trunk breaks and problems with branch outgrowth (Fig.11H). We furthermore observed that the tracheal cells are roundish as it is typical for a loss of E-cadherin-mediated adhesion. We also occasionally see cells detaching from the trachea (Movie8). We did, however, not observe the dramatic cytoplasmic dynamics. To summarize it looks like Rac indeed regulates properties of the AJ in the trachea. Yet, this regulation does not seem to manifest itself specifically on the level of cell intercalation. Additionally some effects might be artifacts of the dominant molecules.

We then went on to study the function of RhoA during tracheal cell intercalation. Dominant active RhoA overexpressed in the trachea largely inhibits autocellular AJ formation and intercalation (Fig.11I). In addition the tracheal lumen in the dorsal trunk appears to be uneven showing constrictions and dilations. Dorsal trunk defects were also observed upon overexpression of dominant negative RhoA. The dorsal trunk is convoluted (Fig.11J), but the AJs in this case are normal. The dorsal trunk shows exclusively intercellular AJs while dorsal and ventral branches show autocellular AJs. These defects resemble the defects seen in the septate junction mutants described above. Given the discrepancy of the dominant negative and the loss of function phenotype described for Rac we checked the RhoA loss of function phenotype. We found that mutants for RhoA displayed a perfectly normal tracheal system (data not shown). Thus also in this case we are not sure whether the defects observed with the dominant molecules represent artifacts.

Non-muscle myosin in tracheal development

As mentioned before non-muscle myosin has been shown to mediate cell intercalation events during germband extension (Bertet et al., 2004; Zallen and Wieschaus, 2004). Therefore we asked whether it may play a similar role during tracheal cell intercalation. *Drosophila* non-muscle myosin consists of a light chain which is encoded by *spaghetti squash* (*sqh*) and a heavy chain which is encoded by *zipper* (*zip*). We examined the AJ pattern in mutations for both genes and found that the mutants showed the regular AJ pattern with intercellular AJ in the dorsal trunk and autocellular AJ in the other branches (Fig.12A,B).

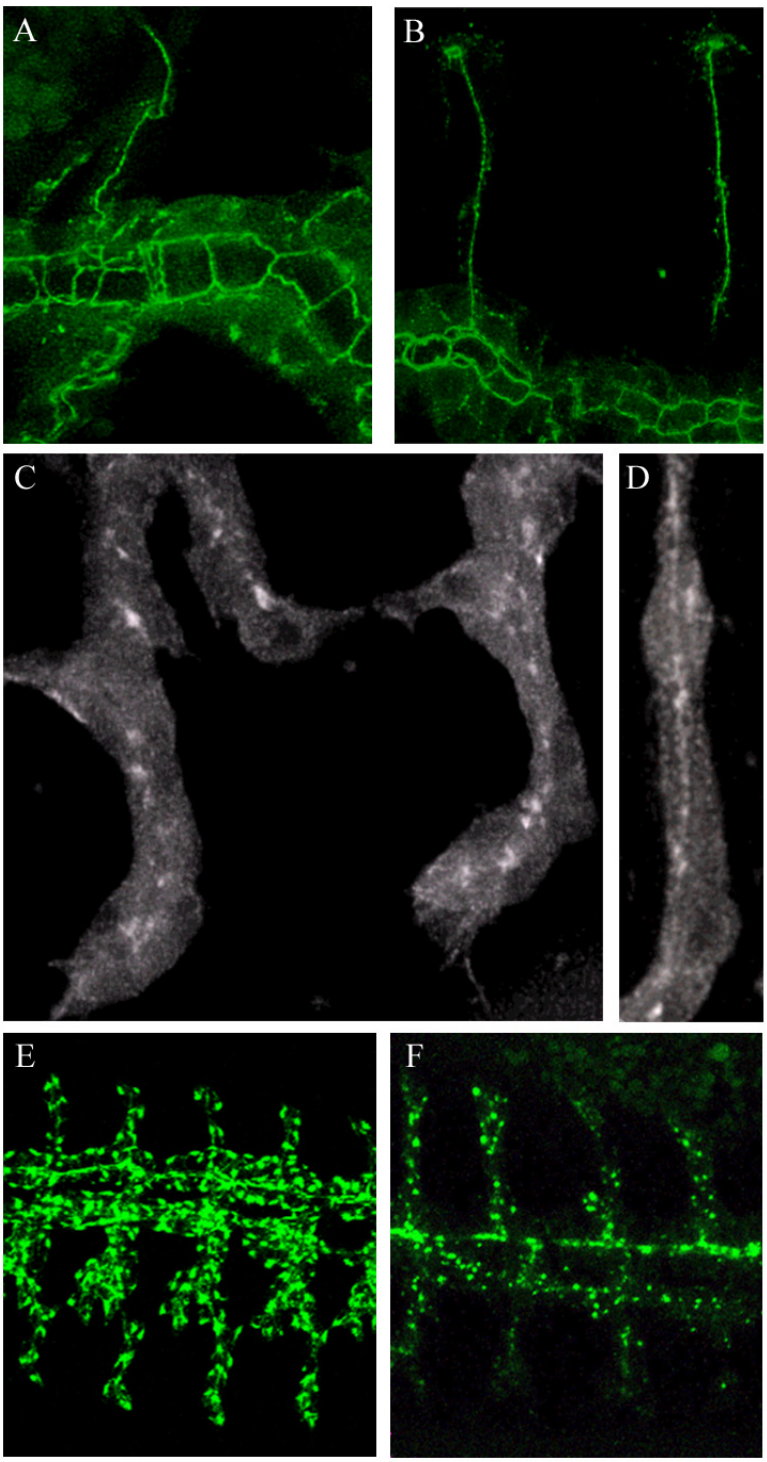

Figure 12 Non muscle myosin is not involved in tracheal cell intercalation.
Mutations in (A) zipper or (B) *spaghetti squash* do not affect intercalation. Neither (C,D) Sqh nor (E,F) Zipper localize to shrinking AJs during intercalation.
Embryos mutant for (A) *zipper* or (B) *spaghetti squash* or (C-F) wildtype embryos expressing (A,B) α-catenin-GFP (C,D) Sqh-GFP, (E) SlamHA or (F) Zip-GFP in the trachea. (A,B,C,D,F) Live embryos. (E) Antibody staining with an HA antibody.

Therefore it looks like non-muscle myosin does not act similarly during tracheal development and germband extension. To further test this conclusion we checked non-muscle myosin localization in the trachea. During germband extension non muscle

myosin localizes to shrinking AJs. This localization has been visualized using different methods (Bertet et al., 2004). Non muscle myosin localization has been visualized using a sqh-GFP fusion under the control of the endogenous promotor. This construct is introduced into a *sqh* mutant background, functioning as a rescue construct. This has been shown to markedly enhance the contrast compared to introduction of the same construct into a wildtype background (Royou et al., 2004). Using this construct we were not able to identify the tracheal Sqh-localization, because of the strong epidermal expression of *sqh* and because the trachea are very close to the epidermis. Even when we labeled the trachea concomitantly with RFPmoe we could not faithfully distinguish between tracheal and epidermal Sqh-GFP. Therefore we cloned Sqh-GFP under UAS control and expressed it in the trachea (see Materials and Methods). We found the Sqh-GFP fusion protein to be homogenously distributed in tracheal cells (Fig.12C) and did not observe any changes in localization during dorsal branch outgrowth (Movie9). Only late we see a slight apical localization (Fig.12D). However this localization is not confined to shrinking junctions. Yet, as this overexpression was done in a wildtype background it is possible that we do not detect localization due to the presence of wildtype protein. Therefore we tried an alternative method to visualize non muscle myosin.

Non muscle myosin localization has also been visualized indirectly by the heterologous expression of HA-tagged Slam (Slow as molasses) (Lecuit et al., 2002). *slam* is exclusively expressed during cellularization and has been shown to bind to *zip*. Ectopic expression of *slam* does not cause any abnormalities. We expressed SlamHA in the trachea and stained for the distribution of the HA-epitope. We observed a spotty localization throughout the trachea that does not show any obvious polarity inside the cells (Fig.12E). We also see a similar localization with two independent GFP-Zip fusions (gift of A. Brand and our own construct). These GFP fusions localize apically in the dorsal trunk. However additionally we see a spotty pattern throughout the trachea (Fig.12F). These spots do not seem to show any prevalence for shrinking junctions and may represent an overexpression artifact. To summarize, we have so far no evidence that non-muscle myosin plays a similar role in tracheal cell intercalation as it does during germband extension.

Components of the AJs

As mentioned above the core components of the AJs are E-cadherin, α-catenin, β-catenin and p120-catenin. Beside their structural role these genes are also involved in the regulation of epithelial adhesiveness and epithelial rearrangement (D'Souza-Schorey, 2005; Gumbiner, 2005).

Unfortunately we could not test all of these components for an involvement in AJ remodeling. For α-catenin, no mutant is available. To assay the role of β-catenin during cell rearrangement is problematic as it mediates *wg* signaling in addition to its role in the AJs. As Sal expression in the dorsal trunk depends on *wg* signaling (Chihara and Hayashi, 2000; Llimargas, 2000) loss of β-catenin also leads to a loss of *sal* and interferes by this means with cell rearrangements.

E-cadherin is the key-component of AJs and in many instances regulation of adhesion is mediated by the regulation of the levels of E-cadherin at the surface (Bryant and Stow, 2004). We asked whether modulation of the levels of E-cadherin interferes with tracheal cell intercalation. E-cadherin is maternally supplied, for this reason progeny of heterozygous mothers develops normally in the early stages of development. Defects only appear in later embryogenesis in morphologically dynamic organs, such as the malphigian tubules and the trachea (Tepass et al., 1996; Uemura et al., 1996). The tracheal defects are largely due to a failure of neighboring branches to fuse (Tanaka-Matakatsu et al., 1996).

To test whether AJ remodeling is also affected in the mutant we expressed α-catenin-GFP in tracheal cells to assay for AJ remodeling defects. Yet, in this case the situation is more complicated. As α-catenin localization relies on the presence of E-cadherin we loose α-catenin-localization as E-cadherin levels decrease. However, we are able to detect localized α-catenin-GFP until late stage 14 when the overall tracheal defects are clearly visible (Fig.13A). At this stage we occasionally see dorsal branches, which have undergone autocellular AJ formation (Fig.13B) arguing that E-cadherin transcription is not required for cell rearrangements to occur properly. At the same time we see a dorsal trunk showing exclusively intercellular AJs (Fig.13B). As long as we can detect localized α-catenin-GFP we do not see any ectopic autocellular AJ formation in the dorsal trunk.

These findings argue that cell intercalation in the tracheal system is not affected by a decrease in E-cadherin. Still, we cannot rule out that AJ-remodeling defects occur only at E-cadherin levels lower than the ones we observe. We then asked whether an increase in E-cadherin would interfere with cell rearrangements. To this end we over-expressed a functional E-cadherin-GFP fusion (Oda and Tsukita, 1999b) in the trachea and used it at the same time to monitor the AJs. We did not see any abnormalities (Fig.13C). Taken together these results imply that AJ-remodeling in the trachea is not tightly controlled by the levels of E-cadherin.

To further investigate the role of E-cadherin- levels and turnover we checked components of the AJs that have been found to regulate these processes. Among them is Hakai an E3-ubiquitin ligase that targets E-cadherin (Fujita et al., 2002) and marks it for degradation. The closest *Drosophila* homologue of Hakai is CG10263. CG10263 has 3 predicted splice forms encoding proteins of 300-450 amino acids. It exhibits 54% identical and 68% similar amino acids in a 100 amino acid range around the characteristic RING-domain We found two partially overlapping deficiencies that delete CG10263. Yet one of these deficiencies deletes *spitz*, the other one *screw*. Mutations in both genes cause severe tracheal defects. However, transheterozygotes of these deficiencies display a wildtype tracheal system at stage 16 (Fig.13D).

Also p120 catenin has been implicated in the regulation of E-cadherin-levels at the surface, though the exact role is still controversial. Mutations in the *Drosophila* p120-catenin are not lethal but show a strong genetic interaction with other AJ components (Myster et al., 2003). The tracheal system in these mutants had been described to be wildtype (Lee et al., 2003). When we tested the mutants for defects in AJ remodeling we could confirm that also on this level no defects can be seen (data not shown).

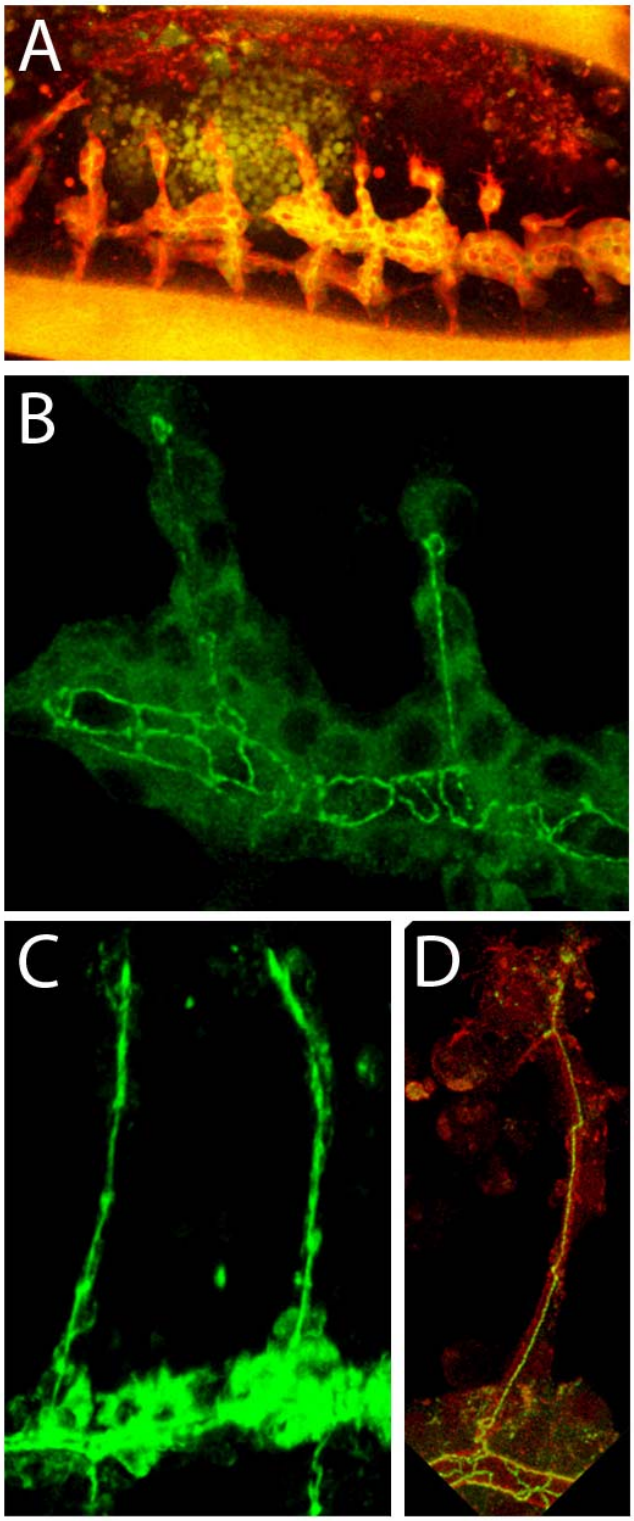

Figure 13 Altered E-cadherin levels do not interfere with intercalation.
(A,B) Loss or (C) gain of E-cadherin situations do not affect intercalation. (D) Mutations in Hakai do not affect intercalation.
Embryos mutant for (A,B) E-cadherin or (D) Hakai expressing α-catenin-GFP and RFPmoe in the trachea. (C) Wildtype embryos expressing E-cadherin-GFP in the trachea.

In situ screen

Many genes show very specific expression patterns during development. A way to identify genes involved in a certain process is to screen for genes that are expressed at the right time and the right place to account for a certain effect. We are particularly interested in genes that are expressed in the tracheal system during embryogenesis.

Extracellular molecules labeling a subset of tracheal cells

As we seek to identify genes that mediate the effect of *sal* the ideal candidate would show the same or a complementary expression pattern. Furthermore we reasoned that regulation of cell rearrangements involves the regulation of cell-cell contacts and therefore is likely to happen extracellularly. Christian Dahmann (MPI Dresden) has performed an in situ screen for several hundred genes encoding extracellular proteins. In collaboration with him we screened this library and identified two candidates that match the above criteria.

CA16 is expressed similar to *sal* in the trachea. The early expression is confined to the central part of the tracheal placodes like *sal* (Fig.14A). In later stages, CA16, like *sal*, is still not expressed in dorsal and ventral branches. Yet, in contrast to *sal,* it is also expressed in the transverse connective (Fig14C,E). It is also expressed in the anal pad (Fig.14B), in imaginal disc precursors (Fig.14F) and in the salivary gland (Fig.14D).

CA16 encodes a cadherin and includes the predicted genes CG4509 and CG4655 (personal communication C. Dahmann). As the expression of CA16 resembles *sal* expression we asked whether it is regulated by *sal*. As described above *sal* expression in the dorsal trunk is induced by *wg* signaling. We checked CA16 expression in an *armadillo* (*arm*) mutant that has been shown to specifically abolish the signaling function of arm without interfering with its role at the AJs. This mutation has been shown to abolish *sal* expression in the dorsal trunk and to display a *sal* like phenotype (Llimargas, 2000). Still, we find CA16 to be expressed in the trachea of these mutants (Fig.14G). We then checked whether overexpression of *sal* in the trachea would induce CA16 expression but we did not see any effect (Fig.14H). Thus despite the very similar expression CA16 is not regulated by *sal*.

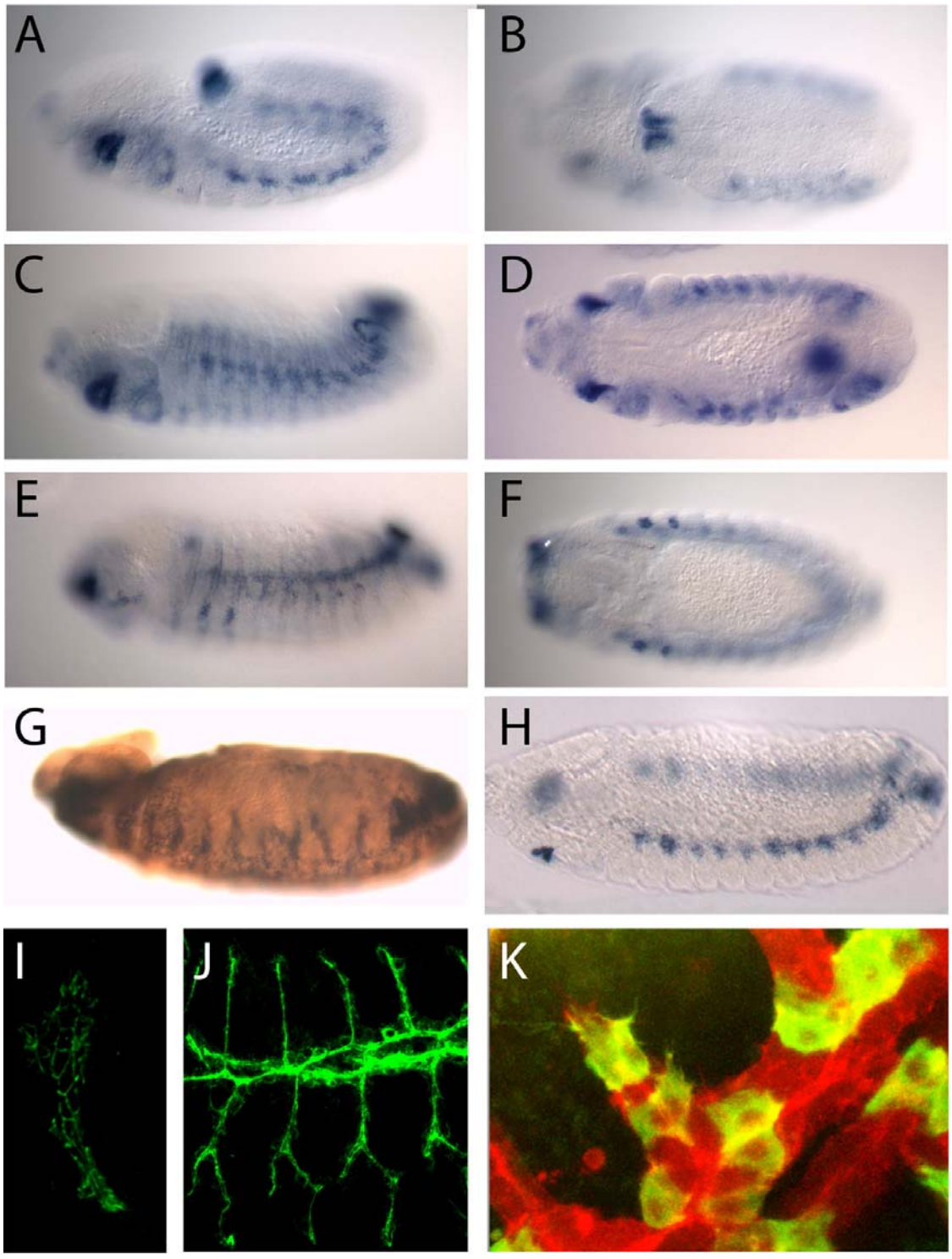
A
B
C
D
E
F
G
H
I
J
K

Figure 14 Characterization of a cadherin that is expressed similar to *spalt*.
(A-H) CA16 is expressed in the central part of the tracheal placode, in the salivary gland, in the anal pad and in imaginal disc precursors. (G) CA16 is expressed in *armadillo* mutants. (H) CA16 is not expanded upon pan-tracheal overexpression of *spalt*. (I,J) CA16 localizes to the AJs and the apical surface. (J) Pan-tracheal overexpression does not cause tracheal defects. (K) Overexpression of CA16 in single tracheal cells does not cause any effect.
In situ hybridization with a probe for CA16 in (A-F) wildtype embryos or embryos mutant for (G) *armadillo* or (H) embryos overexpressing *spalt* throughout the trachea. (I,J) AntiHA antibody staining on embryos expressing CA16HA in the trachea. (K) Overexpression of CA16HA in single tracheal cells that are labeled with GFPactin, while all tracheal cells are labeled with RFPmoe.

Although CA16 is not under *sal* control we were still interested in the role it might play in tracheal development and AJ remodeling. To get a first hint about its function we investigated the subcellular localization of the protein. An HA-tagged version of the molecule (from C. Dahmann) shows a subcellular distribution which looks virtually identical to α-catenin-GFP when expressed in tracheal cells early in tracheal development (Fig.14I). This localization becomes more diffuse in later stages and appears to extend to the apical surface (Fig.14J). This might reflect the real localization, but it may also be an overexpression or a fixation artifact. AJs are affected by methanol fixation. Also α-catenin antibody stainings show a more diffuse localization when compared to *in vivo* visualization (data not shown). Therefore it seems like CA16 is part of the AJs. At the same time we see that the overexpression of this construct does not cause any abnormalities (Fig.14J). We then wanted to know whether the loss of function would affect tracheal development. C. Dahmann generated a null allele of the gene and found the mutants to be homozygous viable and fertile. Examination of the trachea in these mutants revealed no defects with respect to branch specification and outgrowth and with respect to AJ remodeling (data not shown). For some genes, however, it has been shown that while the pure loss or gain of function did not cause any obvious defects on cell sorting and adhesion, gain or loss of function in clones resulted in defects (Milan et al., 2001). Therefore we overexpressed CA16 in single tracheal cells. We did not observe any defects. Furthermore we did not observe any prevalence of the cells for a certain area of the trachea or a tendency to stick to each other (Fig.14K). Taken together we did not find any role of CA16 in tracheal development.

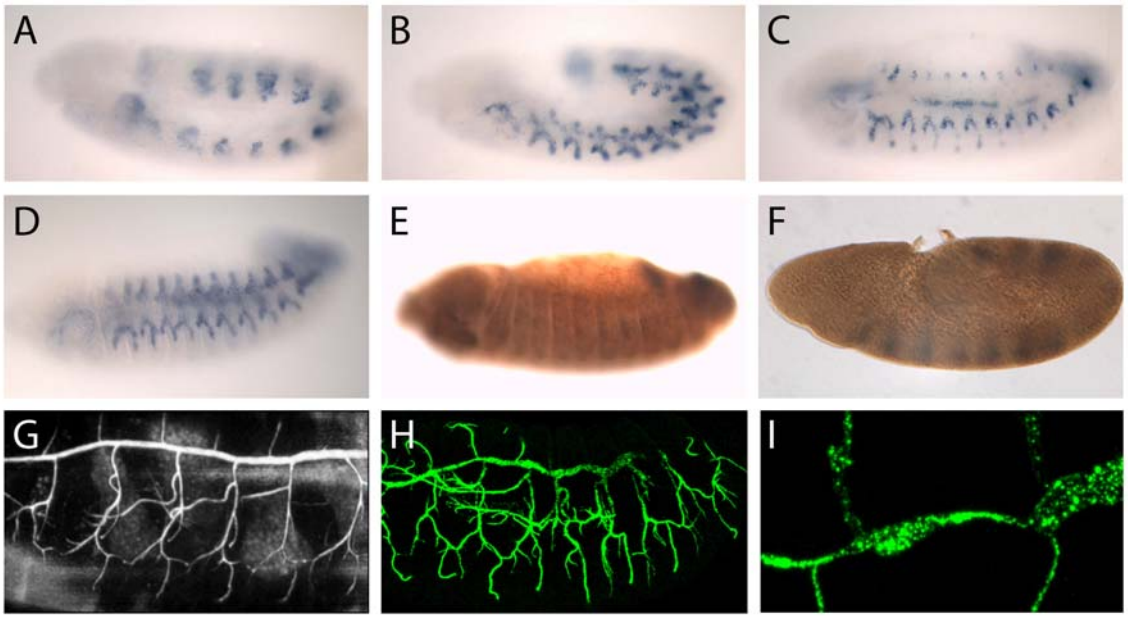

Figure 15 Characterization of a gene that is expressed in a subset of tracheal cells.
(A-C) CA229 is expressed at the tip of growing branches and is excluded from the center of the placode. (D) Overexpreesion of activated *breathless* causes an expansion of the expression. The expression is lost in (E) branchless or (F) breathless mutants. (G) CA229GFP accumulates in the tracheal lumen in stage 16. A deficiency deleting CA229 exhibits (H) lateral trunk breaks and (I) an uneven dorsal trunk lumen.
In situ hybridization with a probe for CA229 in (A-C) wildtype embryos or (D) embryos expressing a dominant active *breathless* receptor or embryos mutant for (E) *branchless* or (F) *breathless.* (G)Live embryo expressing CA229GFP in tracheal cells. (H,I) 2A12 antibody staining of embryos homozygous for a deficiency deleting CA229.

The other candidate -CA229- is exclusively expressed in dorsal and ventral branches and is excluded from the central part of the placode (Fig.15A-C). CA229 is encoded by CG16959. It contains an EGF-domain and a signal peptide. A similar expression as the one of CA229 has been reported for components of the FGF pathway and has been found to be due to an autoregulatory feedback loop (Ohshiro et al., 2002). Thus we checked whether CA229 is under the control of *btl* signaling. Indeed, expression of a dominant active version of the *btl* receptor causes a dramatic expansion of CA229 expression (Fig.15D), while only residual CA229 expression is left in *bnl* (Fig.15E) and in *btl* mutants (Fig.15F). Thus we conclude that *btl* signaling is responsible for the regulation of CA229 expression.

To examine CA229 protein localization we generated a CA229-GFP fusion and expressed it in the trachea under the control of *btl*-Gal4. Surprisingly we only detect GFP after late stage 16 although *btl*-Gal4 is expressed from stage 11 onwards. We have not observed such a phenomenon in any other GFP fusion we analyzed so far. In late stages CA229-GFP is found inside the tracheal lumen (Fig.15G) and we do not observe any overexpression phenotype. However, presently it is not clear whether this localization reflects the localization of the native protein and whether the fusion protein is functional.
To get more insight into CA229 function we wanted to study the loss of function phenotype. Unfortunately no mutant in this gene is available. Therefore we investigated the phenotype of a deficiency that deletes CA229. In Df(3L)Brd15 homozygous flies stained with 2A12 antibody we observe occasional fusion defects in the lateral trunk (Fig.15H) and in dorsal branches. In the dorsal trunk we see occasional breaks and an uneven lumen (Fig.15I). This uneven lumen may also represent fusion defects, but it may also be due to ectopic autocellular junction formation. Unfortunately the deficiency has a very poor viability and we were so far not able to visualize the phenotype with a-catenin-GFP. Anyway the deficiency is rather big and not molecularly mapped. We are currently generating a smaller deficiency with molecularly mapped breakpoints.

Genes showing pan-tracheal expression

The genes that mediate cell rearrangements do not necessarily need to be regulated transcriptionally by *sal*. It is as well possible that they are regulated indirectly in a posttranscriptional way. It is also possible that they act intercellularly for example in the regulation of the AJ-cytoskeleton interaction. Therefore we extended our search to all genes exhibiting tracheal expression. We searched the literature and screened a collection of in situ hybridizations that comprises around 3000 genes (Tomancak et al., 2002). For the most interesting candidates we ordered mutations or deficiencies and checked the loss of function phenotype using the 2A12 antibody that labels the tracheal lumen. Three of these mutants showed trachea-specific defects (Table 1). Df(2L)ast5 that deletes CG4226 shows a phenotype that is reminiscent of mutations in the EGF pathway (Wappner et al., 1997). Indeed the deficiency also includes the EGF-ligand *spitz*. To date there is no

deficiency or mutation available that deletes CG4226 without deleting *spitz*. Therefore we cannot analyze the loss of function of CG4226. A p-insertion in CG4726 that abolishes the tracheal expression (data not shown) causes a convoluted dorsal trunk as it is described for the tube size mutants above. We already know that these defects do not result in cell rearrangement defects. Therefore we did not further analyze this mutant.

Gene	**Deficiency / Mutant**	**Remark**
CG4226	Df(2L)ast5	Deficiency includes *spitz*
CG4726	P{EPgy2}EY00370	Convoluted dorsal trunk
CG10479	P{SUPor-P}KG00023	Trachea wildtype
CG18459	Df(3R)kar-Sz12	Trachea wildtype
CG30023	Df(2R)stan1	Trachea wildtype
CG33275	DF(3L)pbl-X1	Dorsal trunk defects
dachsous		Trachea wildtype
epithelial membrane protein	Df(2R)Kr14	Trachea wildtype
fat	ft[G-rv]	Trachea wildtype
Four jointed	fj[d1]/	Trachea wildtype

Table 1 Genes with a tracheal expression pattern that were tested for a mutant phenotype.

We then focused our analysis on DF(3L)pbl-X1 that deletes CG 33275. First we analyzed the phenotype in more detail. Labeling tracheal actin and α-catenin in live embryos we find that the trachea do form, but that a dorsal trunk is missing. Also dorsal branch outgrowth seems to be impaired (Fig.16A). The AJs in these mutants are present. Autocellular as well as intercellular AJs are found in the ventral half of the trachea. Dorsally no autocellular AJs can be seen (Fig.16B). Therefore it is possible that the CG33275 is required for tracheal development and AJ remodeling. DF(3L)pbl-X1 deletes around 100 genes as estimated by cytology. Thus it is well possible that more than one gene inside this deficiency is involved in tracheal development. Another deficiency that

overlaps with DF(3L)pbl-X1 and does not include CG33275 also displays a mutant tracheal phenotype (Fig.16C). This phenotype, however, is different from the one of DF(3L)pbl-X1, arguing that another gene inside DF(3L)pbl-X1 contributes to the observed tracheal phenotype. This could possibly be CG33275.

The predicted transcript of CG33275 comprises N-terminal spektrin-repeats and a DH (Dbl-homology)-domain followed by a PH (plekstrin homology)-domain (Fig.16D). A consecutive DH and PH domain are characteristic for GEFs that are specific for small GTPases of the Rho family (Cerione and Zheng, 1996). Interestingly the phenotype observed in the deficiency is similar to the one observed for Rac mutants (Compare to Fig).

As a next step we characterized the expression pattern of CG33275 in detail. CG33275 starts to be expressed around stage 12 in all tracheal cells (Fig.16E). The tracheal expression persists during stage 13 (Fig.16G,I). In stage 14 it starts to fade from the center of the trachea (Fig.16F) and is not detected anymore in stage 15. Additional expression is seen in cells in the ventral midline (Fig.16H) and in amnioserosa cells at the end of dorsal closure (Fig.16J).

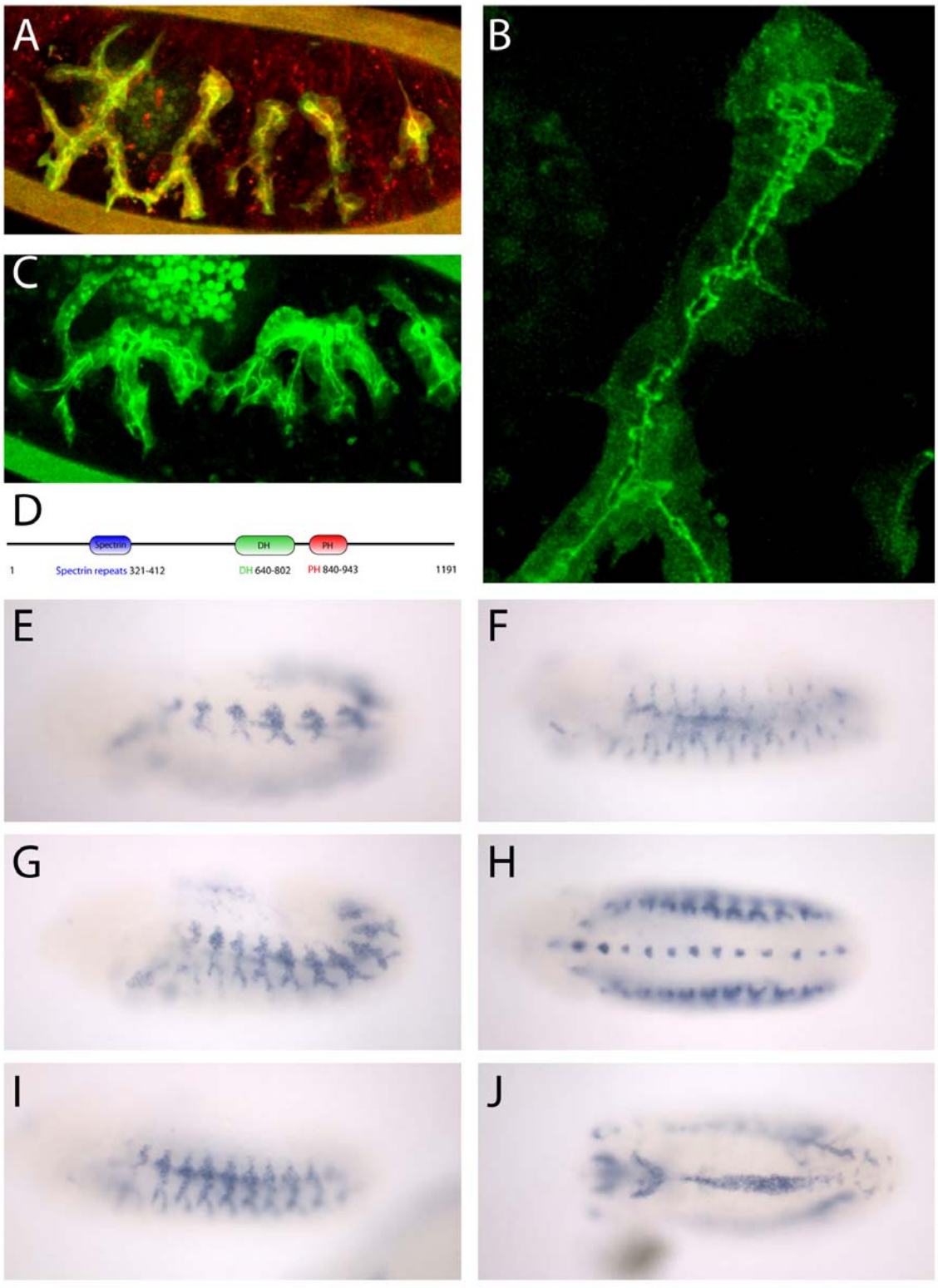
A
B
C
D
Spectrin
DH
PH
1
Spectrin repeats 321-412
DH 640-802
PH 840-943
1191
E
F
G
H
I
J

Figure 16 Analysis of a RhoGEF expressed in the trachea.
(A,B) A deficiency deleting CG33275 causes tracheal defects. (C) A partially overlapping deficiency that does not delete CG33275 also causes tracheal defects but has a different phenotype. (D) CG3375 contains N-terminal spektrin repeats and a consecutive DH and PH domain. (E-J) CG33275 is expressed in the trachea, in cells of the ventral midline and in amnioserosa cells.
(A,B) Deficiency deleting CG33275 or (C) partially overlapping deficiency not deleting CG33275 expressing (A,B,C) α-catenin-GFP and (A) RFPmoe in the trachea. (D) Domain structure of CG33275. (E-J) In situ hybridization using a CG33275 probe on wildtype embryos.

As no mutations in CG33275 or smaller deficiencies deleting the gene are available to test whether the loss of CG33275 causes tracheal abnormalities we sought to generate a smaller deficiency that removes as few other genes as possible. Two similar methods have recently been established to facilitate the construction of new deficiencies (Parks et al., 2004; Ryder et al., 2004). Both methods rely on trans-recombination events. In the one case, transheterozygotes of two P-element insertions are subjected to transposase. In the other case heterozygotes for two FRT insertions are subjected to flipase. In both cases the end result is the removal of the sequence in-between the two insertions (Fig.17A). To complement this tool with an adequate number of insertions the *Drosophila* genome is mutagenized systematically in an ongoing effort with either p-elements (Bellen et al., 2004) or piggy bac or P-elements bearing FRT-sites (Ryder et al., 2004; Thibault et al., 2004). We checked the genomic region around CG33275 for pairs of transposon-insertions we could use to generate a deficiency. Three such pairs were found (Fig.17B); one pair of p-elements (P{GT1}BG02453 / P{EPgy2}EY02000) and two pairs of Exelixis-FRT-insertions (e03004 / f01768 and e01801 / d09052). During the crossing procedure we found that two lines were mapped incorrectly. e03004 and P{GT1}BG02453 did not map to the third chromosome. We therefore only generated one deficiency with the remaining pair.
Using Exelixis FRT insertions, there are several ways to identify a recombination event and therefore the successful generation of the deficiency. For some combinations of FRT elements the white maker is lost upon recombination. Furthermore the recombination event can be confirmed via PCR. There are several PCR strategies that depend on the elements used (Fig.17C). In our case flies in which recombination occurred were selected

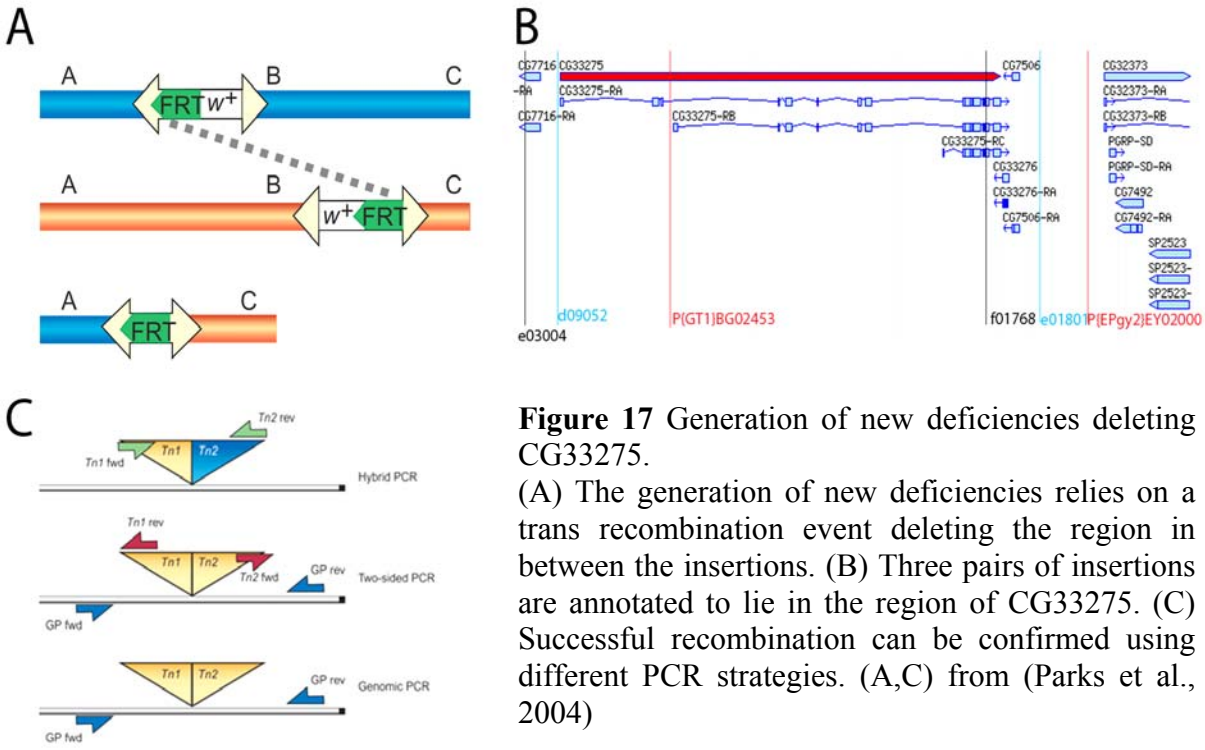

Figure 17 Generation of new deficiencies deleting CG33275.
(A) The generation of new deficiencies relies on a trans recombination event deleting the region in between the insertions. (B) Three pairs of insertions are annotated to lie in the region of CG33275. (C) Successful recombination can be confirmed using different PCR strategies. (A,C) from (Parks et al., 2004)

by the loss of *white*. From 10 *white* lines 8 were homozygous lethal and 2 were homozygous viable and fertile. 5 lines including a homozygous viable one were checked for the recombination event via hybrid PCR (Fig). All lines yielded a PCR product. Although the product is smaller than the published size, it fits the size calculated when looking at the published sequences of the vectors. In an independent recombination event that had been done in our lab we observed the same discrepancy with the published size (personal communication G. Pyrowolakis). Thus the PCR confirms that recombination occurred in all lines. From these lines one lethal and one viable line were tested with genomic PCR. Both were negative. As recombination occurred this result argues that one or both insertions are not correctly mapped. Analyzing the tracheal system of those two lines with α-catenin-GFP we found no defects (data not shown). However, at the moment it is not clear whether the constructed deficiency deletes CG33275 and therefore we cannot conclude whether the gene is essential for tracheal development. We are currently testing whether the gene is still expressed in the deficiencies we generated.

Genetic screen to identify genes involved in tracheal cell rearrangements

One major advantage of *Drosophila* is the possibility to easily perform forward genetic screens, which allows the identification of the function of new genes. This possibility has extensively been used and many novel genes have been identified by this means. Classically these screens were done using EMS which induces random point mutations in the genome. More recently transposons were used to mutagenize the genome (Bellen et al., 2004; Spradling et al., 1999). Yet another possibility is the use of deficiencies, in which larger areas of the genome are deleted. A deficiency kit covering most of the *Drosophila* genome has been available for almost 10 years (see Bloomington Homepage). However, these deficiencies were mapped only by cytology and therefore it is not sure which genes exactly are deleted by these deficiencies. Recently new approaches were initiated to systematically generate molecularly mapped deficiencies as described above (Parks et al., 2004; Ryder et al., 2004).

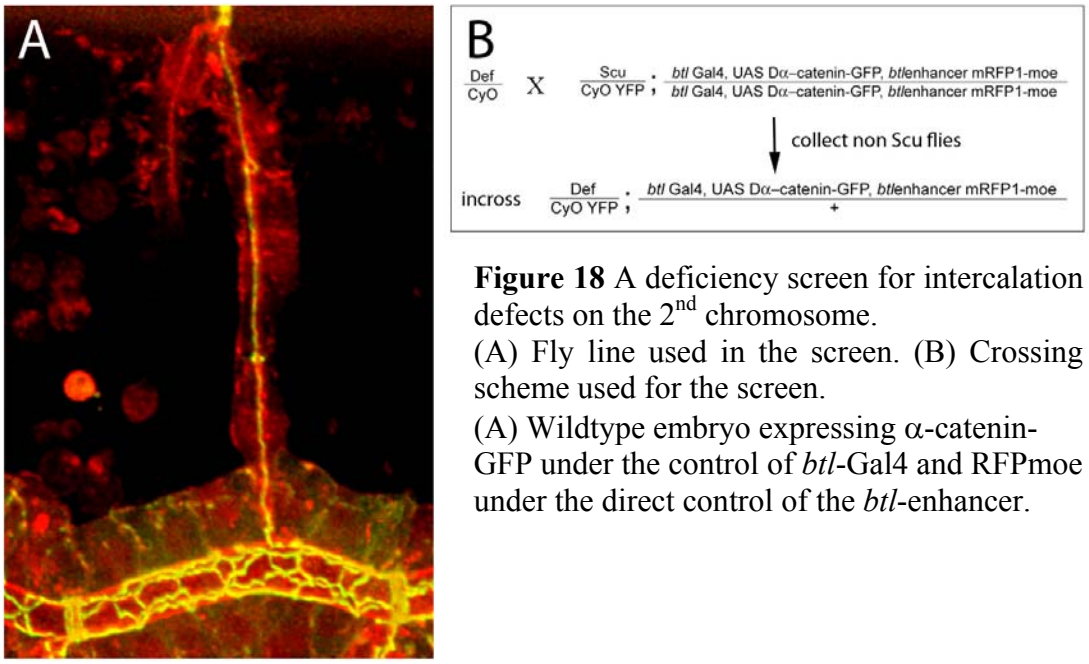

Figure 18 A deficiency screen for intercalation defects on the 2nd chromosome.
(A) Fly line used in the screen. (B) Crossing scheme used for the screen.
(A) Wildtype embryo expressing α-catenin-GFP under the control of *btl*-Gal4 and RFPmoe under the direct control of the *btl*-enhancer.

Setup of the screen

As we have identified a very specific phenotype both for the gain and the loss of *sal* function we wanted to find other factors that when deleted show similar phenotypes in the trachea. The idea of the screen is to express α-catenin-GFP in the trachea and to screen for mutations that either show ectopic autocellular AJs in the dorsal trunk or a loss of autocellular AJ formation in dorsal and ventral branches. Since this phenotype is subtle and requires thorough analysis under the confocal microscope we needed an approach with a limited amount of lines to screen. Thus we performed a screen using deficiencies. Additionally α-catenin-GFP is a weak marker. To allow for a rapid identification of the stage and the orientation of the embryos under the microscope, a direct fusion of the *btl*-enhancer and RFPmoe was recombined onto the same chromosome as α-catenin-GFP. With this line we label the AJs and the actin cytoskeleton at the same time (Fig.18A). Mutants were identified by using a YFP balancer that shows strong YFP-expression in two anterior spots from stage 15 onwards (gift from Greg Beitel). With this setup we screened all available deficiencies of the Exelixis deficiency kit on the 2nd chromosome (Fig18B), which comprises 170 lines covering 80% of the predicted transcripts of 2L and 60% of 2R.

During the screen we identified virtually all known tracheal mutants that fall into these deficiencies including *spalt*, *ribbon*, *escargot*, *star* and *raw*. We also identified various deficiencies with mutant tracheal phenotypes that do not include a gene known to affect tracheal development. The results of the screen are summarized in the supplementary material and discussed below (see discussion). In the following we will focus on the closer analysis of one candidate deficiency that shows a specific cell rearrangement defect in the trachea.

Analysis of a deficiency screen candidate

The Bloomington line BL7782, which corresponds to the Exelixis line Exel7010, displays a tracheal system that is on the whole intact in stage 15. All branches are formed and extend into the right directions (Fig.19A). Yet, while dorsal and ventral branches show the regular α-catenin localization the anterior part of the dorsal trunk shows an

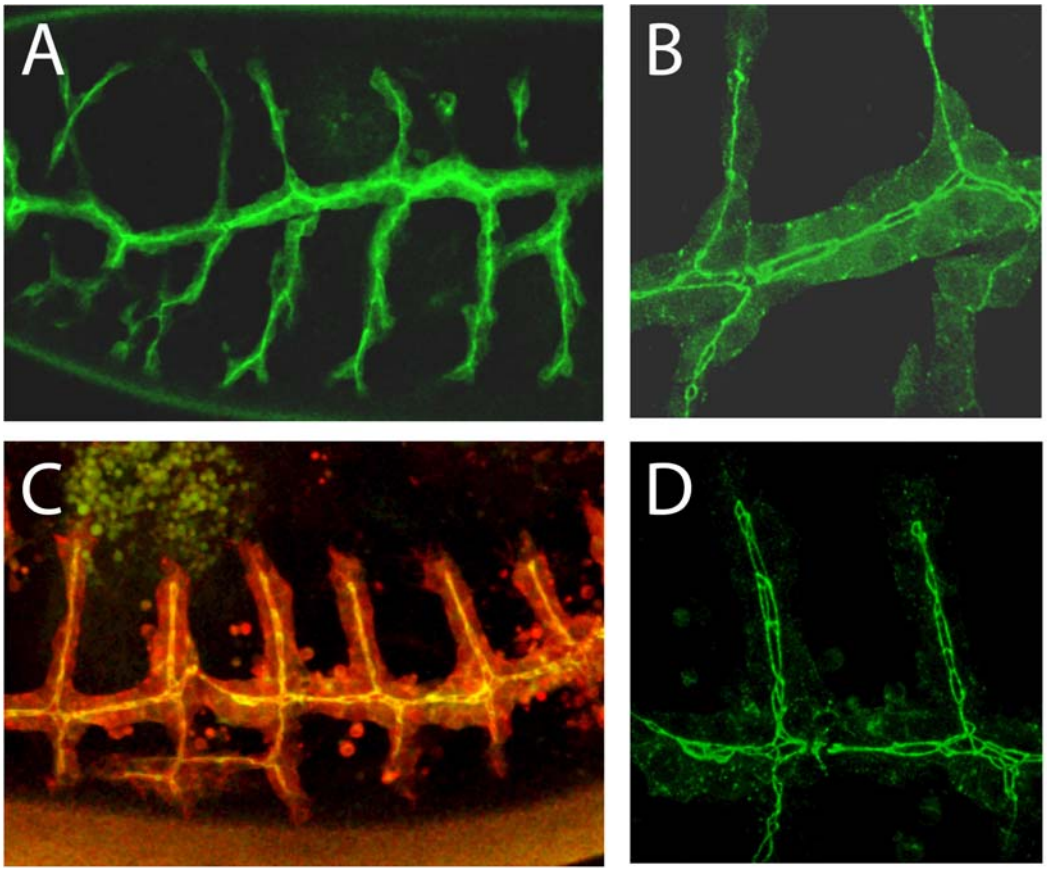

Figure 19 The deficiency Exel7010 displays ectopic intercalation.
(A,B)Homozygous mutant embryos display ectopic intercalation in the anterior dorsal trunk. (C,D) The same phenotype is observed in transheterozygotes with an independent deficiency covering the same region.
(A,B) Embryos homozygous for Exel7010 or (C,D) transheterozygotes of Exel7010 and Df(2L)BSC37 expressing (A-D) α-catenin-GFP and (C) RFPmoe in the trachea.

abnormal pattern of α-catenin localization as it shows stretches of autocellular AJs (Fig.19B). In addition the apical surface appears smaller than in the wildtype. In later stages the embryos display a partial loss of α catenin localization and in very late stages the tracheal system disintegrates. Furthermore we observe some ill-characterized defects in the epidermis that seems to be closer to the trachea making the visualization of the trachea difficult.

The phenotype is only found in homozygous mutant embryos and never in heterozygous ones (data not shown). Thus it is not a dominant phenotype and the defect is not caused by haploinsuffiency. Crossing the deficiency over an independent overlapping deficiency

resulted in the same phenotype (Fig.19C,D), arguing that the phenotype is really due to the deficiency and not due to an unrelated event on the same chromosome.

We then went on to further characterize the phenotype. Given the small apical surface and the thinner lumen resulting from the formation of autocellular AJs we asked whether luminal proteins are localized correctly in embryos homozygous for the deficiency. The antibody, which has been used most routinely to stain the tracheal lumen, is 2A12. It is a monoclonal antibody against a so far unidentified protein that is exclusively found in the lumen of the embryonic trachea from stage 14 onwards. We find that 2A12 is indeed mislocalized in mutant embryos. In contrast to the very even line in the wildtype (Fig.20D), 2A12 in the deficiency shows a bulgy appearance especially in the dorsal trunk (Fig.20C). We also found that 2A12 appears to be trapped during secretion. While in the wildtype only in very early stages a faint cytoplasmic staining is seen (Fig20B), in the mutant excessive cytoplasmic staining is found until late stage 15 (Fig.20A). At the same time the amount of protein that reaches the lumen seems to be smaller than in the wildtype.

We then tested Pio another luminal protein that had been identified in our lab. Pio is required to terminate autocellular AJ formation in dorsal and ventral branches before it goes to completion (Jazwinska et al., 2003). In contrast to 2A12 Pio localization is normal. We do also not observe a massive cytoplasmic retention of Pio (Fig.20E). Thus the defects are not unspecific secretion or luminal localization defects, but are specific for some proteins.

Looking carefully at the 2A12 antibody staining we also found that in the mutant more cells are incorporated into the dorsal branches of anterior segments. While in the wildtype five to six cells make up the dorsal branch (Samakovlis et al., 1996) in the mutant up to nine cells are found to be part of the dorsal branch (Fig.20A). This phenotype resembles a moderate gain of *dpp* function phenotype. Also ectopic AJs in the dorsal trunk are observed upon tracheal overexpression of activated *dpp* receptor or its target gene *kni* (Fig.4D,E in (Ribeiro et al., 2004)).

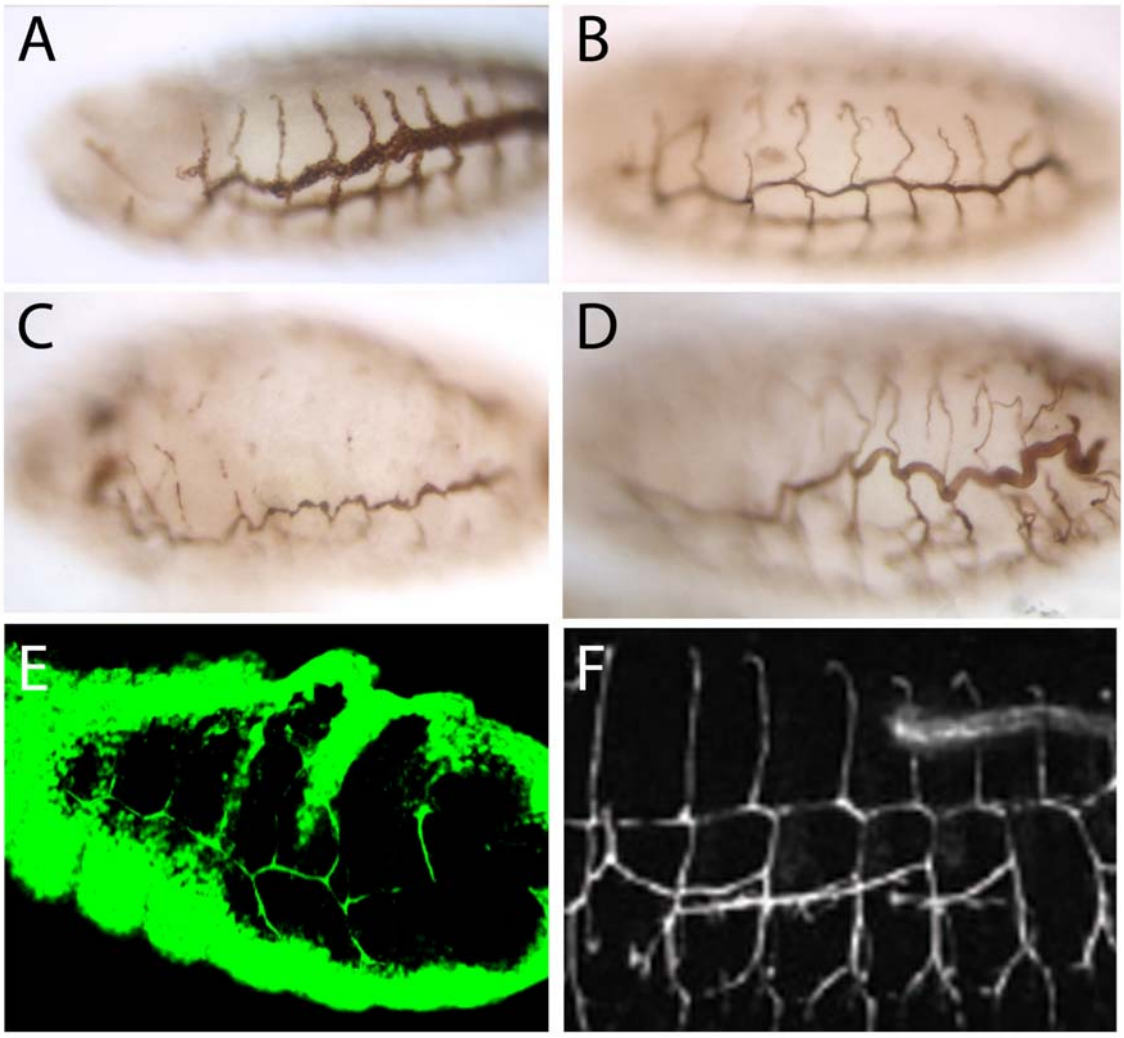

Figure 20 Exel7010 exhibits a cargo specific secretion defect.
The antigen that is detected by the 2A12 antibody is (A) trapped during secretion and (C) does not efficiently reach the lumen and shows an irregular distribution. (E) Similar effects are not observed for Pio.
(A,C,E) Embryos homozygous for Exel7010 or (B,D,F) wildtype embryos, stained with (A-D) 2A12 or (E,F) anti-Pio antibody. (F) From(Jazwinska et al., 2003).

To find out whether the phenotype is due to elevated *dpp* signaling we checked *kni* expression in the deficient embryos. However, *kni* expression looks normal. It is found in dorsal and ventral branches and does not extend to the center of the placode (Fig.21B). To further clarify the phenotype we then checked Sal protein expression itself. The protein expression in early stages looks perfectly normal (Fig.21D). In stage 15 Sal protein is still present in the dorsal trunk of mutant embryos. The expression even seems

to expand into the transverse connective where it is not seen in wildtype embryos (Fig.21E). However, looking more closely it appears like the subcellular localization of Sal is altered in the anterior part of the dorsal trunk. While in the posterior part the characteristic nuclear localization of Sal is seen (Fig.21G) in the anterior part a more uniform staining is observed. No nuclei can be identified with the Sal antibody staining in this region anymore (Fig.21F). This is most likely not due to a general defect in the nuclei as we observe nice round nuclei by the nuclear exclusion of markers as RFPmoe or α-catenin-GFP (Fig.19B).

Thus, it is possible that although Sal protein is present in dorsal trunk cells fewer Sal is found in the nucleus resulting in a weaker signal and a *sal* loss of function phenotype. Consistent with this scenario the intercalation phenotype is mostly observed in the anterior dorsal trunk where the localization defect is observed. To find out whether indeed Sal levels are critical for the intercalation phenotype we overexpressed Sal in mutant trachea. By doing so we could restore intercellular AJs in the dorsal trunk (Fig.21I). We also mimicked the *sal* overexpression phenotype in wildtype with regard to intercalation: Dorsal and ventral branches are blocked in the intercalation process and display intercellular AJs. Hence the intercalation phenotype is due to a lack of *sal* signal. Interestingly with the overexpression of Sal we do not rescue the size of the apical surface. All branches keep a very thin lumen and a small apical surface (Fig). Thus this process seems to be affected independently of the lack of *sal*.

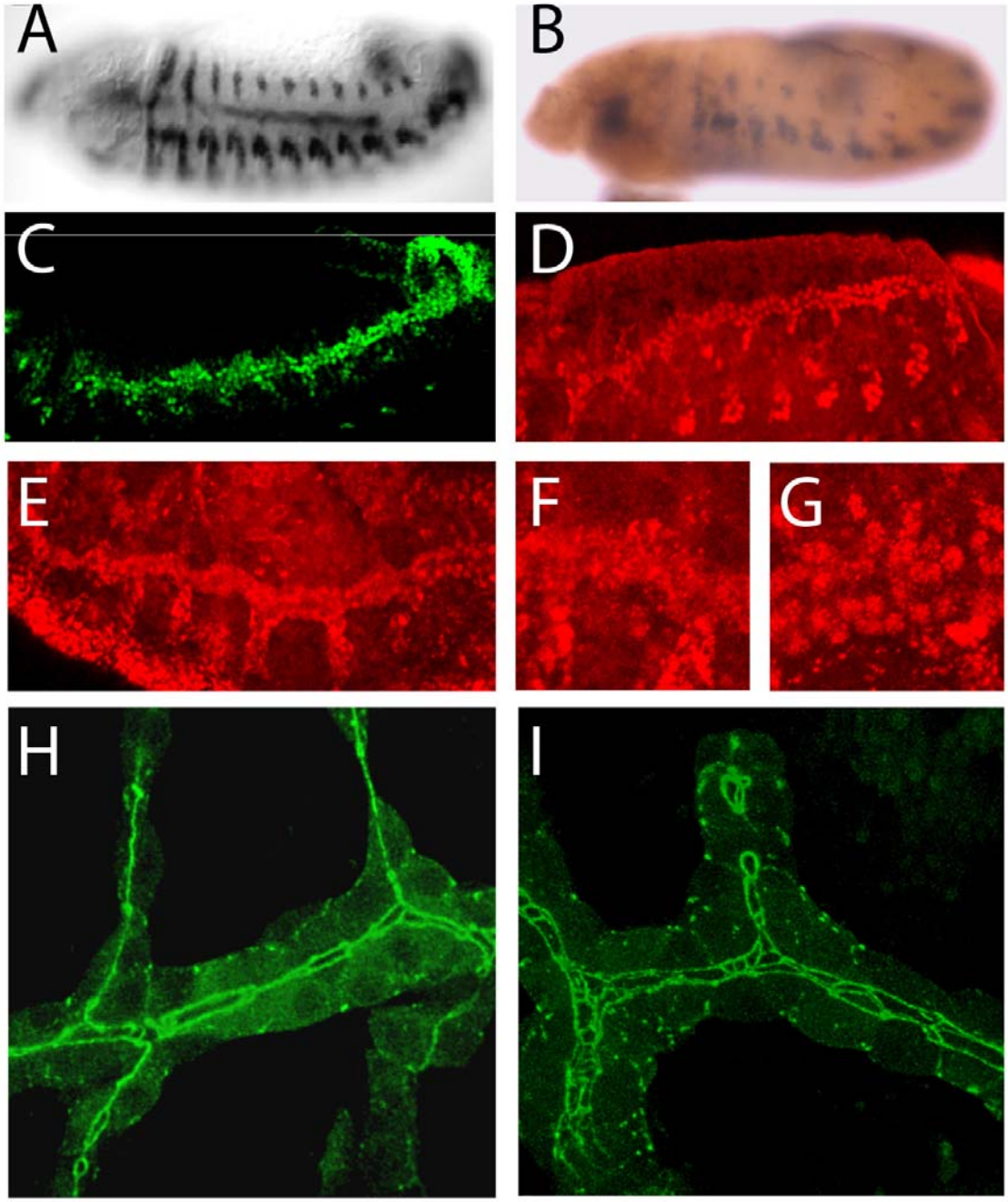
A
B
C
D
E
F
G
H
I

Figure 21 Spalt may not be efficiently localized to the nucleus in the anterior dorsal trunk.
(B) *knirps* and (D) early Spalt are expressed normally in embryos homozygous for Exel7010. (E) Later Spalt is still expressed in the trachea and is localized to the nucleus (G) in posterior segments. (F) It is not specifically localized to the nucleus in anterior segments. (I) Overexpression of *spalt* in the trachea of embryos homozygous for Exel7010 rescues the intercalation phenotype in the dorsal trunk and blocks autocellular AJ formation in the other branches.
In situ hybridization of (A) wildtype or (B) embryos homozygous for Exel7010. Anti-Spalt antibody staining of (C) wildtype or (D-G) embryos homozygous for Exel7010. (H,I) α-catenin-GFP expressed in the trachea of embryos homozygous for Exel7010 (I) overexpressing *spalt* in the trachea. (A) From (Chen et al., 1998), (C) from S. Merabet.

Mapping the deficiency screen candidate

The deficiency Exel7010 was constructed using the original lines f00030 and d09675. It spans a genomic region of 142kb and deletes 26 putative genes based on the release 3.1 of the *Drosophila* genome (Table 2). Among the deficiencies in the screen another deficiency (Exel7009) partially overlaps with Exel7010 (Table 2 black label). This deficiency does not show any of the phenotypes described above as assessed in the screen. To identify the gene that is responsible for the tracheal phenotype observed we performed three different approaches.

First we tried to identify an EMS mutant that shows the same phenotype. To this end we crossed flies that were mutagenized with EMS (in the lab of M. Leptin) against the deficiency and screened for lethality. Then we checked the flies carrying the lethal hit for the intercalation phenotype. In total we checked 1300 lines, each carrying around 1.7 lethal hits per chromosome as estimated by the concentration of EMS used (Luschnig et al., 2004). Therefore an approximate total of 2200 lethal hits on the 2nd chromosome were screened. From this we obtained 10 lines that were lethal over Exel7010. Yet, none of these lines showed the intercalation phenotype.

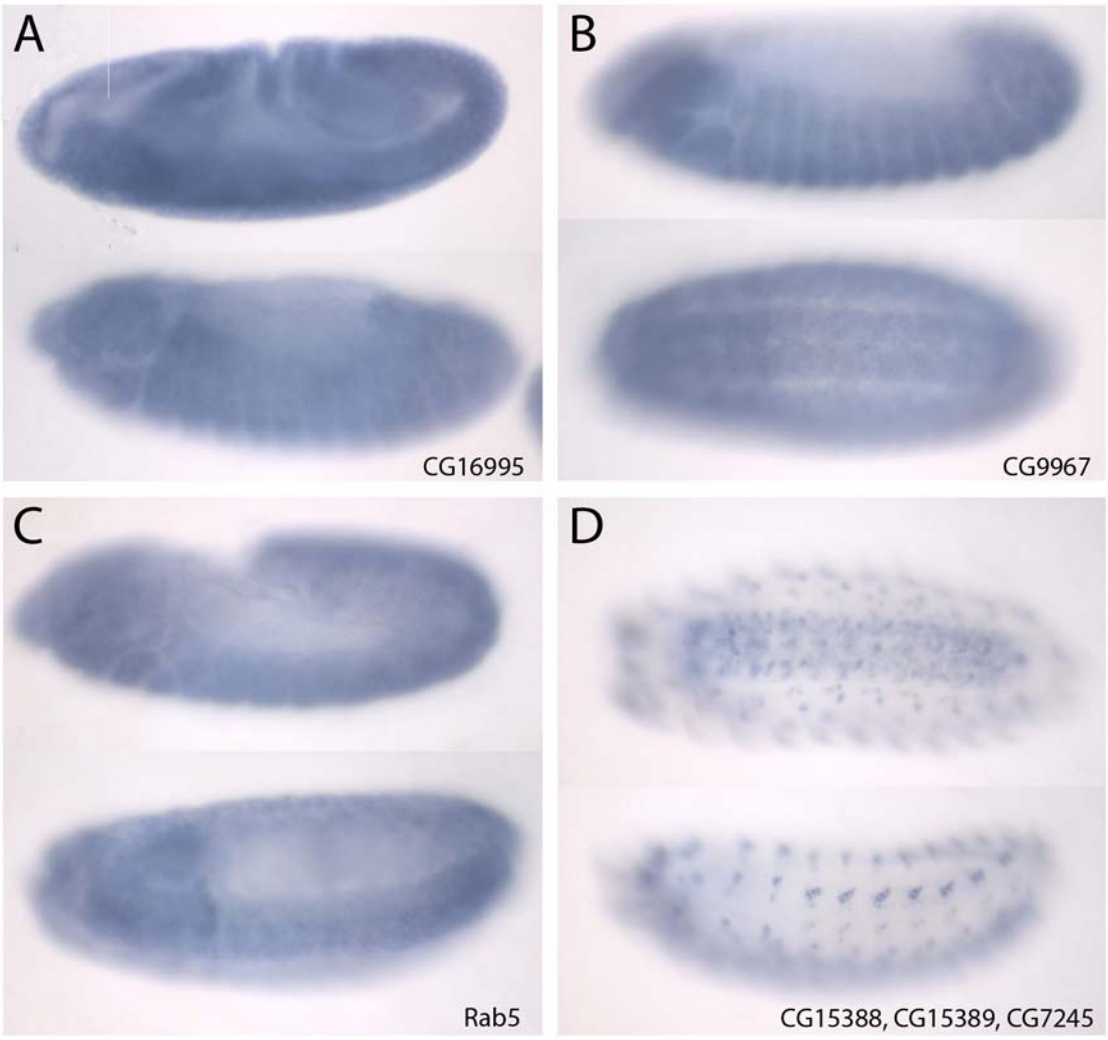

Figure 22 Expression patterns of genes covered by Exel7010.
(A) CG16995 is expressed ubiquitously. (B,C) CG9967 and Rab5 are expressed ubiquitously with a stronger expression in the CNS. (D) CG15388, CG15389 and CG7245 display an identical expression pattern in the CNS and PNS.
In situ hybridizations of wildtype embryos with the stated probes.

In another approach we searched for a gene inside the deficiency that shows an expression pattern which would qualify the gene as a candidate. We identified several embryonic expression patterns (Fig). While some genes (CG31686, CG4279, robl22E, CG31949) do not seem to be expressed during embryogenesis, CG16995 displayed rather ubiquitous expression (Fig.22A). CG9967 and Rab5 showed a ubiquitous staining with higher levels in the CNS (Fig.22B,C). The predicted genes CG15388, CG15389 and CG7245 are likely to encode one transcript as they show an identical expression pattern

in the CNS and the PNS (Fig.22D). None of these patterns strongly implied a function in tracheal development.

We then tried to restrict the region responsible for the phenotype by generating smaller deficiencies as described above. We focused our analysis on the area that is not included in Exel7009 as this deficiency does not show the phenotype we are interested in. We generated seven deficiencies that delete parts of the Exel7010 deficiency (Table 2) and analyzed their phenotype. None of these deficiencies displayed the original phenotype. There are several possible explanations for this.

At first we tried to rule out that this result is due to technical problems. Thus we checked whether recombination occurred properly and whether the integration site of the Exelixis lines used are correctly mapped. The correct recombination was verified by several means. First, all deficiencies were constructed in a way that they loose the *w* marker upon recombination. We then performed PCR on these w^--flies using different primer pairs as suggested in the publication describing the generation of new deficiencies (Fig.17C). The deficiencies were first tested with a hybrid PCR. All lines except for one (Table 2 faint grey label) yielded a PCR-product. We therefore conclude that in these lines recombination occurred properly. We then tested whether the transposon insertion sites were mapped properly. For this we designed genomic primers flanking the insertion site. With these primers we made a PCR spanning the entire recombination region (Fig.17C genomic PCR). For all lines tested we obtained a PCR product. Sequencing this PCR product we identified in all cases a stretch of genomic DNA followed by the respective transposon sequence confirming again that recombination occurred as expected. We also found that the real insertion sites of the transposons differ in no case more than 200bp from the published insertion sites. Additionally we checked the initial line Exel7010 by genomic PCR and obtained the expected PCR product showing that this deficiency deletes the expected genes.

Taken together these results show that the deletion of the region we focused on is not sufficient to reproduce the phenotype of the entire deficiency. Therefore we switched our attention to the region that we excluded from the analysis as it was annotated to overlap with Exel7009. First we retested Exel7009 confirming that the deficiency is indeed

Gene	Annotated function	Exelixis element	Exel7009	Constructed deficiencies						
CG7082	RNA binding	f00030								
CG15387	?									
CG7085	?									
CG10882	COPIIcoat binding, actin binding									
CG31679	Endonuclease									
CG32463	Endonuclease									
CG31682	Endonuclease									
CG4267	Lipase									
CG31686	?	d00854,f01528								
CG17240	Trypsin related	f03416								
CG17239	Trypsin related									
CG17234	Trypsin related									
CG17012	Trypsin related									
CG4270	Gli pathogenesis related 2									
CG17242	Trypsin related	e02526, f07743								
CG4271	Trypsin related									
CG31681	Trypsin related									
CG17237	Calcium binding EF-hands									
CG10838	Dynein associated protein									
CG31949	?									
CG16995	Gli pathogenesis related 2									
CG9967	?	e00929								
CG15388	EGF-domain									
CG15389	Cell adh., Thrombosp.-, EGF-domain	f00112								
CG7245	Thrombosp.-, Laminin-, EGF domain	e02575								
Rab5	Small GTPase, vesicle trafficking	d09675								

Table 2 Genes deleted by Exel7010

wildtype (Fig.23A). We also did not observe any cytoplasmic retention with a 2A12 antibody staining (data not shown). Next we tried to confirm the position of the deficiency with genomic PCR. However, we did not obtain a PCR product arguing that the deficiency is wrongly mapped. We then checked which genes are supposed to be deleted in the deficiency and found that among others *anterior open* (*aop*) should be deleted in the deficiency. However *aop* has been reported to exhibit a tracheal phenotype

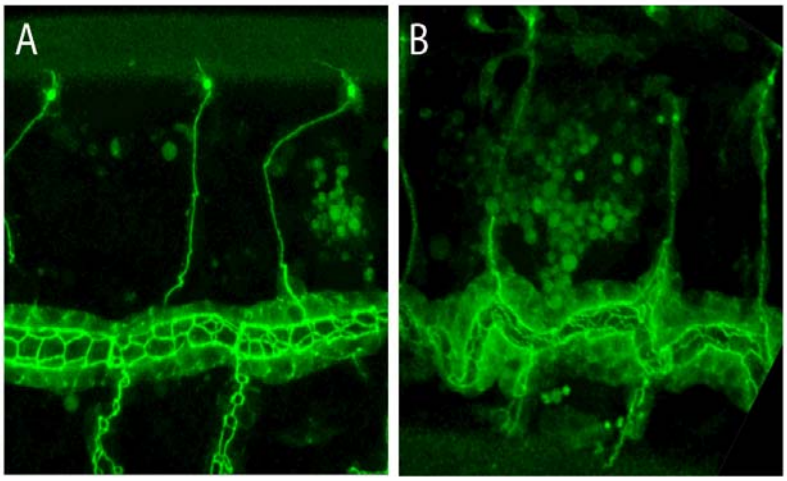

Figure 23 Exel7009 does not delete *anterior open.*
(A) Embryos homozygous for Exel7009 display a wildtype tracheal system. (B) Embryos mutant for *anterior open* display tracheal defects,
Embryos homozygous for (A) Exel7009 or (B) *anterior open* expressing α-catenin-GFP in the trachea.

(Lai and Rubin, 1992). An analysis of the *aop* mutant revealed that the dorsal trunk in *aop* is convoluted and that the dorsal branches are longer than in the wildtype (Fig.23B). These findings argue that Exel7009 does not cover the region it is annotated to cover. Therefore we do not know whether a gene in the overlap region we excluded from the analysis so far is responsible for the phenotype (see discussion). We are currently performing an in situ analysis of the region and generate smaller deficiencies in this region.

In silico *approach to identify* sal *targets*

So far we screened for genes that affect the same process as *sal* by searching for a similar phenotype. Another approach is to screen directly for targets of *sal*. Sal is a well characterized transcription factor and therefore its major effect is probably at the level of transcription. Therefore we attempt a transcriptional profiling of tracheal cell during intercalation using microarray analysis.

Setup of the screen

Several chip experiments have been performed in our lab, but most of them did not work properly. This has mainly been due to two reasons. Some experiments were done using whole embryos to detect transcriptional changes in tracheal cells. As only 10% of all cells of the embryo are tracheal cells the resulting overall changes were probably too low to be faithfully detected. This resulted in a very high fraction of false positives in these experiments (personal communication A. Jung, Thesis C. Ribeiro). Trying to circumvent this problem Carlos Ribeiro tried to FACS (Fluorescence activated cell sorting) sort tracheal cells. Yet, at that time it was not possible to concentrate the cells in a way that allowed obtaining enough RNA for a linear amplification method (see Thesis C. Ribeiro). Nowadays non-linear amplification methods are well established and methods for RNA-extraction even from single cells are readily available. Therefore the amount of cells needed for a chip experiment has decreased dramatically. Also FACS sorting has improved and allows cell sorting in a smaller volume of liquid. In the earlier FACS sorting experiments C. Ribeiro aimed to sort up to 200 000 cells, which resulted in 15 ml of liquid volume (see thesis C. Ribeiro). We now aim to sort 10 000 cells which now can be sorted into 15 µl.

To identify *sal* targets we compare the transciptome of wildtype tracheal cells with the one of tracheal cells that overexpress or lack *sal*. We therefore need to label exactly these cells. To label wildtype cells we use a recombinant of btlGal4 and UAS GFPactin (Fig 24A). To label cells that overexpress *sal* we cross this line to a line that is homozygous for UAS *sal*. To label cells that lack *sal* we generate recombinants carrying either btlGal4 or UAS GFPactin on the same chromosome as a small deficiency removing *sal* and *salr*.

When these two lines are crossed only tracheal cells lacking *sal* are labeled. With these crosses we expect a total of 2,5% of the cells to be GFP-positive, assuming that 10% of the total embryonic cells are tracheal cells.

We then dissociate the embryos using a protocol that has successfully been used to obtain cells of the embryonic nervous system for MACS (magnetic cell sorting) and successive chip analysis (personal communication Y. Fan). Using this protocol with the wildtype cross we can identify single intact green-fluorescent cells via confocal microscopy (data not shown). When FACS sorting cells from this cross we clearly identify a GFP-positive fraction of events (Fig.24B) amounting to 2,6% of the total events. Co-labeling with propidium iodide confirms that these events are not dead cells (Fig.24C). As inferred from the pulse width the events are due to single particles (Fig.24D) Applying all these filters and analyzing the resulting fraction in the forward scatter / side scatter reveals that these events are heterogenous with respect to size and granularity (Fig.24E). As we do not see a clear cluster, the borders for size and granularity of the events to be sorted have to be guessed.

When sorting cells that overexpress or lack *sal* we get an unexpected result. Unlike the wildtype situation we do not obtain a clear cluster of GFP-positive cells (Fig). Currently we do not know the cause of this phenomenon (see Discussion). Yet, only when we are able to faithfully sort cells in wildtype and mutant situations we can proceed to the actual chip experiment.

A

yw x *btl*Gal4, UAS-GFPactin / cyo

UAS-*sal* / UAS-*sal* x *btl*Gal4, UAS-GFPactin /cyo

*btl*Gal4, *sal* /cyo x UAS-GFPactin, *sal* / cyo

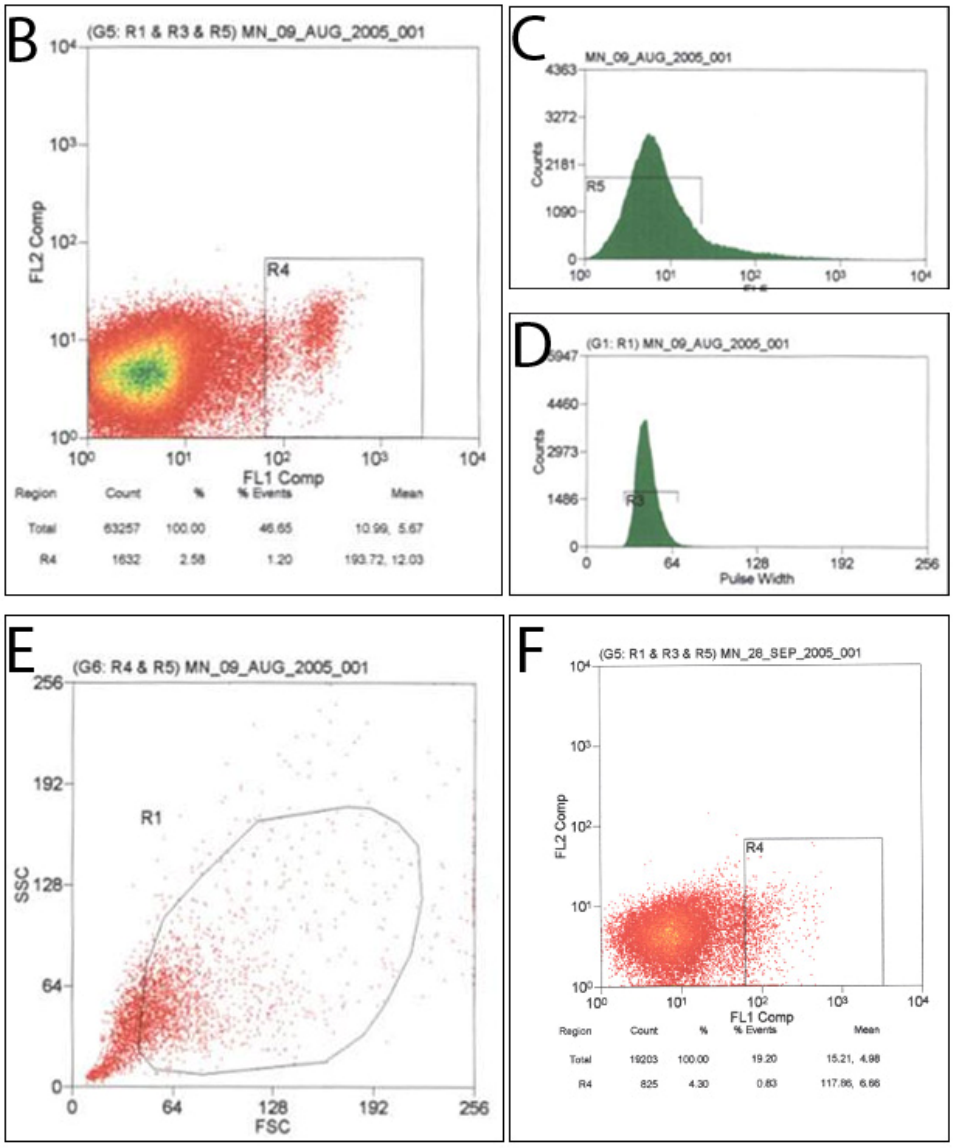

Figure 24 FACS sorting tracheal cells.
Sorting wildtype tracheal cells we clearly identify (B) a GFP-positive fraction that (C) does not represent dead cells and (C) contains of single particles. (E) Applying the indicated filters we obtain a population that is heterogeneous with regard to size and granularity.
(A) Crossing schemes to obtain fluorescently labeled tracheal cells with different Spalt levels. *Drosophila* cells from embryos expressing GFP actin in wildtype tracheal cells during FACS displayed as a function of (B) green and red fluorescence, (C) propidium iodide staining, (D) pulse width or (E) size and granularity. (E) Gated for R4 (in B), R5 (in C) and R3 in (D). (F) *Drosophila* cells from embryos expressing GFP actin and ectopic Spalt in tracheal cells during FACS displayed as a function of green and red fluorescence.

Structure-function analysis of *spalt*

The central molecule in the regulation of autocellular AJ formation is the transcription factor *sal* and we use a variety of approaches to identify *sal* target genes. Once targets are identified we would like to know whether these targets are directly regulated by *sal* and identify a consensus sequence for Sal binding which would then allow for the *in silico* identification of additional target genes. To this end biochemical studies such as electrophoresis mobility shift assay (EMSA) are required. These assays are problematic with large molecules. As Sal is a rather large protein of 1355 amino acids we wondered whether we could generate a smaller version of the molecule that is still capable of blocking autocellular AJ formation. For these purposes we generated a series of deletion constructs (Fig.25A). All deletions were fused to a V5 tag to allow detection and to an NLS to ensure nuclear localization. Then we checked whether overexpression of the constructs would mimic the overexpression phenotype of the full-length protein (Fig.25B) when expressed in the trachea.

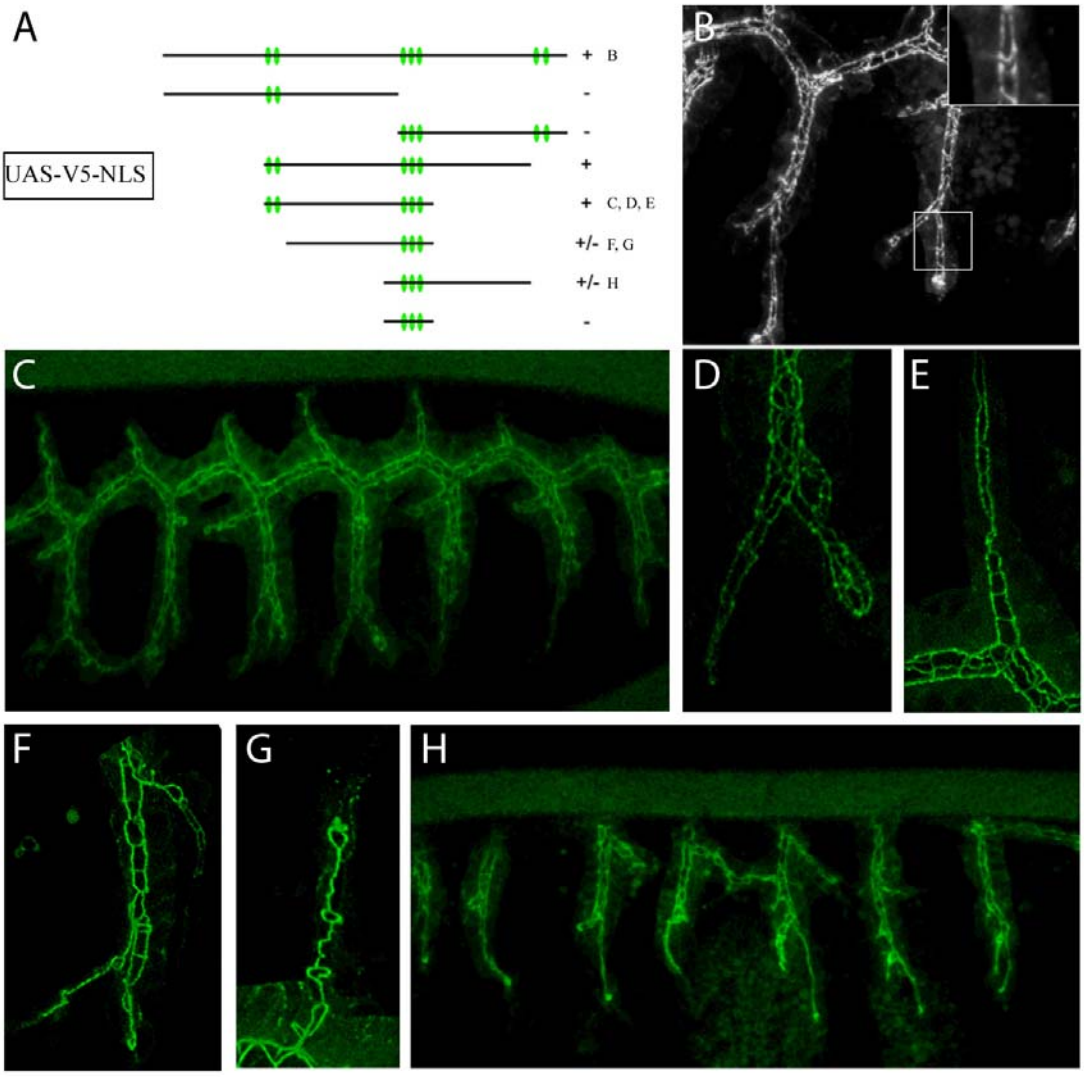

Figure 25 Structure function analysis of Spalt.
(C-E) A Spalt deletion construct containing the central 600 amino acids including the first 5 zinc fingers perfectly mimics the overexpression phenotype of (B) the full-length protein. (F,G) Removal of the N-terminal zinc-fingers from this construct results in a partial loss of function. (H) A similar phenotype is seen when using the conserved region around the zinc-finger triplet and the adjacent downstream region.
(B-H) Embryos expressing α-catenin-GFP together with various deletion constructs of Spalt (as indicated in A) in the trachea.

The Sal protein contains two doublets and one triplet of zinc fingers (Fig.25A). In the deletion analysis we found that the central part of the molecule including the N-terminal doublet and the triplet is required and sufficient to mimic the overexpression phenotype of the full-length molecule (Fig.25C). It blocks intercalation in ganglionic branches

(Fig.25D) as well as in dorsal branches (Fig25E). Removal of the doublet in this construct resulted in a partial loss of this capability. Although some branches are still blocked in intercalation (Fig25F) others are not (Fig.25G). A similar phenotype was observed when a conserved region upstream of the triplet was kept and additionally the region downstream of the triplet just until the next doublet (Fig.25H). The conserved region around the zinc-finger-triplet alone was not sufficient to block intercalation (Data not shown). However removal of the zinc finger triplet in any case completely abolished *sal* function (data not shown) despite the presence of protein (shown by an antibody staining detecting the V5 epitope; data not shown). Taken together, we have identified a 600 amino acid fragment of Sal that perfectly mimics Sal function during intercalation. This size will allow a biochemical analysis in the future.

FGF signaling and the force driving intercalation

A physical force is required for intercalation to occur. To better understand the mechanism of intercalation we wanted to find out more about the origin of this force. It could either be generated inside the intercalating cells or could be applied from other cells. As tracheal cells are attached via AJs the force could for example be generated by the leading cells that react to the *bnl*/FGF signal and that pull the rest of the cells during branch outgrowth. Alternatively the surrounding mesodermal cells could generate a pressure that results in intercalation.

Based on the observation that in *bnl*/FGF mutants no branch outgrowth (Klambt et al., 1992; Sutherland et al., 1996) occurs and on the fact that only the tip cells respond to FGF signals with the formation of filopodia (Ribeiro et al., 2002) we favored the model that FGF induced migration in the leading cells at the tip of the branch is generating the force. Consistent with this model we do not observe any intercalation in *btl* mutants (Fig).

To test the model we tried to alter this force and monitor the effect on the AJs. We reasoned that the force inside the individual intercalating cells could be decreased if either the distance of branch outgrowth would be decreased or if the number of intercalating cells would be increased. To check a situation where branch outgrowth is decreased we examined “dorsal open” mutants. Dorsal closure is a process in which the epidermis is stretched over the amnioserosa and is eventually sealed at the dorsal midline. Tracheal cells were proposed to be tightly associated with the dorsal epidermis (Dorfman et al., 2002) and dorsal branch outgrowth runs in parallel to dorsal closure. In *kayak* (*kay*) mutants stretching of the epidermis during dorsal closure does not occur properly (Zeitlinger et al., 1997) leaving the embryo dorsal open. Examining the AJs of dorsal branches in these mutants reveals that autocellular AJ formation is not impaired despite the fact that the distance the dorsal branches have to span is considerably shorter than in wildtype embryos (Fig). Even more surprising, the branches look compressed as if they try to extend despite the lack of pulling force. Yet, at the moment we do not know whether the branches have indeed never been stretched. To rule out this possibility we have to make time lapse movies of tracheal development in dorsal open mutants.

To check a situation where more cells are integrated into the dorsal branch we investigated *brinker* (*brk*) mutants. *brk* mutants show dorsal branches with different cell numbers. While dorsal branches in the posterior part comprise the normal number of 5-6 cells, dorsal branches in anterior segments consist of up to 10 cells. We find that anterior dorsal branches undergo normal autocellular AJ formation (Fig) like posterior ones (Fig) arguing again that a reduction in the pulling force does not affect intercalation. However, as *brk* is an integral part of the *dpp* signaling network alterations in *brk* levels also affect Sal levels. Therefore it might be that the reduction in pulling force is compensated by a reduction in Sal levels in this situation.

To summarize we have so far no evidence that intercalation is driven by the force generated by the migration of FGF-responsive tip cells. Yet, as described above *bnl*/FGF is required to induce branch outgrowth and intercalation and its effect seems to be confined to the tip cells. To specify the role of FGF signaling we investigated how a genetically mosaic tracheal system would develop. To this end we used the single cell labeling system described above to rescue single tracheal cells in *btl* mutants. Only the cells that express the *btl* receptor display the characteristic cytoplasmic extensions of tip cells, while *btl* mutant cells stay inert (Fig.). However, we did not observe any branch outgrowth. Thus, it looks like apart from its function to induce filopodia in tip cells, FGF has also a function in the other tracheal cells, allowing them to branch out.

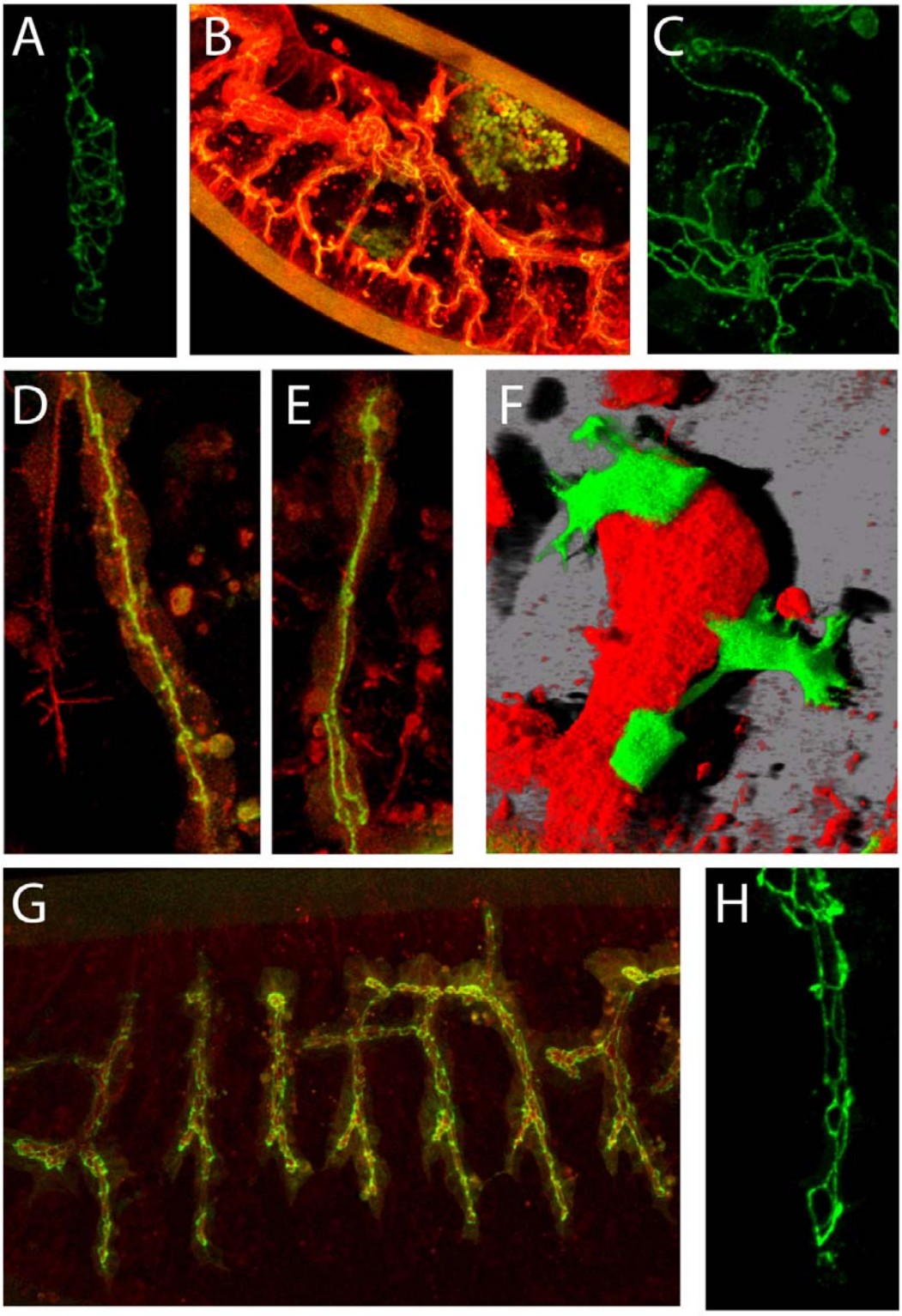
A
B
C
D
E
F
G
H

Figure 26 Contribution of FGF signaling and the pulling force to intercalation.
(A) In *breathless* mutants no intercalation takes place. (B,C) Dorsal branches in dorsal open mutants intercalate. (D) Dorsal branches in anterior segments of *brinker* mutants intercalate as well as (E) dorsal branches in posterior segments. (F) Expression of *breathless* in single tracheal cells of otherwise *breathless* mutant embryos rescues filopodia formation but not branch outgrowth. (G,H) Intercalation is blocked in *pointed* mutants.
(A-E, G,H) Embryos expressing α-catenin-GFP and (B,D,E,G) RFPmoe in the trachea. (A) *breathless* mutant. (B,C) *kayak* mutant. (D,E) *brinker* mutant, (G,H) *pointed* mutant. (F) *breathless* mutant embryo expressing *breathless* in single actinGFP-expressing tracheal cells.

We then wanted to know how this effect of FGF is mediated. Apart from its role in the induction of filopodia FGF also regulates transcription. One well-characterized FGF target is the ETS transcription factor Pointed (Pnt). We wanted to know whether *pnt* mutants also show cell rearrangement defects. *pnt* mutants were shown before to exhibit tracheal defects. Unlike mutants in *bnl* or *btl* that show no tracheal outgrowth, the primary outgrowth in *pnt* mutants is not affected (Samakovlis et al., 1996). However, later branch outgrowth stalls. Interestingly in these branches no autocellular AJs are found (Fig). Thus *pnt* is required for autocellular AJ formation showing a direct requirement of FGF signaling for cell intercalation.

Discussion

In this study we have characterized the morphological events underlying cell intercalation in the *Drosophila* tracheal system and we have found how this process is regulated. Based on these findings we attempted to molecularly understand intercalation using various approaches. In the following we will discuss different models for cell intercalation based on our findings and will outline the future direction of our research. We will also discuss how our findings might be extended to higher organisms.

A four step model of cell intercalation

We characterized intercalation to be a four step process consisting of (1) pairing, (2) reaching around the lumen, (3) zipping and (4) termination. While for the termination a mechanistical model has been proposed (Jazwinska et al., 2003), the mechanistics of the other steps remain largely elusive.

Pairing is a logical prerequisite for the intercalation process as we describe it since it allows cells to slip in-between their neighbours without displacing them from the lumen. The actual intercalation process starts only after pairing. It is interesting to note that *sal* overexpression apparently blocks intercalation specifically at this step. Though, due to resolution limitations we can not rule out that some cells start to reach around the lumen in most cases the AJs clearly show the paired arrangement. To position cells in this paired arrangement also requires cell rearrangements. Yet, *sal* specifically regulates the cell rearrangements involved in intercalation and autocellular AJ formation, suggesting that they are mechanistically distinct from the rearrangements that occur before. We have so far no evidence for a regulation of pairing. Pairing may therefore be a passive process representing the energetically favorable arrangement under the given forces of the environment. Alternatively it is regulated by yet unidentified genes.

The actual steps of intercalation are “reaching around the lumen” and “zipping”. We have described them as two distinct steps. Yet, in principle zipping could also be regarded as a continuation of reaching around the lumen meaning that the same molecular events underlie both processes. This would mean that we would need to find a molecular

mechanism that would explain both movements. During the reaching around the lumen step, the shrinking of a common AJ between neighboring cells might pull the two ends of an intercalating cell around the lumen (Fig.27A). During the "zipping" process, however, it looks more like if the cell that forms autocellular AJ complexes does so at the expense of the intercellular AJ complexes it initially formed with the neighboring cell. This process does not intuitively resemble a junctional shrinking but rather a junctional zipping involving the remodeling of junctional proteins of one cell (the exchange of binding partners located on a neighboring cell with binding partners located on the same cell), accompanied by a relocalization/degradation of the unliganded junctional complexes of the neighbor (Fig.27B). The same mechanism could also account for the process by which cells reach around the lumen (Fig27C). In this case, one and the same cell would shrink its junctional surface at either the distal or proximal end, and by doing so induce both steps ("reach around the lumen" and "zipping") during the intercalation process.

To gain insight into the exact mechanisms by which cell intercalation occurs we follow

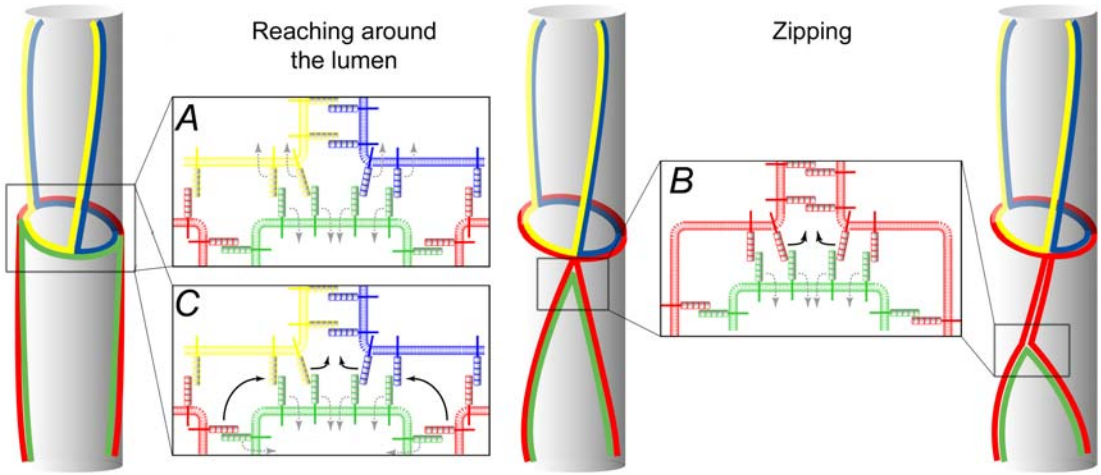

Figure 27 Speculative models for AJ remodelling.
(A) The "reaching around the lumen" might be mediated by the shrinking of a common AJ between neighbouring cells. (B) In contrast the "zipping" process might rely on the exchange of cadherin interactions between different cells. (C) A similar mechanism could also account for the "reaching around the lumen".

up a variety of different approaches. We want to establish pulse-chase labeling techniques that would allow to visualize how newly synthesized E-cadherin is incorporated into existing AJs during the intercalation process. Such methods are available but have so far only been used in cell culture (Griffin et al., 1998; Keppler et al., 2003). In the lab the protocols are currently adapted for a use in live *Drosophila* embryos and larvae (personal communication S. Lueders and E. Ellertsdottir). Similarly E-cadherin turnover at the AJs can be visualized using FRAP (fluorescence recovery after photobleaching). In the dorsal trunk we see that E-cadherin-GFP is reincorporated homogenously into the AJs (Movie10). We did so far not succeed to perform FRAP on intercalating dorsal branch cells as the laser we use cannot be focused on a small enough area.

We also analyze the tracheal AJs at an ultrastructural level (Fig.28) searching for differences in *sal* loss and gain of function situations. Additionally we want to make use of the single cell labeling system described above to analyze the behavior of the basal side of tracheal cells during intercalation. It has been proposed that in *C. elegans* the basal side is sending out protrusions which are then filled via cortical flow (Williams-

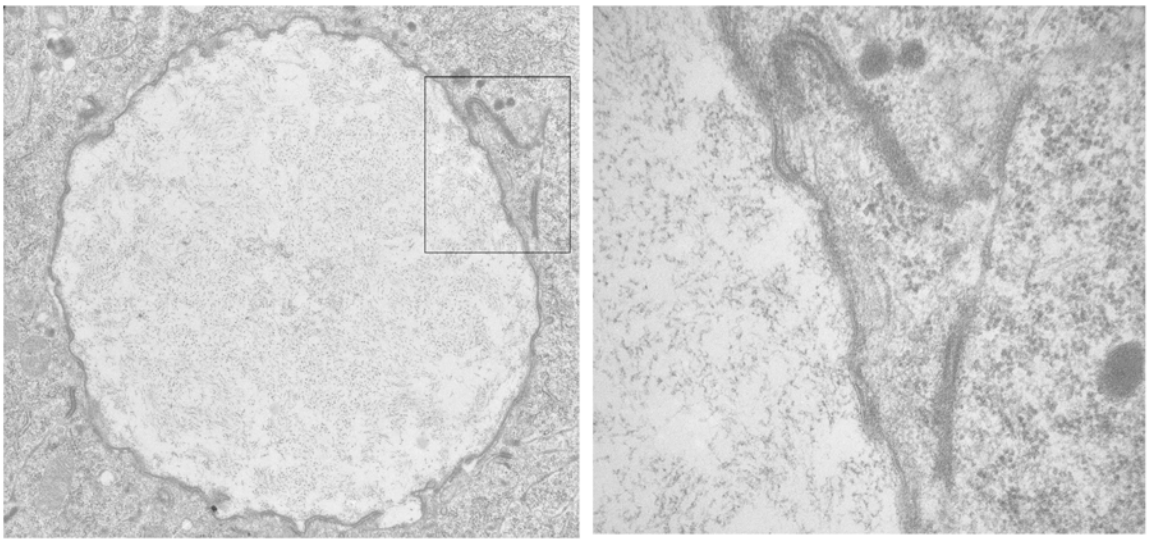

Figure 28 Ultrastructural analysis of tracheal cells during intercalation.
Tracheal lumen and AJs of tracheal cells in the transverse connective that overexpress Spalt.

Masson et al., 1998). We have preliminary evidence that this is not the case during tracheal cell intercalation as we do not observe these protrusions (data not shown). Finally we hope that the identification of mutants that impair the process will lead to a better understanding of the mechanism.

Comparison to cell intercalation during germband extension

As mentioned above epithelial cell intercalation drives germband extension and this process seems to depend on the asymmetric mutually exclusive localization of Non-muscle Myosin and Bazooka (Bertet et al., 2004; Zallen and Wieschaus, 2004). On an abstract level, the AJ rearrangements during this process are strikingly similar to the one occurring during tracheal development and it has been suggested that a similar mechanism might be at work (Lecuit, 2005). However, apart from these similarities there are also profound differences between the two systems. While the force driving intercalation during germband extension is most likely generated in the germband itself the situation for the trachea is much less clear. Though there seems to be some intrinsic force to intercalate as shown by the reduction of the pulling force, the external FGF signal is still strictly required for intercalation to occur (See also discussion below). Furthermore, we could by no means detect any asymmetric distribution of non muscle myosin in the trachea, though we still have to check whether Bazooka shows any localization inside tracheal cells. Thus it looks like different mechanisms are at work.

It has been proposed that the AJ remodeling events during germband extension are due to shrinkage of AJs. As discussed above it is difficult to describe the complete intercalation in the trachea by this means only.

Taken together, these considerations pose the question whether the morphological resemblance has any molecular parallels. It has actually been postulated already a long time ago that the type of AJ remodeling events described to occur during germband extension represent the paradigm of remodeling events during intercalation and that virtually any intercalation movement can be described in these terms on an abstract level (Weliky and Oster, 1990). Thus it looks like the uniting theme between the two processes

is only that they both represent intercalation movements but that nature has used a variety of different ways to drive and regulate these movements.

E cadherin levels and cell rearrangements

E-cadherin is a key component of epithelia. It organizes the AJs and physically mediates the adhesion among neighboring cells. Overexpression of E-cadherin leads to the aggregation of mesenchymal cells, while loss of E-cadherin results in the loss of epithelial properties and an epithelial to mesenchymal transition (Thiery, 2003). In contrast to this well established role in the establishment of epithelial character its role in epithelial remodeling is less well understood.

We have performed gain and loss of function analyses of E-cadherin and did not observe any effect on cell rearrangement and intercalation. Although we can not rule out that we did not modulate the range of E-cadherin expression enough to observe an effect it seems for sure that there is a wide range of E-cadherin levels that does allow proper cell rearrangements. Given these results it also seems unlikely that differences in E-cadherin levels control cell rearrangements as it has been shown in other systems (Bryant and Stow, 2004). To specifically address this question E-cadherin-levels have to be modulated in single tracheal cells using the single cell labeling system. To further clarify this question it is also necessary to closer examine molecules that are involved in the regulation of E-cadherin levels at the surface. We have solid data that p120 catenin does not have any influence on cell rearrangements. We also tested a zygotic mutation in a gene encoding a putative homologue of Hakai without observing any effect. However, we can not rule out that there is a maternal contribution. There are also other candidates to be checked. Src has been implicated in the regulation of E-cadherin levels via hakai (Fujita et al., 2002). Recently, double mutants in the two *Drosophila* src genes were shown to exhibit a tracheal phenotype (Takahashi et al., 2005). Also *abnormal wing discs* the homologue of the nucleoside diphosphate kinase NM23H, which is recruited by Arf6 to facilitate the internalization of E-cadherin (Palacios et al., 2002), exhibits tracheal defects (Dammai et al., 2003). Mutations in these genes have not been examined yet with regard to cell rearrangements. Additionally it may be worthwhile to recheck some genes more

carefully. It is possible that in some instances cell intercalation is not completely abolished, but is occurring less efficiently. For example, mutations in p120 catenin were recently shown to complete dorsal closure considerably slower than wildtype embryos (Fox et al., 2005).

Rac has been found to regulate levels of E-cadherin in the fly and has been proposed to regulate cell rearrangements during tracheal morphogenesis by regulating the incorporation of E-cadherin into the AJs (Chihara et al., 2003). Although we could confirm the dramatic effects elicited by the overexpression of dominant negative and dominant active Rac in the trachea, we found that these effects are not connected to the intercalation movements we describe. We see a loss of E-cadherin localization in both instances, yet this is not accompanied by ectopic autocellular AJ formation or a block in autocellular AJ formation. Thus it looks like tracheal cells loose their epithelial character and undergo EMT rather than undergoing a controlled regulation of cell rearrangement. This interpretation is supported by the fact that we observe strong cytoskletal dynamics upon overexpression of dominant negative Rac as it is often observed during an EMT.

Currently we do not know whether this phenotype indeed reflects the loss of function phenotype or whether it is an artifact of the dominant negative molecule. We do not observe the same effect in double mutants for *rac1* and *rac2*. Yet a third Rac like protein (*mig-2-like* (*mtl*)) is present in the *Drosophila* genome and the triple mutant has been shown to exhibit stronger defects than the double mutant (Ng et al., 2002). Unfortunately *mtl* is on another chromosome and we are currently not able to visualize these double balanced mutants with our GFP/RFP lines. At the moment we check the effect of the double mutant on AJ remodeling.

Other mechanisms to control cell rearrangements

Instead of controlling E-cadherin levels to control cell-rearrangements it would also be possible to control the adhesiveness of E-cadherin. It has been hypothesized that E-cadherin adhesion -similar to the integrins- might be controlled via inside-out signaling (Gumbiner, 2005). Although this is an interesting idea it is so far not clear which molecules would be involved in such a mechanism.

More evidence is available for a regulation of adhesion via the regulation of the interaction of E-cadherin with the cytoskeleton. The small GTPases Rac and Rho were implicated in this regulation (Braga et al., 1997). As discussed above we could so far not confirm a specific role of Rac in the cell intercalation movements we analyze.

We also see defects using dominant versions of RhoA (discussed above). Yet also in this situation the problem remains that the genetic loss of function phenotype does not resemble the phenotype obtained by using the dominant molecules.

Small GTPases of the Rho family are difficult to study. Due to their involvement in a large variety of cellular processes they tend to exhibit pleiotropic effects making an interpretation of the results difficult. Furthermore it is not clear which small GTPases can substitute for each other or which other small GTPases are affected using dominant molecules. Instead of studying the small GTPases themselves it might therefore be more informative to study molecules upstream or downstream of them.

In this context it is interesting that we find a RhoGEF that is specifically expressed in the trachea. Unfortunately we can not yet conclude whether or how a loss of function of this gene affects tracheal development. However, apart from the loss of function phenotype it will also be interesting to analyze the gain of function phenotype and the subcellular localization of the protein to find out whether this RhoGEF acts similar to TIAM that is localized to AJs.

In vertebrates convergent extension and intercalation depend on non-canonical Wnt-signalling (Wallingford et al., 2002). In *Drosophila* this pathway is well known to regulate planar cell polarity (PCP) and to rely on the asymmetric localization of some molecules such as Frizzled or Dishevelled (Mlodzik, 2002). We checked the loss of function of several genes that are implicated in PCP and are expressed inside or around the trachea such as *dachsous*, *fat* or *four jointed* without observing major tracheal defects. We also checked the subcellular localization of Frizzled and did not find it to be asymmetrically localized in tracheal cells (data not shown). Thus it looks like tracheal cell intercalation does not involve non–canonical Wnt-signalling.

Contribution of other junctions to intercalation

In this study we have focused our analysis on the AJs and on the subapical region. However epithelial cells are also connected via other structures. Septate junctions –the equivalent of the vertebrate tight junction- serve as a diffusion barrier. Gap-junctions connect neighboring cells and allow cytoplasmic exchange between them. Both of these structures are located at the baso-lateral side of the cells. During autocellular AJ formation, cells move from a side-by-side to an end-to-end configuration. During this process the area of baso-lateral contact appears to be minimized and it seems likely that extensive remodeling takes place in this area as well. It is so far not clear whether these junctions also interfere with the rearrangements we describe.

We have tested mutants of various septate junction components and did not find any intercalation defects. Therefore the septate junctions do not seem to be required for AJ remodeling. Yet, we have only tested loss of function situations so far. It may still be that intercalation can be blocked in a gain of function situation. In this context it is interesting that dominant negative Rho expressed in the trachea results in a phenotype, reminiscent of the loss of function phenotype of septate junction components. In contrast, dominant active Rho results in a block of autocellular AJ formation. Yet, the hypothesis that Rho regulates properties of the septate junctions remains to be tested.

We also do not yet know whether gap junctions and innexins play a role during AJ remodeling and cell rearrangements. However the innexins Ogre and Innexin2 are strongly expressed in the trachea (Stebbings et al., 2002) and for mutants in *innexin2* tracheal defects have been reported (Bauer et al., 2004). It will be interesting to see whether cell intercalation is affected in these mutants.

The role of hemiadherens junction for cell intercalation is also unclear. Hemiadherens-junctions are integrin-based structures. Integrins have been shown to specifically affect some tracheal branches (Boube et al., 2001), yet the dorsal trunk vs. dorsal branch development is unaffected in these mutants. Thus, it seems likely that these junctions do not play a general role during intercalation.

Screening for genes involved in tracheal cell intercalation

In a genetic screen we used the Exelixis deficiency kit to search for defects in tracheal cell intercalation upon removal of genes on the second chromosome. We blindly identified virtually all genes that have already been described to have a tracheal phenotype. Furthermore we have identified many other deficiencies that show tracheal phenotypes but do not include genes known to be involved in tracheal development. Among them is a candidate deficiency with specific tracheal intercalation defects (see also discussion below). Taken together, this shows that the design of the screen works well and it seems worthwhile to extend the screen.

One possibility would be to screen the other chromosomes. As described above the screen requires a fly line that carries a fluorescent balancer on the chromosome of interest and the α-catenin-GFP and RFPmoe on another chromosome. We tried to generate a fly line that would allow a screen of the 3rd chromosome but with the fluorescent balancers we had at hand we were not able to generate a viable double balanced line. We have recently received other balancer lines and are trying to establish a stable line with them. Another possibility is to use another set of deficiencies to increase the coverage of the genome. With the lines we tested we achieved coverage of around 50% of the second chromosome. There is an ongoing project that generates molecularly mapped deficiencies that are independent of the Exelixis lines we used (Ryder et al., 2004). Using these lines it would be possible to increase the coverage up to around 80%.

In addition it is important to complement the genetic approach with other approaches. We have screened for candidates based on their expression pattern. Yet a high fraction of the genes we tested does not exhibit any tracheal abnormalities despite the expression in the trachea. We also checked the genes that are reported to have a tracheal expression (Tomancak et al., 2002) and fall into one of the deficiencies we used in the screen. Out of six deficiencies that include the predicted genes CG15151, CG6055, CG16798, CG9336, CG16820 and CG7279 only the one including CG9336 exhibits a phenotype. This deficiency shows a convoluted dorsal trunk. However this phenotype is probably due to another gene deleted by the deficiency that has been described before to exhibit this defect (Beitel and Krasnow, 2000). Taken together it seems like many genes that are expressed in the trachea do not have a major function or act redundantly or generate a

loss of function phenotype that is not visible with the markers we used. A screen based on the expression pattern is therefore only of limited use.

Genes affecting cell intercalation

In addition to *sal* we have identified two transcription factors that affect intercalation. In mutants of *rib* and *pnt* no autocellular AJs form. Therefore these genes have an opposing effect to *sal*; they are allowing intercalation. For both genes our analysis is at an early stage.

We found that *rib* is not sufficient to induce remodeling ectopically when expressed in the trachea. This is not surprising as *rib* is anyway expressed throughout the trachea (Bradley and Andrew, 2001). So far we did not address the question whether we can rescue the intercalation phenotype by expression of *rib* in the trachea. Yet this seems likely, as the tracheal defects in *rib* mutants can be rescued by tracheal expression of *rib* (Bradley and Andrew, 2001). As *rib* is required for intercalation it would be interesting to know more about *rib* target genes. It would be possible that *rib* induces a factor allowing intercalation that is then repressed by *sal* in the dorsal trunk (or vice versa). Yet, a gene chip experiment designed to identify *rib* target genes did not identify a target gene with such an expression pattern (personal communication S. Luschnig). Therefore either the situation is more complex or the corresponding genes were not found in the screen.

The results for *pnt* are very recent and we so far only know that it is required for intercalation. We do not yet know whether the phenotype can be rescued or whether we observe an altered phenotype upon tracheal overexpression of *pnt*. However, as *pnt* is known to be a target of FGF signaling we have identified an interesting link between the FGF-pathway that is required for branch outgrowth and the *dpp*/*wg* signaling system that regulates intercalation. It is intriguing to speculate that there is a crosstalk between branch outgrowth and intercalation. It has recently been shown that both *btl* and *pnt* are required for the efficient expression of *kni* (Myat et al., 2005). Therefore the observed intercalation defect in dorsal branches could be due to a loss of *kni* causing ectopic expression of *sal* in dorsal branches. To clarify this we will check *sal* expression in *pnt* mutants. Nevertheless we also observe a block of intercalation in ventral branches. In

these branches intercalation does not depend on a *dpp* signal (Fig.4F in (Ribeiro et al., 2004)). A thorough analysis of the epistasis of *pnt* with the FGF-, *dpp*- and Wg- signaling systems with regard to intercalation will be required to better understand the role of *pnt* in tracheal development.

Candidates in the genetic deficiency screen

Many deficiencies in the screen show defects in tracheal development. A considerable number of these deficiencies is severely messed up making it likely that the tracheal phenotype is due to more general defects. The largest class of defects that is likely to be trachea specific is a convoluted dorsal trunk. A considerable number of such phenotypes has already been identified in another genetic screen (Beitel and Krasnow, 2000) and has in some instances been assigned to mutations in septate junction components (Wu and Beitel, 2004). It is, however, not clear how this phenotype can be explained by defects in the septate junctions. Recently it has been shown that genes involved in chitin synthesis also result in a similar phenotype and that intact septate junctions are required for the correct assembly of luminal chitin fibres (Tonning et al., 2005). This may explain the frequency of the phenotype and also why the defects are specifically seen in the trachea. It also enables us to guess a role of luminal chitin for tracheal development. The luminal proteins Pio and Dumpy, for example, are required to terminate the intercalation process (Jazwinska et al., 2003). Yet, none of the mutants that show the convoluted trachea phenotype and that therefore might be defective in their luminal chitin, shows intercalation defects. Thus it looks like chitin is needed to correctly shape the trachea but not for intercalation.

Another phenotype that is observed frequently and that looks fairly trachea specific are branch fusion defects. Branch fusion has been studied in some detail and a number of components necessary for fusion have been identified (Lee et al., 2003; Lee and Kolodziej, 2002; Tanaka-Matakatsu et al., 1996; Tanaka et al., 2004). In collaboration with H. Chanut we started a closer investigation of some candidate genes.

Finally, we identified a deficiency (Exel7010) that displays ectopic autocellular AJs in the dorsal trunk, while the overall organization of the trachea is not affected. We could

show that despite the phaenotypical similarity this is not due to an expansion of *kni* and that *sal* is still present in the mutants. Yet, especially in the anterior part of the embryo, where the phenotype is most prominent, Sal does not localize specifically to the nucleus any more. This may indicate that nuclear levels of Sal are not high enough to block autocellular AJ formation. Indeed, when overexpressing *sal* in the mutant we do block intercalation arguing that the mutation is upstream of *sal*.

An alternative explanation would be that in the mutant a *sal* dependent process is not working as efficiently as in the wildtype and that it therefore needs higher levels of Sal for this process to do its job. This would fit with the observation that anterior Sal levels in the dorsal trunk are generally lower than posterior ones.

As a matter of fact secretion of some luminal proteins is impaired in the mutants. Only little of the unknown protein that is detected by the 2A12 antibody reaches the lumen, while most of the protein is retained in the cytoplasm. As mentioned above luminal proteins are involved in blocking the intercalation process in the dorsal branch (Jazwinska et al., 2003). Thus it could be that the secretion of a luminal protein that has yet to be identified is reduced in the deficiency, causing the intercalation defects. In this context it is interesting that Pio –the luminal protein responsible for the block of intercalation in the dorsal branch- is secreted normally. These findings argue that the defects are not due to general secretion defects but selectively affect only some luminal proteins.

Identification of the candidate gene within the deficient region

The deficiency comprises 25 predicted genes and we tried to identify the gene that causes the tracheal phenotype. At first we tried to identify candidates via in situ hybridization. Although we did not positively identify a candidate with this approach, we can rule out some of the genes. It is possible that the genes for which we do not detect any embryonic expression are expressed and functional at extremely low levels. However it seems more likely that their absence not the cause for the phenotype. Also the three predicted genes that presumably encode one transcript that is expressed in the CNS and PNS are no likely candidates. The assembled transcript encodes a membrane bound molecule and the

expression is not in contact with the dorsal trunk. Therefore, among the genes we checked, the two predicted genes CG9967 and CG16995 and the gene Rab5 are likely candidates. Still, it is also possible that the loss of one or several of the proteases we excluded from the in situ analysis are causing the phenotype.

To further address this question we constructed a series of smaller deficiencies that delete parts of the original deficiency. We excluded a region that was assigned to be covered by another partially overlapping deficiency (Exel7009) we tested in the screen and which has a wildtype tracheal system. None of the deficiencies we generated showed a phenotype despite the fact that they cover the entire region that was not covered by the overlapping deficiency except for 200bp. There are three possible interpretations for this finding. It is formally possible that the cause of the phenotype resides in the 200 base pairs we did not cover. Yet, this seems unlikely as no transcript lies in this region. Another possibility is that more than one gene is responsible for the phenotype and one of the genes lies in the region we did not cover. This is well possible and there would be two obvious candidates for such a scenario. We see defects in cellular trafficking in the mutants and indeed we find two genes that are implicated in cell trafficking inside the deficiency. These genes are Rab5 and a COPII-binding protein. The COPII-binding protein lies in the region we excluded from the analysis and the partially overlapping deficiency that does not include Rab5 does not show the trafficking defects. Conversely Rab5 mutants alone do not display a tracheal phenotype (data not shown). These findings would be consistent with a model in which the loss of both genes is required to generate the trafficking defect and the abnormalities at the AJs.

The third possibility is that the partially overlapping deficiency is wrongly mapped. Indeed we could not confirm the annotated insertion by PCR. Additionally, we have found that though the gene *aop* is supposed to be deleted in the deficiency, the mutants do not show an *aop* phenotype. Thus, Exel7009 was not mapped correctly. At the moment we are generating in situ probes to test which of the genes deleted in Exel7010 are also deleted in Exel7009 and how the genes in the overlap region are expressed. We also generate an independent deficiency that is based on confirmed insertions and that deletes the region of the overlap (including the 200bp that have so far not been included),

to test whether it displays the tracheal phenotype. If this was the case the COPII binding protein alone is a strong candidate due to the secretion defects observed.

Characterizing the forces that drive intercalation

As we aim to understand branching and intercalation on a mechanistic level, we need to understand the nature and the source of the forces driving these processes. To this end we try, on the one hand, to identify the molecules that mediate *sal* function and block the intercalation process. On the other hand we also need to understand the forces that drive intercalation. As mentioned above, these forces can either be generated cell autonomously by the intercalating cells or by the leading cells that respond to FGF and guide branch outgrowth.

At the moment we have conflicting evidence on this question. Like discussed above intrinsic forces generated by non muscle myosin do not seem to play a role for tracheal cell intercalation. On the other hand we also have evidence that branch outgrowth is not the driving force of intercalation as branches that grow less or include more cells still intercalate normally. However, these situations are not easy to interpret as they rely on mutations in signaling pathways that also interfere with tracheal development. To circumvent these problems we will try to laser-ablate the leading cells or cut the branches during branch outgrowth and monitor the effect on intercalation in the stalk cells (personal communication E. Caussinus).

Alternatively, the forces could be generated by the pressure of the surrounding tissue. Indeed, dorsal branches have been shown to grow through a narrow path flanked by mesoderm and intercalation is initiated as the cells enter the narrow region(Franch-Marro and Casanova, 2000). Yet, as we can block intercalation by tracheal expression of *sal* this force is clearly not sufficient to drive intercalation. To test whether the force is required we would need to monitor intercalation in embryos with defects in the mesoderm. Unfortunately mesoderm mutants also exhibit severe tracheal phenotypes (Franch-Marro and Casanova, 2000) due to the multiple requirements of the mesoderm as a source for signals, as for example the FGF signal (Merabet et al., 2005).

Direct tests for forces are technically demanding and to apply them in whole embryos is almost impossible. The development of tools that show fluorescence in response to physical forces may facilitate such an analysis. At the moment, however, only indirect evidence for forces can be collected. The most promising approach to get hands on the forces at the moment is probably to identify genes that interfere with intercalation and to guess their contribution to the force based on their phenotype, their expression pattern and subcellular localization.

AJ-remodeling during tubular organ formation in higher organisms

Epithelial remodeling and intercalation are central processes in the shaping of an embryo. We have used the *Drosophila* tracheal system as a model system to study these processes during tubular organ formation. We have found that intercalation is this system is coupled to the formation of autocellular AJs, leading to morphological distinct branches. The branches that undergo intercalation become thin and long, while the other branches stay shorter and thicker. Virtually any organ that is formed via branching morphogenesis consists of thicker main branches and smaller terminal branches. At the moment it is not clear whether morphologically distinct branches in these organs are formed in a similar way. In principle there are two different ways to generate new epithelial branches out of existing ones. Either this is done by budding as described in this study or by the migration of a group of non-epithelial cells away from the initial branch, followed by secondary lumen formation (Hogan and Kolodziej, 2002). These examples are not mutually exclusive. An organ can be generated by a combination of both mechanisms. Also in the tracheal systems both mechanisms are used. While dorsal branches, ganglionic branches visceral branches and others are formed via budding, the terminal branches (where the actual gas exchange is happening) are formed via de novo formation of lumen (Samakovlis et al., 1996). The two types of branches can be easily distinguished based on their AJs. Branches that arose via budding display autocellular AJs as described above. Branches that arose via de novo lumen formation do not show any AJs lining the

lumen. This characteristic can be used to find out which branches in a given organ arise by which mechanism.

The formation of the vascular system in the zebrafish trunk has been characterized in detail and is strikingly similar to tracheal development on the morphological level (Isogai et al., 2003). Yet, the AJ complexity of the branches has not been analyzed. In a pilot experiment we wanted to gain first insight into the mechanism by which these branches are formed. We reasoned that during budding the vessels immediately form a lumen, while in the other case the lumen is only formed later. In collaboration with A. Vogel we injected Rhodamin-dextrane into the heart of live zebrafish embryos that express GFP in the vascular system and monitored the distribution of rhodamin with respect to GFP using confocal microscopy. We found that the small vessels did not contain a lumen

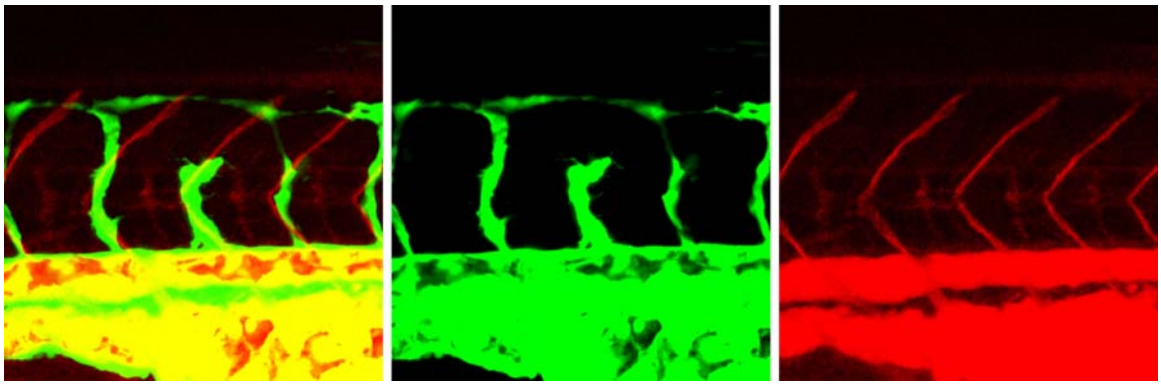

Figure 29 Intersegemental vessels in the zebrafish do not have an open lumen during vessel outgrowth.
Injection of rhodamin-dextrane into the heart of live zebrafish embryos that express GFP in all cells of the vascular system shows that branch outgrowth precedes the formation of an open lumen in intersegmental vessel.

during their outgrowth (Fig.29) arguing that they form the lumen secondarily. An exhaustive analysis of the complexity of the AJs in the vascular system is underway (personal communication H.G. Belting E. Ellertsdottir and Y. Blum). This will answer the question which vessels arise via which mechanism. It will also be interesting to analyze the AJ complexity in other branched organs like the lung and the kidney as this immediately implies a mechanism for their generation.

Remodeling epithelial tubes via cell rearrangements

From cells to molecules

Marc Neumann and Markus Affolter

Submitted to EMBO reports as a concept paper

Summary

Epithelial cell movements such as those that occur during cell intercalation largely contribute to the formation of epithelial structures during the morphogenesis of multicellular organisms. Since the architecture of epithelial tissues relies on strong adhesion between cells at adherens junctions (AJs), intercalation or rearrangements of epithelial cells might be controlled by modulating the adhesion dynamics of the AJs by internal or external forces. We describe recent progress in understanding cell rearrangements during epithelial tube remodeling, and discuss a number of models that might account for the developmental control of the spatial dynamics of AJs.

Introduction

During development and homeostasis, epithelial tissues are remodeled extensively to account for their structural needs. In some cases, tissue morphogenesis is dependent on changes in either cell shape or oriented cell division. In other cases, morphogenesis is accompanied by cells exchanging their neighbors through "intercalation". Different types of intercalations (radial intercalation, axial intercalation) have been described and are at the heart of the restructuring of early embryos before and during gastrulation (Keller, 2002). The importance of cell intercalation in epithelial remodeling in development in general and in morphogenesis in particular has been recognized decades ago (Fristrom, 1988), but molecular scenarios underlying the astonishing capacity of epithelial cells to remodel while remaining tightly attached to each other via adherens junctions (AJs), and molecular mechanisms controlling the extent of remodeling, have only started to unveil in a few well studied cases (Gumbiner, 2005). Here, we briefly discuss emerging cellular mechanisms and molecules involved in the remodeling of epithelial tubes via cell intercalation, a process that has recently been described in the *Drosophila* tracheal system by a combination of live imaging, genetic and cellular assays. Whether similar mechanisms remodel epithelial tubes in other tissues and/or organisms remains to be investigated, but parallels to cell intercalation in more simple situations are apparent.

Epithelial remodeling in tubulogenesis

Over the past few years, a number of laboratories have tried to answer the question of how the ordered formation of distinct tracheal tubes is orchestrated during embryonic development in *Drosophila*. It has been known for quite some time that starting from epithelial invaginations called tracheal placodes, tracheal cells migrate towards localized sources of the secreted ligand Branchless/Fgf (Bnl/Fgf) (Sutherland et al., 1996) by forming dynamic filopodial and lamellopodial extensions from their basal side (Ribeiro et al., 2002). The developmentally controlled expression of Bnl/Fgf in the *Drosophila* embryo prefigures the direction of branch formation, and in a first phase, bud-like epithelial outgrowths are formed, extending away from the sac present at the onset of the process (reviewed in (Affolter et al., 2003; Ghabrial et al., 2003; Uv et al., 2003). Tracheal cells keep their adhesive contacts throughout the morphogenetic process; the apical side of the tracheal cells faces the luminal side and will later be covered by cuticle structures. Since tracheal cells do not divide after invagination, the morphological transformations that accompany branch outgrowth and elongation are brought about by cell shape changes and cell intercalation.

The tracheal network formed via branching morphogenesis consists of tubes of different cellular composition (Samakovlis et al., 1996; Uv et al., 2003). Large tubes are made of several cells wrapped around the lumen, with more than one cell contributing the apical side to the luminal circumference. Cells in such tubes are held together by intercellular AJs, established at a subapical position between neighboring cells (Fig.1 A,B). Finer tubes consist of single cells wrapped around the lumen. Most of the AJ in such tubes represent autocellular AJ; they seal single cells along the lumen. To maintain this chain-like alignment of tube cells, ring-shaped intercellular AJs connect adjacent cells (Fig.1C). The finest tubes at the periphery of the tracheal system are seamless, intracellular tubes, which lack AJ complexes along the lumen (Manning and Krasnow, 1993; Samakovlis et al., 1996).

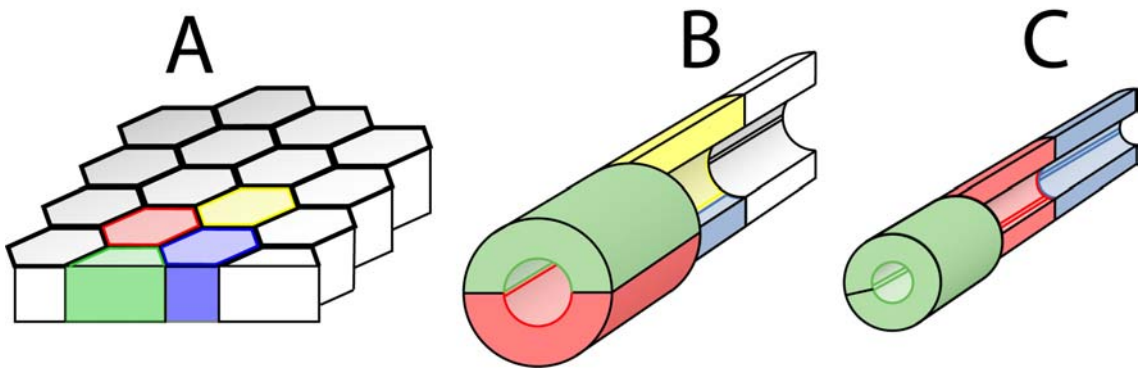

Figure 1 Cellular architecture of epithelial tubes
(A) All tubes of the tracheal system originate from a flat epithelial sheet. By invagination, this flat epithelium is transformed into an epithelial sac from which epithelial tubes form via cell migration, cell intercalation and cell shape changes. (B) Initially, cells in larger tubes retain their intercellular AJs connecting them to their neighbours. In such cases, several cells make up the circumference of the lumen. (C) In certain branches, cells intercalate and eventually transform most of their intercellular AJs into autocellular AJs. In these cases, single cells make up the circumference of the lumen.

Recent studies taking advantage of methods that allow the imaging of the outline of individual cells *in vivo* in real time during branch elongation started to provide significant insight into how cell intercalations transforms the epithelial sheet into tubes of different cellular architecture. In particular, these studies have shown how larger tubes with intercellular AJs are remodeled into finer tubes with mostly autocellular AJs via cell intercalation, a process which must be accompanied by dramatic rearrangement of the AJ complexes.

Tube remodeling occurs via distinct steps

By following the rearrangement of AJ during tracheal remodeling *in vivo* with the help of an α–Catenin-GFP protein, which specifically labels the AJ complexes in *Drosophila* (Oda and Tsukita, 1999a), a number of distinct steps have been identified during the process of tube elongation (Jazwinska et al., 2003; Ribeiro et al., 2004); see Fig.2). Starting from a bud-like extension, tracheal cells first appear to align in a pair-wise fashion along the tube, with two cells making up the luminal circumference in a cross

section, a process we referred to as pairing (step 1). Pairing appears to precede intercalation, and such an arrangement is conceptually critical since it allows cells to "squeeze" in-between their neighbors. Upon pairing, cells start to intercalate. The intercalation process is accompanied by extensive AJ remodeling, and we have subdivided this phase into three distinct steps. At the onset, one of the two neighboring cells starts to reach around the lumen (step 2), a process that ultimately leads to the formation of the first autocellular contact and the formation of the first autocellular AJ, as a cell touches its own membrane extension at the opposite side of the tube circumference. For intercalation to proceed properly both of the paired cells eventually reach around the lumen but they do so at opposite ends, one cell on the proximal side and its neighbor on the distal side along the axis of elongation. Once the initial autocellular AJ contact has been established, cells appear to zip up or extend their autocellular junctions by continuously replacing intercellular AJ complexes with autocellular AJs in a process referred to as zipping (step 3). During this zipping, cells transform most of their AJs into autocellular AJs, and only small, ring-like intercellular AJ remain intact and connect neighboring cells. To ensure that this contact remains intact and holds the cells together in the head to tail arrangement, the zipping process has to be stopped before it goes to completion and leads to the complete loss of intercellular AJs (termination (step4)).

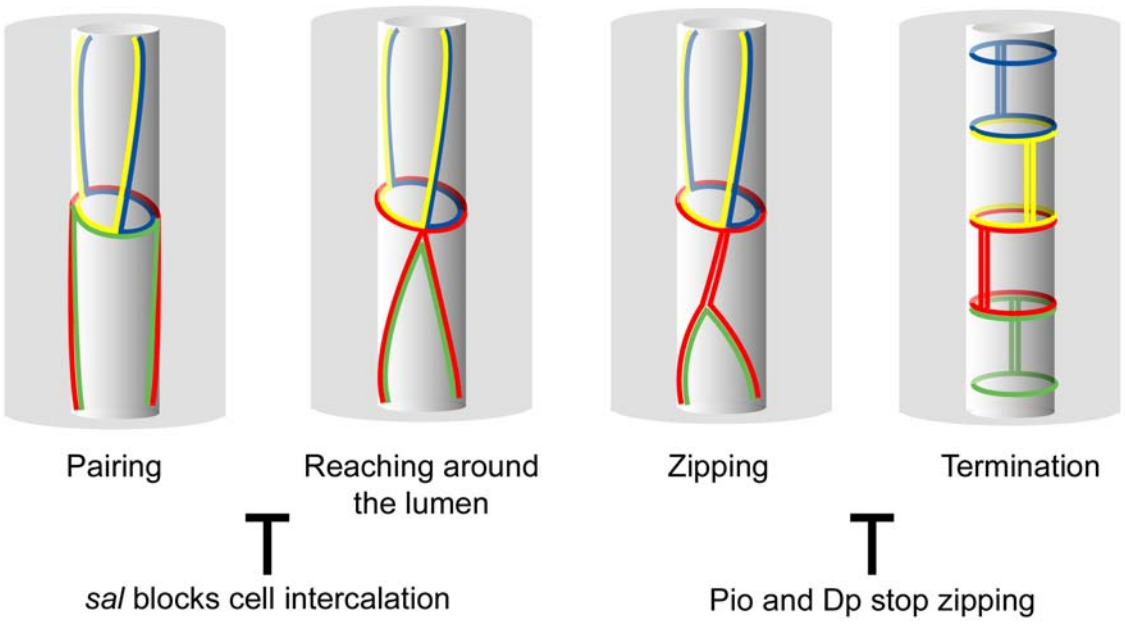

Figure 2 Steps of AJ remodelling during cell intercalation and tube elongation.
At the onset of intercalation, cells are paired (**pairing**). Upon pairing, one cell reaches around the lumen with its apical surface leading to the formation of the first autocellular AJ contact (**reaching around the lumen**). Starting from this initial autocellular contact, conversion of intercellular AJs into autocellular AJs proceeds via a process that resembles a zipping mechanism (**zipping**). The zipping process is stopped by proteins (Piopio (Pio) and Dumpy (DP)) that are deposited in the tracheal lumen (**termination**). The entire intercalation-process can be blocked by *spalt* (*sal*).

Cell intercalation is genetically controlled during tracheal morphogenesis

Using this four-step model as a conceptual framework, a variety of questions needs to be answered to better understand how cell intercalation is controlled during tube formation. Where do the forces that trigger cell intercalation come from? What are the molecules that are implicated in exerting or regulating the different steps of intercalation? Why do certain branches undergo intercalation while others do not?

In the last decade, many genes involved in tracheal development have been identified. A number of interesting observations were made when the functions of these genes were re-examined with regard to intercalation. It was shown that the intercalation process can be blocked by the expression of the zinc finger transcription factor Spalt (Sal) in groups of tracheal cells (Ribeiro et al., 2004). In fact, the *Drosophila* embryo makes use of this transcription factor to inhibit cell intercalation in the dorsal trunk; as a result of this

inhibition by Sal, the dorsal trunk remains a large, multicellular tube entirely consisting of cells sharing intercellular AJs with neighboring cells (Kuhnlein and Schuh, 1996; Ribeiro et al., 2004). The expression of *sal* is induced by Wnt signaling in dorsal cells of the tracheal sac (Chihara and Hayashi, 2000; Llimargas, 2000). In a few of the dorsal-most cells that ultimately form a neighboring, finer branch, the dorsal branch, *sal* transcription is turned off by the transcription factors Knirps and Knirps-related, which are themselves induced by *dpp* signaling in these dorsal-most tracheal cells (Chen et al., 1998). Therefore, the Wnt and *dpp* signaling systems generate two distinct groups of tracheal cells. One group lacks Sal and undergoes intercalation by proceeding with steps 2 to 4 (Fig.2 reaching around the lumen, zipping and termination), generating an elongated tube with autocellular AJs. The other group of cells in the dorsal trunk can not initiate the intercalation process due to the presence of Sal and thus remains in a multicellular arrangement (Ribeiro et al., 2004). The important role of the Sal transcription factor in the developmental control of intercalation obviously asks for the identification of those genes that are regulated by Sal in an attempt to better understand, at the molecular level, how their products interfere with cell intercalation and AJ remodeling.

Little is known about molecules which could be involved in cell pairing (step 1), in cells reaching around the lumen (step 2) or in the zipping process (step 3). However, it seems likely that the regulation of adhesion is crucial for these steps to occur properly. Although many proteins are involved in the establishment and maintenance of epithelial cell-cell contacts, E-cadherin is probably the most important protein for the formation of tight intercellular adhesion. E-cadherin is a single-pass transmembrane protein, in which the extracellular domain forms homophilic transdimers between adjacent cell membranes. The cytoplasmic domain interacts with p120 catenin and β-Catenin and with Hakai, an ubiquitin-ligase. β -Catenin binds to α-Catenin, which in turn associates with actin filaments. The anchoring of Cadherin-Catenin complexes to the actin cytoskeleton contributes to the strong adhesiveness of cadherin-based cell-cell contacts, and must presumably be modulated during cell rearrangements. Regulation could occur at many levels, for example by the control of E-cadherin turnover or recycling, by the modulation of the interaction of E-cadherin with the cytoskeleton, or by the regulation of adhesive

strength via inside-out signaling (reviewed in (Bryant and Stow, 2004; D'Souza-Schorey, 2005; Gumbiner, 2005). Promising candidates to analyze with regard to the intercalation process would be Src that has been shown to induce dissociation of epithelial cells and Hakai, an E3-ubiquitin ligase targeting E-cadherin (Fujita et al., 2002) or Arf6, a GTPase that mediates the internalization of E-cadherin (Paterson et al., 2003). Candidates implicated in the regulation of the interaction with the actin cytoskeleton are, for example, the small GTPases Rho, Rac and Cdc42 (reviewed in (Fukata and Kaibuchi, 2001)) and the Ras family member Rap1 (Hogan et al., 2004; Price et al., 2004). In addition, various components of the AJ-complex itself, including α- Catenin, β- Catenin and p120 catenin, may have specific functions in the regulation of intercalation.

Interestingly, mutations in genes encoding some of these molecules show tracheal defects. The *Drosophila* homologue of the nucleoside diphosphate kinase NM23H, which is recruited by Arf6 to facilitate the internalization of E-cadherin (Palacios et al., 2002), shows defect in all tracheal branches (Dammai et al., 2003). Also double mutants in both *Drosophila* Src genes show tracheal defects (Takahashi et al., 2005). In addition, the small GTPase Rac1 has been shown to influence cell rearrangements during tracheal development (Chihara et al., 2003). These phenotypes have not been analyzed yet in detail with regard to cell rearrangements, making it difficult to relate the defects to different steps of intercalation. In addition, Rac and Src affect diverse cellular function, making it difficult to assign direct and indirect roles on the adhesive state of tracheal cells.

The identification of two other mutations, however, provided significant insight into the last step of the intercalation process, the termination of the conversion of intercellular AJs into autocellular AJs (Jazwinska et al., 2003). Two genes, *piopio* (*pio*) and *dumpy* (*dp*) were shown to be required for the integrity of the fine, autocellular AJ-containing branches; in the absence of either *pio* or *dp*, all fine tubes were transformed into epithelial cysts, disconnected from the multicellular tubes in the embryo. No obvious defects were observed in the multicellular as well as in the intracellular, seamless tubes in these two mutants. Both *pio* and *dp* encode Zona Pellucida (ZP)-domain-containing proteins produced by all tracheal cells and secreted apically into the luminal space. Since it has been shown that several ZP domains trigger the formation of extracellular filaments

(Wassarman et al., 2004), it was proposed that Pio and Dp might form rigid heteromeric filaments deposited in the lumen; such filaments could provide a physical barrier and hinder tracheal cells to continue the zipping process to the very end. Live imaging of the disruption process in the mutant conditions indeed supports such a model (Jazwinska et al., 2003).

What about the role of other proteins linking neighboring tracheal cells, such as septate junction and desmosomal proteins, in cell intercalation during tube elongation? Quite a large number of proteins localizing to the lateral membrane of tracheal cells have been identified in the past few years and many of them display an irregular tube size (Bauer et al., 2005; Wu and Beitel, 2004). Whether these molecules influence the intercalation process remains to be shown.

A model for AJ shortening during cell intercalation in the tracheal system

As outlined above, the transformation of an epithelial sheet into a network of distinct tracheal tubes requires extensive AJ remodeling, in particular during cell intercalation. Yet, AJ contacts between neighboring cells have to be maintained such as to keep cells attached to each other and form an interconnected, tubular network throughout the rearrangement procedure. Relatively little is known about how epithelial cells physically exchange their neighbors in a coordinated manner, and which molecules are involved in and control this process.

Two recent studies, however, have started to shed some light on these issues (Bertet et al., 2004; Zallen and Wieschaus, 2004). During *Drosophila* gastrulation cell intercalation is used to elongate the body axis. It has now been shown that this intercalation depends on the differential localization of at least two molecules. Myosin II is localized in the vicinity of AJs oriented along the dorsal-ventral axis, while Bazooka is excluded form these junction but present on the junctions oriented along the anterior-posterior axis. It turns out that Myosin II and its activation by Rho kinase is required to destabilize and shorten the AJs oriented along the dorsal-ventral axis; in contrast, Bazooka might stabilize the other AJs.

On an abstract level, the AJ remodeling events in epidermis of the early fly embryo have been proposed to resemble the AJ rearrangements during cell intercalation in the tracheal system described above (Lecuit, 2005) (compare Fig 3 A-C with the corresponding tubes shown below) and it has been hypothesized that similar mechanisms drive these two intercalation processes.

Apart from these apparent similarities, there are also profound differences between the two systems. While the forces that control the axial extension of the germ band in the *Drosophila* embryo are cell intrinsic and might be spatially displayed via the localization of Myosin II, the forces driving tracheal cell intercalation most likely originate from the migration of tip cells away from the sac-like structure towards the more distant sources of Bnl/Fgf, producing a pulling force exerted upon the attached, non-migrating cells. It is not known whether this pulling force is the only force tracheal cells experience during the intercalation process, but clearly there is no cell-autonomously driven intercalation in the absence of Fgf signaling. Indeed, it has been shown previously that application of external force can be sufficient to induce intercalation of epithelial cells in Xenopus explants (Beloussov et al., 2000).

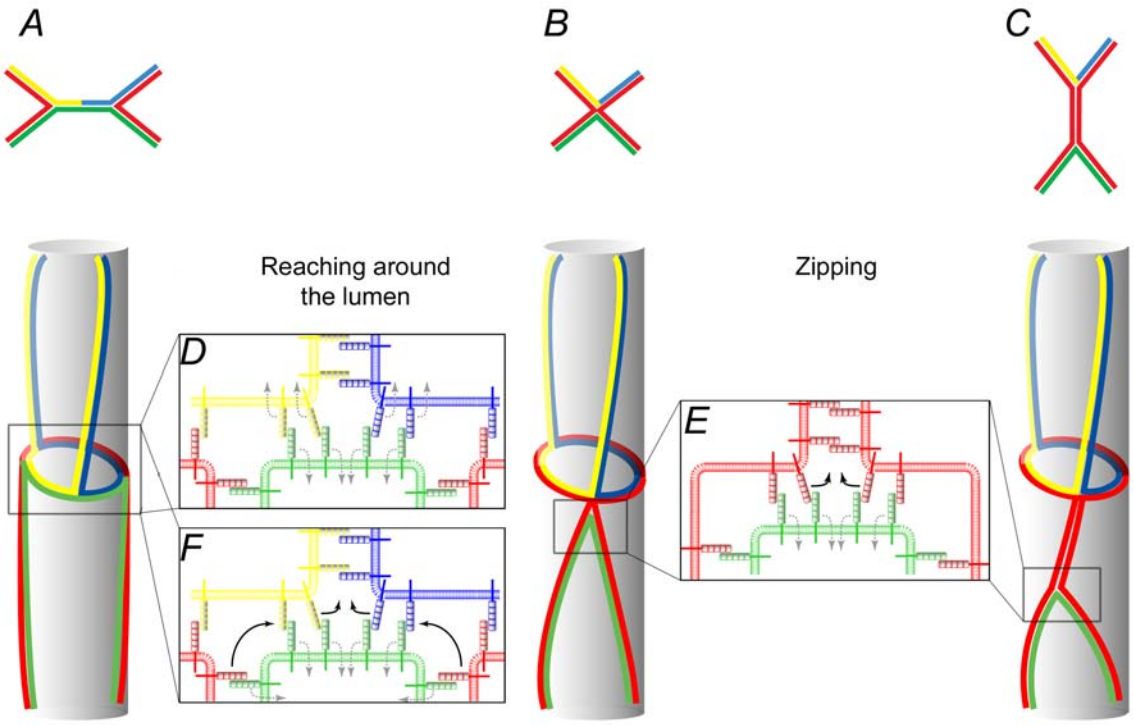

Figure 3 Speculative models for AJ remodelling
(A-C) Stages of AJ remodelling during germband extension as proposed in (Bertet et al., 2004) (note that A-C are drawn with anterior being up). The AJs are coloured to correspond to the tracheal AJs. (D) Analogous to this model the "reaching around the lumen" might be mediated by the shrinking of a common AJ between neighbouring cells. (E) In contrast the "zipping" process might rely on the exchange of cadherin interactions between different cells. (F) A similar mechanism could also account for the "reaching around the lumen".

Despite the apparent differences in the force-producing mechanism, we have schematically compared the remodeling of AJs during germband extension and tracheal tube morphogenesis. In analogy to germ band extension, the shrinking of a common AJ between neighboring tracheal cells might pull the two ends of an intercalating cell around the lumen (Fig.3D). In this particular scenario, the cell pairing with the intercalating cell shrinks its common AJ with the two cells sitting above it in the tubular arrangement, leading to an AJ arrangement similar to Fig.3B. During the "zipping" process, however, it looks more like if the cell that forms autocellular AJ complexes does so at the expense of the intercellular AJ complexes it initially formed with the neighboring cell. This process does not intuitively resemble a junctional shrinking but rather a junctional

"zipping" involving the extracellular remodeling of junctional complexes of one cell (the exchange of the homophilic Cadherin binding partners located on neighboring cells for Cadherin molecules located on the same cell), accompanied by a relocalization/degradation of the unliganded junctional complexes of its neighbor (see Fig.3E). In principle, the same mechanism could also account for the process by which cells reach around the lumen (see Fig.3F). In this case, one and the same cell would shrink its junctional surface at either the distal or proximal end, and, by doing so, induce both steps ("reaching around the lumen" and "zipping") during the intercalation process. In molecular terms, it is thus possible that somewhat different mechanisms are at work during germband extension and tracheal cell intercalation. Other models for epithelial rearrangements, in which intercalating epithelial cells behave similarly to mesenchymal cells and form lateral protrusions in-between individual cells, have also been proposed (cortical tractor model; see (Jacobson et al., 1986; Williams-Masson et al., 1998).

At present, most of these models explaining cell rearrangement in tightly adhering epithelial sheets are rather speculative. To better understand the events that occur at the AJs during cell rearrangements, it will be essential to molecularly dissect the process using genetic and reverse genetic approaches. In addition, it might be essential to introduce novel molecular tools into well-defined systems such as the ones described here. Pulse chase labeling of AJ proteins during intercalation would be very helpful to get a better view at AJ dynamics and remodeling in different situations. Such methods are in principle available (Griffin et al., 1998; Keppler et al., 2003), but have not yet been well adapted for applications in living multicellular organisms. In addition, the dynamics of the lateral membranes have to be investigated in single intercalating cells in order to find out whether this membrane compartment actively forms protrusive activities, or participates in the process relatively passively. Using these and other approaches will eventually provide a molecular view of epithelial remodeling, allowing both for an appreciation of an astonishing biological process and for an eventual interference with the process in certain situation, be it experimental or clinical.

Materials and methods

Drosophila strains

The followoing fly strains were used in addition to the ones explicitly mentioned in the text: $Lac^{BG01462}$ (Llimargas et al., 2004); $mega^{Goo44}$ (Behr et al., 2003); $sinu^{06524}$ (Wu et al., 2004); sqh^{AX3} (Jordan and Karess, 1997); zip^{IIX62} (Young et al., 1993); UAS-slamHA (Lecuit et al., 2002); UAS tau-GFP, UAS-GFPzip (A. Brand unpublished); $p120ctn^{308}$ (Myster et al., 2003); UAS-E-cadherin-GFP (UAS DEFL 6.3) (Oda et al., 1998); *btl-Gal4* (Shiga et al., 1996); UAS-GFP-actin (Verkhusha et al., 1999); UAS-*Dα-cat-GFP* (Oda and Tsukita, 1999a); UAS-*sal* (Kuhnlein and Schuh, 1996); *UAS-GFPN-lacZ (2-1)* (Shiga et al., 1996); UAS-*kni* (Chen et al., 1998); UAS-tkv^{QD} (Haerry et al., 1998); *Df(5)* (removing *sal* and *salr*) (Barrio et al., 1999); UAS-*dad* (Tsuneizumi et al., 1997); btl^{LG19} (Klambt et al., 1992); UAS-*btl* (Dossenbach et al., 2001); UAS-torso-*btl* (Dominant active) (Reichman-Fried et al., 1994); aop^{1} (Rogge et al., 1995); $Rab5^{2}$ (Wucherpfennig et al., 2003); shg^{2} (Uemura et al., 1996); UAS-HA-CA16, CA16 null-mutant (C. Dahmann unpublished); $Rac1^{J10}$, $Rac2^{\Delta}$ (Ng et al., 2002); Drac1L89, Drac1N17, Drac1V12 (Luo et al., 1994); $RhoA^{720}$ (Strutt et al., 1997)

Drosophila genetics

To obtain labeled tracheal flipout clones *hs flp; btlenhancer>y^{+}>Gal4, UAS*-D*α-cat-GFP; btlenhancer-mRFP1-moe* or *hs flp; btlenhancer>y^{+}>Gal4, UAS GFP-actin; btlenhancer-mRFP1-moe* (see below) embryos were collected overnight at 18°C, heat shocked for 30min at 37°C and raised at 25°C for 5-12h. For single cell overexpression these lines were crossed to *UAS-sal* or *UAS* tkv^{QD} and the effect was monitored at least 9h after the heatshock.

For the single cell rescue of *btl* mutant embryos the following cross was performed and the progeny was subjected to a similar heatshock regime*: hs flp; btlenhancer-mRFP1-moe; UAS-btl,* btl^{LG19} *x btlenhancer>y^{+}>Gal4, UAS-actinGFP;* btl^{LG19}.

Embryos lacking Dpp and Wnt signaling in the trachea were generated by first crossing *arm*^{XM19} (an allele affecting only the signaling functions of Arm) virgins to *btl-Gal4, UAS-*D*α-cat-GFP#8* or *UAS-GFPN-lacZ (2-1)/CyO; btl-Gal4 (3-1)/TM3, Sb, Ser* males. Virgins carrying the *arm*^{XM19} allele and the reporter constructs were then crossed to males of a homozygous *UAS-Dad* line. Embryos lacking Dpp and Wnt signaling in trachea were recognized by the expression of the reporter constructs and the lack of dorsal trunk formation.

Cloning

To generate *btlenhancer>y*$^{+}$*>Gal4,* the P[B123] fragment upstream of the *btl* gene (Ohshiro and Saigo, 1997) was amplified by PCR and subcloned upstream of the *Gal4* sequence into pP{Car20.1} whose *ry*$^{+}$ gene was deleted. A flip-out cassette containing the *y*$^{+}$-gene (Basler and Struhl, 1994) was then inserted between the enhancer and the *Gal4* CDS.

To generate *btlenhancer-mRFP1-moe, mRFP1* (Campbell et al., 2002) was amplified by PCR and cloned upstream of the actin binding domain of *moesin* (Ohashi et al., 2002). This construct was cloned into pP{CaSper} carrying the P[B123] fragment.

To generate a *spaghetti squash* GFP fusion under UAS control we amplified *sqh*GFP form transgenic flies (Royou et al., 2004) and cloned it into pUAST.

To generate a *zipper* GFP fusion we amplified the zip coding sequence (Young et al., 1993) from a cDNA of the short isoform lacking the first 45 amino acids and cloned it downstream of GFP. The resulting fusion was then cloned into pUAST.

To generate CA229GFP we amplified the CA229 coding sequence from the EST clone GH11627 and cloned it upstream of GFP. The resulting fusion was then cloned into pUAST.

To generate the Spalt deletion costructs we first generated pUAST-V5-NLS. To this end we inserted a nuclear localization signal into pUAST-V5 (see Thesis B. Hartmann). The different Spalt-deletion constructs were obtained by PCR form a cDNA (Kuhnlein et al., 1994) and then cloned into pUAST-V5-NLS.

Immunohistochemistry and whole-mount in situ hybridization

The following primary antibodies were used: a rabbit anti-Sal antibody (1:20) (Kuhnlein et al., 1994) a tracheal lumen specific mouse monoclonal antibody IgM 2A12 (1:20, provided by N. Patel) and mouse anti-GFP antibody (1:500; Roche), a rabbit anti-Pio antibody (1.20) (Jazwinska et al., 2003), rat anti-HA antibody (1.500; Roche) and anti-V5 antibody (1:500; Invitrogen). Embryos were fixed and immunostained as described before (Patel, 1994) with minor modifications.

In situ hybridization was performed as described before(Tautz and Pfeifle, 1989) with minor modifications. Templates for the probe generation were usually obtained by PCR and ranged in size from 200 to 1000 base pairs. To decrease the background the probe were hydrolyzed as described before (Cox et al., 1984) with minor modifications.

Time-lapse Confocal Microscopy

Embryos expressing the *GFP* construct of interest were collected overnight, dechorionated for three minutes using 3-4% chlorax and mounted in 10s Voltalef oil using the hanging drop method. Images were collected on a Leica TCS SP2 confocal system using the Leica Confocal Software (Version 2.5). For excitation, the 488nm emission line of an Argon laser and the 568nm emission line of a Krypton laser were used. The spacing of the focal sections was chosen in order to comply with the critical sampling distance of the objective.

Deconvolution, 3D and 4D reconstructions

Images were deconvoluted using Huygens Essential (Version 2.3.0) from SVI and subsequently processed using the Volocity 2.61 software (Improvision) or the Imaris 4.0.4 software (Bitplane) or later. Some images were treated with Photoshop (Adobe) to enhance the contrast.

Dissociation of embryos for FACS

Dechorionate the embryos in 3-4% chlorax for 4'. Collect them in a mesh and rinse them with water. Add 1 ml PBS + 60 units/ml proteinase K onto the mesh and incubate for 2' at RT. Wash with PBS. Transfer the embryos to 1ml 10x Trypsin. Pass 30 times through a 21G needle with a 1 ml syringe. Add 4ml PBS and shake for 40' at 25^{o}C and 800 rpm. Filter the lysate through a 40 μm cell strainer. Pellet the cells at 1500rpm at 4^{o}C for 5'. Resuspend in PBS + 2% BSA + 2mm EDTA in a tube that has been coated overnight with 2% BSA. Keep on ice until FACS starts.

References

Affolter, M., Bellusci, S., Itoh, N., Shilo, B., Thiery, J. P., and Werb, Z. (2003). Tube or not tube: remodeling epithelial tissues by branching morphogenesis. Dev Cell *4*, 11-18.

Bang, A. G., and Kintner, C. (2000). Rhomboid and Star facilitate presentation and processing of the Drosophila TGF-alpha homolog Spitz. Genes Dev *14*, 177-186.

Barrio, R., de Celis, J. F., Bolshakov, S., and Kafatos, F. C. (1999). Identification of regulatory regions driving the expression of the Drosophila spalt complex at different developmental stages. Dev Biol *215*, 33-47.

Basler, K., and Struhl, G. (1994). Compartment boundaries and the control of Drosophila limb pattern by hedgehog protein. Nature *368*, 208-214.

Bauer, R., Lehmann, C., Martini, J., Eckardt, F., and Hoch, M. (2004). Gap Junction Channel Protein Innexin 2 Is Essential for Epithelial Morphogenesis in the Drosophila Embryo. Mol Biol Cell *15*, 2992-3004.

Bauer, R., Loer, B., Ostrowski, K., Martini, J., Weimbs, A., Lechner, H., and Hoch, M. (2005). Intercellular communication: the Drosophila innexin multiprotein family of gap junction proteins. Chem Biol *12*, 515-526.

Behr, M., Riedel, D., and Schuh, R. (2003). The claudin-like megatrachea is essential in septate junctions for the epithelial barrier function in Drosophila. Dev Cell *5*, 611-620.

Behrens, J., Vakaet, L., Friis, R., Winterhager, E., Van Roy, F., Mareel, M. M., and Birchmeier, W. (1993). Loss of epithelial differentiation and gain of invasiveness correlates with tyrosine phosphorylation of the E-cadherin/beta-catenin complex in cells transformed with a temperature-sensitive v-SRC gene. J Cell Biol *120*, 757-766.

Beitel, G. J., and Krasnow, M. A. (2000). Genetic control of epithelial tube size in the Drosophila tracheal system. Development *127*, 3271-3282.

Bellen, H. J., Levis, R. W., Liao, G., He, Y., Carlson, J. W., Tsang, G., Evans-Holm, M., Hiesinger, P. R., Schulze, K. L., Rubin, G. M.*, et al.* (2004). The BDGP Gene Disruption Project: Single Transposon Insertions Associated With 40% of Drosophila Genes. Genetics *167*, 761-781.

Beloussov, L. V., Louchinskaia, N. N., and Stein, A. A. (2000). Tension-dependent collective cell movements in the early gastrula ectoderm of <SMALL>Xenopus laevis</SMALL> embryos. Development Genes and Evolution *210*, 92-104.

Bertet, C., Sulak, L., and Lecuit, T. (2004). Myosin-dependent junction remodeling controls planar cell intercalation and axis elongation. Nature *429*, 667-671.

Bloor, J. W., and Kiehart, D. P. (2002). Drosophila RhoA regulates the cytoskeleton and cell-cell adhesion in the developing epidermis. Development *129*, 3173-3183.

Boube, M., Martin-Bermudo, M. D., Brown, N. H., and Casanova, J. (2001). Specific tracheal migration is mediated by complementary expression of cell surface proteins. Genes Dev *15*, 1554-1562.

Bradley, P. L., and Andrew, D. J. (2001). ribbon encodes a novel BTB/POZ protein required for directed cell migration in Drosophila melanogaster. Development *128*, 3001-3015.

Braga, V. M., Machesky, L. M., Hall, A., and Hotchin, N. A. (1997). The small GTPases Rho and Rac are required for the establishment of cadherin-dependent cell-cell contacts. J Cell Biol *137*, 1421-1431.

Braga, V. M., and Yap, A. S. (2005). The challenges of abundance: epithelial junctions and small GTPase signalling. Curr Opin Cell Biol *17*, 466-474.

Brown, N. H., Gregory, S. L., and Martin-Bermudo, M. D. (2000). Integrins as Mediators of Morphogenesis in Drosophila. Developmental Biology *223*, 1-16.

Bryant, D. M., and Stow, J. L. (2004). The ins and outs of E-cadherin trafficking. Trends in Cell Biology *14*, 427-434.

Campbell, R. E., Tour, O., Palmer, A. E., Steinbach, P. A., Baird, G. S., Zacharias, D. A., and Tsien, R. Y. (2002). A monomeric red fluorescent protein. Proc Natl Acad Sci U S A *99*, 7877-7882.

Cerione, R. A., and Zheng, Y. (1996). The Dbl family of oncogenes. Curr Opin Cell Biol *8*, 216-222.

Chen, C. K., Kuhnlein, R. P., Eulenberg, K. G., Vincent, S., Affolter, M., and Schuh, R. (1998). The transcription factors KNIRPS and KNIRPS RELATED control cell migration and branch morphogenesis during Drosophila tracheal development. Development *125*, 4959-4968.

Chihara, T., and Hayashi, S. (2000). Control of tracheal tubulogenesis by Wingless signaling. Development *127*, 4433-4442.

Chihara, T., Kato, K., Taniguchi, M., Ng, J., and Hayashi, S. (2003). Rac promotes epithelial cell rearrangement during tracheal tubulogenesis in Drosophila. Development *130*, 1419-1428.

Colas, J. F., and Schoenwolf, G. C. (2001). Towards a cellular and molecular understanding of neurulation. Dev Dyn *221*, 117-145.

Cox, K. H., DeLeon, D. V., Angerer, L. M., and Angerer, R. C. (1984). Detection of mrnas in sea urchin embryos by in situ hybridization using asymmetric RNA probes. Dev Biol *101*, 485-502.

D'Souza-Schorey, C. (2005). Disassembling adherens junctions: breaking up is hard to do. Trends in Cell Biology *15*, 19-26.

Dammai, V., Adryan, B., Lavenburg, K. R., and Hsu, T. (2003). Drosophila awd, the homolog of human nm23, regulates FGF receptor levels and functions synergistically with shi/dynamin during tracheal development. Genes Dev *17*, 2812-2824.

Detrick, R. J., Dickey, D., and Kintner, C. R. (1990). The effects of N-cadherin misexpression on morphogenesis in Xenopus embryos. Neuron *4*, 493-506.

Dorfman, R., Shilo, B. Z., and Volk, T. (2002). Stripe provides cues synergizing with branchless to direct tracheal cell migration. Dev Biol *252*, 119-126.

Dossenbach, C., Rock, S., and Affolter, M. (2001). Specificity of FGF signaling in cell migration in Drosophila. Development *128*, 4563-4572.

Fox, D. T., Homem, C. C. F., Myster, S. H., Wang, F., Bain, E. E., and Peifer, M. (2005). Rho1 regulates Drosophila adherens junctions independently of p120ctn. Development *132*, 4819-4831.

Franch-Marro, X., and Casanova, J. (2000). The alternative migratory pathways of the Drosophila tracheal cells are associated with distinct subsets of mesodermal cells. Dev Biol *227*, 80-90.

Franch-Marro, X., and Casanova, J. (2002). spalt-induced specification of distinct dorsal and ventral domains is required for Drosophila tracheal patterning. Dev Biol *250*, 374-382.

Fristrom, D. (1988). The cellular basis of epithelial morphogenesis. A review. Tissue Cell *20*, 645-690.

Fujimori, T., Miyatani, S., and Takeichi, M. (1990). Ectopic expression of N-cadherin perturbs histogenesis in Xenopus embryos. Development *110*, 97-104.

Fujita, Y., Krause, G., Scheffner, M., Zechner, D., Leddy, H. E. M., Behrens, J., Sommer, T., and Birchmeier, W. (2002). Hakai, a c-Cbl-like protein, ubiquitinates and induces endocytosis of the E-cadherin complex. *4*, 222-231.

Fukata, M., and Kaibuchi, K. (2001). Rho-family GTPases in cadherin-mediated cell-cell adhesion. Nat Rev Mol Cell Biol *2*, 887-897.

Fukata, M., Nakagawa, M., Itoh, N., Kawajiri, A., Yamaga, M., Kuroda, S., and Kaibuchi, K. (2001). Involvement of IQGAP1, an Effector of Rac1 and Cdc42 GTPases, in Cell-Cell Dissociation during Cell Scattering. Mol Cell Biol *21*, 2165-2183.

Ghabrial, A., Luschnig, S., Metzstein, M. M., and Krasnow, M. A. (2003). Branching morphogenesis of the Drosophila tracheal system. Annu Rev Cell Dev Biol *19*, 623-647.

Griffin, B. A., Adams, S. R., and Tsien, R. Y. (1998). Specific Covalent Labeling of Recombinant Protein Molecules Inside Live Cells. Science *281*, 269-272.

Gumbiner, B. M. (2005). Regulation of Cadherin-mediated adhesion in morphogenesis. Nat Rev Mol Cell Biol *6*, 622-634.

Haerry, T. E., Khalsa, O., O'Connor, M. B., and Wharton, K. A. (1998). Synergistic signaling by two BMP ligands through the SAX and TKV receptors controls wing growth and patterning in Drosophila. Development *125*, 3977-3987.

Hogan, B. L., and Kolodziej, P. A. (2002). Organogenesis: molecular mechanisms of tubulogenesis. Nat Rev Genet *3*, 513-523.

Hogan, C., Serpente, N., Cogram, P., Hosking, C. R., Bialucha, C. U., Feller, S. M., Braga, V. M., Birchmeier, W., and Fujita, Y. (2004). Rap1 regulates the formation of E-cadherin-based cell-cell contacts. Mol Cell Biol *24*, 6690-6700.

Hordijk, P. L., ten Klooster, J. P., van der Kammen, R. A., Michiels, F., Oomen, L. C., and Collard, J. G. (1997). Inhibition of invasion of epithelial cells by Tiam1-Rac signaling. Science *278*, 1464-1466.

Ireton, R. C., Davis, M. A., van Hengel, J., Mariner, D. J., Barnes, K., Thoreson, M. A., Anastasiadis, P. Z., Matrisian, L., Bundy, L. M., Sealy, L.*, et al.* (2002). A novel role for p120 catenin in E-cadherin function. J Cell Biol *159*, 465-476.

Isaac, D. D., and Andrew, D. J. (1996). Tubulogenesis in Drosophila: a requirement for the trachealess gene product. Genes Dev *10*, 103-117.

Isogai, S., Lawson, N. D., Torrealday, S., Horiguchi, M., and Weinstein, B. M. (2003). Angiogenic network formation in the developing vertebrate trunk. Development *130*, 5281-5290.

Jacobson, A. G., Oster, G. F., Odell, G. M., and Cheng, L. Y. (1986). Neurulation and the cortical tractor model for epithelial folding. J Embryol Exp Morphol *96*, 19-49.

Jazwinska, A., Ribeiro, C., and Affolter, M. (2003). Epithelial tube morphogenesis during Drosophila tracheal development requires Piopio, a luminal ZP protein. Nat Cell Biol *5*, 895-901.

Jordan, P., and Karess, R. (1997). Myosin Light Chain-activating Phosphorylation Sites Are Required for Oogenesis in Drosophila. J Cell Biol *139*, 1805-1819.

Keller, R. (2002). Shaping the Vertebrate Body Plan by Polarized Embryonic Cell Movements. Science *298*, 1950-1954.

Keller, R., and Danilchik, M. (1988). Regional expression, pattern and timing of convergence and extension during gastrulation of Xenopus laevis. Development *103*, 193-209.

Keller, R., Shih, J., and Sater, A. (1992). The cellular basis of the convergence and extension of the Xenopus neural plate. Dev Dyn *193*, 199-217.

Keppler, A., Gendreizig, S., Gronemeyer, T., Pick, H., Vogel, H., and Johnsson, K. (2003). A general method for the covalent labeling of fusion proteins with small molecules in vivo. *21*, 86-89.

Klambt, C., Glazer, L., and Shilo, B. Z. (1992). breathless, a Drosophila FGF receptor homolog, is essential for migration of tracheal and specific midline glial cells. Genes Dev *6*, 1668-1678.

Kuhnlein, R. P., Frommer, G., Friedrich, M., Gonzalez-Gaitan, M., Weber, A., Wagner-Bernholz, J. F., Gehring, W. J., Jackle, H., and Schuh, R. (1994). spalt encodes an

evolutionarily conserved zinc finger protein of novel structure which provides homeotic gene function in the head and tail region of the Drosophila embryo. Embo J *13*, 168-179.
Kuhnlein, R. P., and Schuh, R. (1996). Dual function of the region-specific homeotic gene spalt during Drosophila tracheal system development. Development *122*, 2215-2223.
Lai, Z. C., and Rubin, G. M. (1992). Negative control of photoreceptor development in Drosophila by the product of the yan gene, an ETS domain protein. Cell *70*, 609-620.
Le, T. L., Yap, A. S., and Stow, J. L. (1999). Recycling of E-Cadherin: A Potential Mechanism for Regulating Cadherin Dynamics. J Cell Biol *146*, 219-232.
Lecuit, T. (2005). Adhesion remodeling underlying tissue morphogenesis. Trends in Cell Biology *15*, 34-42.
Lecuit, T., Samanta, R., and Wieschaus, E. (2002). slam Encodes a Developmental Regulator of Polarized Membrane Growth during Cleavage of the Drosophila Embryo. Developmental Cell *2*, 425-436.
Lee, M., Lee, S., Zadeh, A. D., and Kolodziej, P. A. (2003). Distinct sites in E-cadherin regulate different steps in Drosophila tracheal tube fusion. Development *130*, 5989-5999.
Lee, S., and Kolodziej, P. A. (2002). The plakin Short Stop and the RhoA GTPase are required for E-cadherin-dependent apical surface remodeling during tracheal tube fusion. Development *129*, 1509-1520.
Leung, B., Hermann, G. J., and Priess, J. R. (1999). Organogenesis of the Caenorhabditis elegans intestine. Dev Biol *216*, 114-134.
Llimargas, M. (2000). Wingless and its signalling pathway have common and separable functions during tracheal development. Development *127*, 4407-4417.
Llimargas, M., and Casanova, J. (1997). ventral veinless, a POU domain transcription factor, regulates different transduction pathways required for tracheal branching in Drosophila. Development *124*, 3273-3281.
Llimargas, M., and Casanova, J. (1999). EGF signalling regulates cell invagination as well as cell migration during formation of tracheal system in Drosophila. Dev Genes Evol *209*, 174-179.

Llimargas, M., Strigini, M., Katidou, M., Karagogeos, D., and Casanova, J. (2004). Lachesin is a component of a septate junction-based mechanism that controls tube size and epithelial integrity in the Drosophila tracheal system. Development *131*, 181-190.

Lubarsky, B., and Krasnow, M. A. (2003). Tube morphogenesis: making and shaping biological tubes. Cell *112*, 19-28.

Luo, L., Liao, Y. J., Jan, L. Y., and Jan, Y. N. (1994). Distinct morphogenetic functions of similar small GTPases: Drosophila Drac1 is involved in axonal outgrowth and myoblast fusion. Genes Dev *8*, 1787-1802.

Luschnig, S., Moussian, B., Krauss, J., Desjeux, I., Perkovic, J., and Nusslein-Volhard, C. (2004). An F1 genetic screen for maternal-effect mutations affecting embryonic pattern formation in Drosophila melanogaster. Genetics *167*, 325-342.

Magie, C. R., Pinto-Santini, D., and Parkhurst, S. M. (2002). Rho1 interacts with p120ctn and {alpha}-catenin, and regulates cadherin-based adherens junction components in Drosophila. Development *129*, 3771-3782.

Manning, G., and Krasnow, M. A. (1993). Development of the Drosophila tracheal system, In The development of Drosophila melanogaster, M. Bate, and A. Martinez-Arias, eds. (Cold Spring Harbor, NY: Cold Spring Harbor Laboratory Press), pp. 609-685.

Melnick, M., and Jaskoll, T. (2000). Mouse submandibular gland morphogenesis: a paradigm for embryonic signal processing. Crit Rev Oral Biol Med *11*, 199-215.

Merabet, S., Ebner, A., and Affolter, M. (2005). The Drosophila Extradenticle and Homothorax selector proteins control branchless/FGF expression in mesodermal bridge-cells. EMBO Rep *6*, 762-768.

Milan, M., Weihe, U., Perez, L., and Cohen, S. M. (2001). The LRR proteins capricious and Tartan mediate cell interactions during DV boundary formation in the Drosophila wing. Cell *106*, 785-794.

Mlodzik, M. (2002). Planar cell polarization: do the same mechanisms regulate Drosophila tissue polarity and vertebrate gastrulation? Trends in Genetics *18*, 564.

Myat, M. M., Lightfoot, H., Wang, P., and Andrew, D. J. (2005). A molecular link between FGF and Dpp signaling in branch-specific migration of the Drosophila trachea. Developmental Biology *281*, 38.

Myster, S. H., Cavallo, R., Anderson, C. T., Fox, D. T., and Peifer, M. (2003). Drosophila p120catenin plays a supporting role in cell adhesion but is not an essential adherens junction component. J Cell Biol *160*, 433-449.

Ng, J., Nardine, T., Harms, M., Tzu, J., Goldstein, A., Sun, Y., Dietzl, G., Dickson, B. J., and Luo, L. (2002). Rac GTPases control axon growth, guidance and branching. Nature *416*, 442-447.

Nose, A., Nagafuchi, A., and Takeichi, M. (1988). Expressed recombinant cadherins mediate cell sorting in model systems. Cell *54*, 993-1001.

Oda, H., and Tsukita, S. (1999a). Dynamic features of adherens junctions during Drosophila embryonic epithelial morphogenesis revealed by a Dalpha-catenin-GFP fusion protein. Dev Genes Evol *209*, 218-225.

Oda, H., and Tsukita, S. (1999b). Nonchordate Classic Cadherins Have a Structurally and Functionally Unique Domain That Is Absent from Chordate Classic Cadherins. Developmental Biology *216*, 406.

Oda, H., Tsukita, S., and Takeichi, M. (1998). Dynamic behavior of the cadherin-based cell-cell adhesion system during Drosophila gastrulation. Dev Biol *203*, 435-450.

Ohashi, T., Kiehart, D. P., and Erickson, H. P. (2002). Dual labeling of the fibronectin matrix and actin cytoskeleton with green fluorescent protein variants. J Cell Sci *115*, 1221-1229.

Ohshiro, T., Emori, Y., and Saigo, K. (2002). Ligand-dependent activation of breathless FGF receptor gene in Drosophila developing trachea. Mechanisms of Development *114*, 3.

Ohshiro, T., and Saigo, K. (1997). Transcriptional regulation of breathless FGF receptor gene by binding of TRACHEALESS/dARNT heterodimers to three central midline elements in Drosophila developing trachea. Development *124*, 3975-3986.

Palacios, F., Schweitzer, J. K., Boshans, R. L., and D'Souza-Schorey, C. (2002). ARF6-GTP recruits Nm23-H1 to facilitate dynamin-mediated endocytosis during adherens junctions disassembly. *4*, 929-936.

Parks, A. L., Cook, K. R., Belvin, M., Dompe, N. A., Fawcett, R., Huppert, K., Tan, L. R., Winter, C. G., Bogart, K. P., Deal, J. E*., et al.* (2004). Systematic generation of high-

resolution deletion coverage of the Drosophila melanogaster genome. Nat Genet *36*, 288-292.

Patel, N. H. (1994). Imaging neuronal subsets and other cell types in whole-mount Drosophila embryos and larvae using antibody probes. Methods Cell Biol *44*, 445-487.

Paterson, A. D., Parton, R. G., Ferguson, C., Stow, J. L., and Yap, A. S. (2003). Characterization of E-cadherin Endocytosis in Isolated MCF-7 and Chinese Hamster Ovary Cells: THE INITIAL FATE OF UNBOUND E-CADHERIN. J Biol Chem *278*, 21050-21057.

Pauline Phelan, T. A. S. (2001). Innexins get into the gap. BioEssays *23*, 388-396.

Perez-Moreno, M., Jamora, C., and Fuchs, E. (2003). Sticky business: orchestrating cellular signals at adherens junctions. Cell *112*, 535-548.

Price, L. S., Hajdo-Milasinovic, A., Zhao, J., Zwartkruis, F. J. T., Collard, J. G., and Bos, J. L. (2004). Rap1 Regulates E-cadherin-mediated Cell-Cell Adhesion. J Biol Chem *279*, 35127-35132.

Reichman-Fried, M., Dickson, B., Hafen, E., and Shilo, B. Z. (1994). Elucidation of the role of breathless, a Drosophila FGF receptor homolog, in tracheal cell migration. Genes Dev *8*, 428-439.

Ribeiro, C., Ebner, A., and Affolter, M. (2002). In vivo imaging reveals different cellular functions for FGF and Dpp signaling in tracheal branching morphogenesis. Dev Cell *2*, 677-683.

Ribeiro, C., Neumann, M., and Affolter, M. (2004). Genetic control of cell intercalation during tracheal morphogenesis in Drosophila. Curr Biol *14*, 2197-2207.

Rogge, R., Green, P., Urano, J., Horn-Saban, S., Mlodzik, M., Shilo, B., Hartenstein, V., and Banerjee, U. (1995). The role of yan in mediating the choice between cell division and differentiation. Development *121*, 3947-3958.

Royou, A., Field, C., Sisson, J. C., Sullivan, W., and Karess, R. (2004). Reassessing the role and dynamics of nonmuscle myosin II during furrow formation in early Drosophila embryos. Mol Biol Cell *15*, 838-850.

Ryder, E., Blows, F., Ashburner, M., Bautista-Llacer, R., Coulson, D., Drummond, J., Webster, J., Gubb, D., Gunton, N., Johnson, G.*, et al.* (2004). The DrosDel collection: a

set of P-element insertions for generating custom chromosomal aberrations in Drosophila melanogaster. Genetics *167*, 797-813.

Samakovlis, C., Hacohen, N., Manning, G., Sutherland, D. C., Guillemin, K., and Krasnow, M. A. (1996). Development of the Drosophila tracheal system occurs by a series of morphologically distinct but genetically coupled branching events. Development *122*, 1395-1407.

Sato, M., and Kornberg, T. B. (2002). FGF is an essential mitogen and chemoattractant for the air sacs of the drosophila tracheal system. Dev Cell *3*, 195-207.

Schulte, J., Tepass, U., and Auld, V. J. (2003). Gliotactin, a novel marker of tricellular junctions, is necessary for septate junction development in Drosophila. J Cell Biol *161*, 991-1000.

Shiga, Y., Tanaka-Matakatsu, M., and Hayashi, S. (1996). A nuclear GFP β-galactosidase fusion protein as a marker for morphogenesis in living *Drosophila*. Dev Growth Differ *38*, 99-106.

Shih, J., and Keller, R. (1992). Cell motility driving mediolateral intercalation in explants of Xenopus laevis. Development *116*, 901-914.

Shim, K., Blake, K. J., Jack, J., and Krasnow, M. A. (2001). The Drosophila ribbon gene encodes a nuclear BTB domain protein that promotes epithelial migration and morphogenesis. Development *128*, 4923-4933.

Spradling, A. C., Stern, D., Beaton, A., Rehm, E. J., Laverty, T., Mozden, N., Misra, S., and Rubin, G. M. (1999). The Berkeley Drosophila Genome Project Gene Disruption Project: Single P-Element Insertions Mutating 25% of Vital Drosophila Genes. Genetics *153*, 135-177.

Stebbings, L. A., Todman, M. G., Phillips, R., Greer, C. E., Tam, J., Phelan, P., Jacobs, K., Bacon, J. P., and Davies, J. A. (2002). Gap junctions in Drosophila: developmental expression of the entire innexin gene family. Mechanisms of Development *113*, 197-205.

Steinberg, M. S., and Takeichi, M. (1994). Experimental specification of cell sorting, tissue spreading, and specific spatial patterning by quantitative differences in cadherin expression. Proc Natl Acad Sci U S A *91*, 206-209.

Strutt, D. I., Weber, U., and Mlodzik, M. (1997). The role of RhoA in tissue polarity and Frizzled signalling. Nature *387*, 292-295.

Sutherland, D., Samakovlis, C., and Krasnow, M. A. (1996). branchless encodes a Drosophila FGF homolog that controls tracheal cell migration and the pattern of branching. Cell *87*, 1091-1101.

Takahashi, M., Takahashi, F., Ui-Tei, K., Kojima, T., and Saigo, K. (2005). Requirements of genetic interactions between Src42A, armadillo and shotgun, a gene encoding E-cadherin, for normal development in Drosophila. Development *132*, 2547-2559.

Tanaka-Matakatsu, M., Uemura, T., Oda, H., Takeichi, M., and Hayashi, S. (1996). Cadherin-mediated cell adhesion and cell motility in Drosophila trachea regulated by the transcription factor Escargot. Development *122*, 3697-3705.

Tanaka, H., Takasu, E., Aigaki, T., Kato, K., Hayashi, S., and Nose, A. (2004). Formin3 is required for assembly of the F-actin structure that mediates tracheal fusion in Drosophila. Developmental Biology *274*, 413.

Tautz, D., and Pfeifle, C. (1989). A non-radioactive in situ hybridization method for the localization of specific RNAs in Drosophila embryos reveals translational control of the segmentation gene hunchback. Chromosoma *98*, 81-85.

Tepass, U., Gruszynski-DeFeo, E., Haag, T. A., Omatyar, L., Torok, T., and Hartenstein, V. (1996). shotgun encodes Drosophila E-cadherin and is preferentially required during cell rearrangement in the neurectoderm and other morphogenetically active epithelia. Genes Dev *10*, 672-685.

Tepass, U., Tanentzapf, G., Ward, R., and Fehon, a. R. (2001). Epithelia cell polarity and cell junctions in Drosophila. Annual Review of Genetics *35*, 747-784.

Thibault, S. T., Singer, M. A., Miyazaki, W. Y., Milash, B., Dompe, N. A., Singh, C. M., Buchholz, R., Demsky, M., Fawcett, R., Francis-Lang, H. L.*, et al.* (2004). A complementary transposon tool kit for Drosophila melanogaster using P and piggyBac. Nat Genet *36*, 283-287.

Thiery, J. P. (2003). Epithelial-mesenchymal transitions in development and pathologies. Current Opinion in Cell Biology *15*, 740.

Tomancak, P., Beaton, A., Weiszmann, R., Kwan, E., Shu, S., Lewis, S. E., Richards, S., Ashburner, M., Hartenstein, V., Celniker, S. E., and Rubin, G. M. (2002). Systematic

determination of patterns of gene expression during Drosophila embryogenesis. Genome Biol *3*, RESEARCH0088.

Tonning, A., Hemphala, J., Tang, E., Nannmark, U., Samakovlis, C., and Uv, A. (2005). A transient luminal chitinous matrix is required to model epithelial tube diameter in the Drosophila trachea. Dev Cell *9*, 423-430.

Tsuneizumi, K., Nakayama, T., Kamoshida, Y., Kornberg, T. B., Christian, J. L., and Tabata, T. (1997). Daughters against dpp modulates dpp organizing activity in Drosophila wing development. Nature *389*, 627-631.

Uemura, T., Oda, H., Kraut, R., Hayashi, S., Kotaoka, Y., and Takeichi, M. (1996). Zygotic Drosophila E-cadherin expression is required for processes of dynamic epithelial cell rearrangement in the Drosophila embryo. Genes Dev *10*, 659-671.

Uv, A., Cantera, R., and Samakovlis, C. (2003). Drosophila tracheal morphogenesis: intricate cellular solutions to basic plumbing problems. Trends Cell Biol *13*, 301-309.

Verkhusha, V. V., Tsukita, S., and Oda, H. (1999). Actin dynamics in lamellipodia of migrating border cells in the Drosophila ovary revealed by a GFP-actin fusion protein. FEBS Lett *445*, 395-401.

Vincent, S., Ruberte, E., Grieder, N. C., Chen, C. K., Haerry, T., Schuh, R., and Affolter, M. (1997). DPP controls tracheal cell migration along the dorsoventral body axis of the Drosophila embryo. Development *124*, 2741-2750.

Wallingford, J. B., Fraser, S. E., and Harland, R. M. (2002). Convergent extension: the molecular control of polarized cell movement during embryonic development. Dev Cell *2*, 695-706.

Wappner, P., Gabay, L., and Shilo, B. Z. (1997). Interactions between the EGF receptor and DPP pathways establish distinct cell fates in the tracheal placodes. Development *124*, 4707-4716.

Wassarman, P. M., Jovine, L., and Litscher, E. S. (2004). Mouse zona pellucida genes and glycoproteins. Cytogenetic and Genome Research *105*, 228-234.

Weliky, M., and Oster, G. (1990). The mechanical basis of cell rearrangement. I. Epithelial morphogenesis during Fundulus epiboly. Development *109*, 373-386.

Williams-Masson, E. M., Heid, P. J., Lavin, C. A., and Hardin, J. (1998). The cellular mechanism of epithelial rearrangement during morphogenesis of the Caenorhabditis elegans dorsal hypodermis. Dev Biol *204*, 263-276.

Wu, V. M., and Beitel, G. J. (2004). A junctional problem of apical proportions: epithelial tube-size control by septate junctions in the Drosophila tracheal system. Current Opinion in Cell Biology *16*, 493-499.

Wu, V. M., Schulte, J., Hirschi, A., Tepass, U., and Beitel, G. J. (2004). Sinuous is a Drosophila claudin required for septate junction organization and epithelial tube size control. J Cell Biol *164*, 313-323.

Wucherpfennig, T., Wilsch-Brauninger, M., and Gonzalez-Gaitan, M. (2003). Role of Drosophila Rab5 during endosomal trafficking at the synapse and evoked neurotransmitter release. J Cell Biol *161*, 609-624.

Young, P. E., Richman, A. M., Ketchum, A. S., and Kiehart, D. P. (1993). Morphogenesis in Drosophila requires nonmuscle myosin heavy chain function. Genes Dev *7*, 29-41.

Zallen, J. A., and Wieschaus, E. (2004). Patterned gene expression directs bipolar planar polarity in Drosophila. Dev Cell *6*, 343-355.

Zeitlinger, J., Kockel, L., Peverali, F. A., Jackson, D. B., Mlodzik, M., and Bohmann, D. (1997). Defective dorsal closure and loss of epidermal decapentaplegic expression in Drosophila fos mutants. Embo J *16*, 7393-7401.

Zhong, Y., Brieher, W. M., and Gumbiner, B. M. (1999). Analysis of C-cadherin Regulation during Tissue Morphogenesis with an Activating Antibody. J Cell Biol *144*, 351-359.

Supplementary material

Lines screened in the deficiency screen

For pictures refer to the file DefScreen2nd.fp5 on the attached CD (requires Filemaker Pro 6).

Map Position	Bloomington No.	Exelixis No.	Description
21A4;21B1	7488	6001	wildtype
21B4;21B7	7772	7002	wildtype
21B7;21B8	7773	8001	convoluted DB, DB fusion defects?
21B7;21B8	7773	8001	convoluted DB?, fusion defects?
21D2;21D3	7489	6002	wildtype
21D2;21D4	7775	7005	wildtype
21D3;21E3	7490	6003	ventral mess, DT breaks, LT fusion defects, includes Star
21E3;21F2	7491	6004	includes Star
21F2;21F4	7776	7006	wildtype
21F4;22A3	7777	8004	wildtype
22A3;22B1	7492	6005	wildtype
22B1;22B5	7778	7007	wildtype
22B2;22B8	7779	8005	convoluted DT
22B8;22D1	7780	7008	wildtype
22D1;22D5	7781	7009	wildtype
22D4;22E1	7782	7010	dorsal open, inter AJ defect, DT thin with auto AJ, partial loss of catenin localization, roundish cells?, late mess
22F3;23A3	7494	6008	wildtype
23A2;23B1	7744	6277	wildtype
23C4;23D1	7784	7014	wildtype (subtle defect at DB-DT border: no auto AJ?)
23D1;23E3	7785	7015	wildtype
23E3;23E5	7786	8008	wildtype
23E5;23F5	7787	7016	wildtype

Map Position	Bloomington No.	Exelixis No.	Description
23F6;24A2	7788	7017	wildtype
24A1;24C2	7789	7018	severe defects, DT breaks, abnormal ventral branches
24C3;24C8	7495	6009	severe defects
24C8;24D4	7790	8010	wildtype
24D8;25A1	7791	8011	wildtype
25B1;25B1	7792	9062	wildtype
25B1;25B8	7793	8012	wildtype
25B10;25C3	7794	7022	wildtype
25B3;25B9	7795	7021	wildtype
25B8;25B10	7796	8013	wildtype
25D5;25E6	7498	6012	wildtype
25E5;25F1	7797	7023	wildtype
25E6;25F2	7798	8016	wildtype (GB guidance defects?)
25F2;25F5	7499	6013	wildtype
25F5;26A3	7500	6014	wildtype
26A1;26A8	7799	7024	wildtype
26B9;26C1	7501	6015	wildtype
26C1;26D1	7502	6016	early lethal defects, no trachea form
26C2;26C3	7800	9038	DB guidance defects?, VB guidance defects?
27C4;27D4	7802	7029	wildtype
27E2;27E4	7803	8019	wildtype
27E4;27F5	7503	6017	severe defects, branches undistinguishable, auto AJ present, huge amount of tracheal cells close to the epidermis, some branches below
27F3;28A1	7804	7031	wildtype
28B1;28C1	7504	6018	wildtype
28B4;28C1	7805	9031	wildtype
28E1;28F1	7807	7034	extremely convoluted DT, auto AJ curled, DB absent or abnormal, uneven DT lumen
29C1;29D1	7808	8021	wildtype
29C4;29D4	7809	7038	wildtype
29D5;29F1	7810	7039	severe defects, dorsal open, distinction of branches difficult, auto and inter AJ present, includes raw

Map Position	Bloomington No.	Exelixis No.	Description
29F1;29F6	7811	7040	convoluted DT, TC abnormally thick and long?, no autoAJ in TC?, no LT
29F7;30A2	7505	6021	wildtype
30B10;30C1	7812	7042	wildtype
30B3;30B5	7813	8022	wildtype
30B4;30B5	7814	9064	wildtype (VB defects?)
30B5;30B11	7506	6022	wildtype
30C1;30C1	7815	9040	wildtype
30C1;30C9	7507	6024	severe defects, hardly any trachea
30C9;30E1	7508	6025	wildtype
30D1;30F1	7816	7043	wildtype
31A2;31B1	7817	8024	wildtype
31A2;31D7	7509	6026	wildtype
31A3;31B1	7818	9032	wildtype
31C3;31D9	7819	7046	wildtype
31F5;32B1	7820	8026	wildtype
32B1;32C1	7821	7049	wildtype
32D2;32D5	7510	6027	wildtype
32E4;32F2	7512	6029	includes Sal
33A2;33B3	7513	6030	wildtype
33B3;33C2	7514	6031	convoluted DT, dorsal open?
33C2;33D4	7515	6032	wildtype
33E4;33F2	7516	6033	wildtype
34A1;34A2	7822	8028	wildtype
34A2;34A7	7823	7055	wildtype
34A6;34A7	7824	9023	wildtype
34A6;34B2	7825	8029	wildtype
34D3;34E1	7826	7059	wildtype
34F1;35A3	7827	8032	wildtype
35B1;35B8	7828	8033	wildtype
35B7;35C1	7829	7061	wildtype
35C5;35D2	7830	8034	fusion defects, includes escargot
35D2;35D4	7831	7063	severe defects, hardly any trachea

Map Position	Bloomington No.	Exelixis No.	Description
35D4;35D6	7520	6037	wildtype
35F8;36A3	7832	7065	wildtype
36A1;36A12	7833	7066	wildtype
36A12;36B2	7834	7067	wildtype
36B1;36C9	7835	8036	wildtype
36C10;36C11	7836	9044	wildtype
36C10;36D1	7837	7069	wildtype
36C7;36C10	7838	7068	wildtype
36D2;36E1	7839	7070	wildtype
36D3;36E3	7840	8038	sometimes severe defects, spotty AJ, no GB?, convoluted DT
36E1;36E1	7841	9033	wildtype
36E1;36E1	7842	9063	wildtype
36F5;37A2	7523	6041	wildtype
37A1;37A4	7843	7071	wildtype
37A2;37B6	7844	7072	germband retraction defects DB outgrowth defect DT breaks anteriorly, DT thicker?, slightly convoluted DT
37B8;37B11	7846	8039	wildtype
37C1;37C5	7847	8040	wildtype
37C5;37D7	7525	6043	wildtype
37D2;37E1	7848	7075	wildtype
37F2;38A4	7526	6044	no auto AJ, big dorsal clumps of tracheal cells, less metameres, includes screw and spitz
38A4;38A7	7527	6045	dorsal open, some neighboring DB fuse
38A7;38B2	7850	7077	convoluted DT, occasional DT breaks, occasional fusion defects
38C2;38C7	7528	6046	wildtype
38E6;38F3	7852	7079	extremely convoluted DT, auto AJ curled
39A2;39B4	7529	6047	wildtype
39A7;39B2	7854	9027	wildtype
39B4;39D1	7530	6048	wildtype
39E3;40B3	7856	7082	wildtype
40A5;40D3	7531	6049	slightly convoluted DT

Map Position	Bloomington No.	Exelixis No.	Description
40A5;40D3	7531	6049	slightly convoluted DT
41E6;41F2	7857	9021	wildtype
42C7;42D4	7532	6050	wildtype
42D4;42E4	7533	6051	wildtype
43D1;43E5	7534	6052	occasional DB fusion defects
43E5;43E12	7858	7092	wildtype
43E9;43E18	7536	6054	sporadic DB fusion defects
43F1;44A4	7537	6055	wildtype
44A4;44B4	7859	7094	wildtype
44A4;44C2	7538	6056	convoluted DT
44B3;44C2	7860	7095	occasional fusion defects in all branches
44B7;44B9	7861	9022	wildtype
44B9;44C4	7539	6057	wildtype
44C4;44D1	7540	6058	wildtype
44D4;44D5	7863	8047	DB defects, shorter DBs, no fusion, 2 terminal cells?, or no fusion cell?
44D5;44E3	7864	7098	trachea abnormal, LT fusion defects, DB outgrowth defects, ventrally +- outgrowth defects, slightly convoluted DT
45F1;46A1	7866	8049	wildtype
47B13;47C3	7868	7112	wildtype
47C3;47D6	7541	6059	convoluted DT
49E6;49F1	7544	6062	wildtype
49F10;50A1	7872	7124	severe defects, moesin and catenin in a spotty distribution, most DB stalled, DT looks thinner but AJ normal, dorsal open?
50C5;50C9	7873	7128	DT breaks, also in heterozygotes
50C9;50D7	7874	7129	wildtype
50D4;50E4	7875	7130	wildtype
50E4;50F6	7876	7131	convoluted DT, DT breaks
51B1;51C1	7878	7133	wildtype
51E2;51E11	7879	7135	+-wildtype
51F11;51F12	7880	9015	no tracheal outgrowth, Filopodia present, sometimes (late?) trachea almost gone, similar to dominant negative Rac?

Map Position	Bloomington No.	Exelixis No.	Description
52A13;52A13	7881	9026	wildtype
52D1;52D12	7883	7138	wildtype
52D11;52E4	7884	7139	wildtype
52F6;53C3	7545	6063	wildtype
53A4;53C4	7886	7142	wildtype
53C13;53D14	7887	7145	wildtype
53D14;53F9	7547	6065	DB fusion defects, sometimes also LT, terminal cell defects?
53F9;54B6	7548	6066	wildtype
54B1;54B16	7889	7147	wildtype
54E1;54E9	7891	7150	wildtype
55B1;55B8	7892	7152	wildtype
55B9;55C1	7893	7153	slightly convoluted DT
55E9;55F6	7895	7158	wildtype
55F8;56A1	7549	6067	wildtype
56B5;56C11	7551	6069	severe defects, outgrowth of all branches stalled, dorsal open, cells dissociate and loose polarity, lots of cell debris, no late embryos, like dominant negative Rac?
56F11;56F16	7896	7162	wildtype
57A2;57A6	7897	7163	wildtype
57A6;57A9	7898	7164	wildtype
57A6;57B3	7552	6070	convoluted DT
57B16;57C7	7555	6073	severe defects, trachea completely messed up
57B16;57C7	7899	7167	wildtype
57B16;57D4	7554	6072	wildtype
58A3;58B1	7900	7169	wildtype
58B1;58C1	7901	7170	wildtype?
58C1;58D2	7902	7171	wildtype
58D4;58E5	7903	7173	wildtype
58E5;58F3	7904	7174	wildtype
59B4;59C2	7905	7176	wildtype
59C3;59D2	7906	7177	wildtype
59D11;59E3	7907	7179	wildtype

Map Position	Bloomington No.	Exelixis No.	Description
59E3;59F6	7909	7180	severe early defects, hardly any trachea
60A13;60A16	7910	7182	wildtype
60A16;60A16	7911	9024	wildtype
60B4;60C6	7560	6081	wildtype
60C4;60C7	7561	6082	wildtype
60C7;60C7	7913	9043	wildtype
60C8;60D3	7914	7185	wildtype

Movies

The movies are found on the attached CD.

Movie1 Branching morphogenesis of the *Drosophila* tracheal system.
GFPactin expressed under the control of btl-Gal4 in wildtype embryos. Approximately 0.2 frames/minute.

Movie2 Filopodial dynamics in tracheal tip cells.
GFPactin expressed under the control of btl-Gal4 in wildtype embryos. Approximately 6 frames/minute.

Movie3 Single cell labeling *in vivo.*
tauGFP expressed in a single tracheal cell in the ganglionic branch of a wildtype embryo. Approximately 0.7 frames/minute.

Movie4 Mutations in *ribbon* block intercalation.
α-catenin-GFP expressed in the trachea of embryos mutant for *ribbon*. Approximately 0.7 frames/minute.

Movie5 Dominant active Rac1 interferes with branch outgrowth.

GFPactin and dominant active Rac1 expressed under the control of btl-Gal4. Approximately 1 frame/minute.

Movie6 Dominant negative Rac1 induces lammelipodia in the trachea.
GFPactin and dominant negative Rac1 expressed under the control of btl-Gal4. Approximately 5 frames/minute.

Movie7 Dominant negative Rac leads to a disintegration of the trachea.
GFPactin and dominant negative Rac1 expressed under the control of btl-Gal4. Approximately 0.7 frames/minute.

Movie8 Phenotype of a Rac1, Rac2 double mutant.
GFPactin expressed under the control of btl-Gal4 in embryos mutant for Rac1 and Rac2. Approximately1 frame/minute.

Movie9 *sqh*GFP is homogenously distributed in the trachea.
*sqh*GFP expressed under the control of btl-Gal4 in wildtype embryos. Approximately 1 frame/minute.

Movie10 E-cadherinGFP is reincorporated evenly into AJs of dorsal trunk cells after FRAP.
E-cadherinGFP expressed under the control of btl-Gal4 in wildtype embryos. Approximately 1 frame/minute.

Appendix

Erklärung

Ich erkläre, dass ich die Dissertation “Epithelial cell rearrangements during tubular organ formation” nur mit der darin angegebenen Hilfe verfasst und bei keiner anderen Universität und keiner anderen Fakultät der Universität Basel eingereicht habe.

Basel, den 4. 11. 2005 Marc Neumann

Curriculum vitae

Personal Details

Marc Neumann

Institute address

Department of Cell Biology
Biozentrum, University of Basel
Klingelbergstrasse 50-70
CH-4056 Basel, Switzerland
Marc.Neumann@unibas.ch
Tel.: +41 61 267 20 70
Fax: +41 61 267 20 78

Private address

Mörsbergerstr. 3
4057 Basel
Tel.: +41 61 683 03 89

Date of birth:	24th April 1974
Place of birth:	Bonn, Germany
Citizenship:	German
Marital status:	Unmarried
Children:	One daughter (6 months)

Education

1980-1984	Grundschule Buschhoven
1984-1993	Vinzenz-Palotti-Kolleg, Rheinbach
1993-1994	Alternative service
1994-2001	Diploma in biology at the Albert-Ludwigs-Universität Freiburg, Germany

	Thesis: Molecular analysis of a novel germline marker in the zebrafish
2002-2005	PhD in the lab of Markus Affolter at the Biozentrum Basel Title: Epithelial cell rearrangements during tubular organ formation

Scientific positions

1998	Part time position in the lab of Erez Raz at the University of Freiburg, Germany
2001	Position in the lab of Talila Volk at the Weizmann Institute of Science, Rehovot, Israel

Publications

Cabernard, C., Neumann, M., and Affolter, M. (2004). Cellular and molecular mechanisms involved in branching morphogenesis of the Drosophila tracheal system. J Appl Physiol *97*, 2347-2353.

Ribeiro, C., Neumann, M., and Affolter, M. (2004). Genetic control of cell intercalation during tracheal morphogenesis in Drosophila. Curr Biol *14*, 2197-2207.

Blaser, H., Eisenbeiss, S., Neumann, M., Reichman-Fried, M., Thisse, B., Thisse, C., and Raz, E. (2005). Transition from non-motile behaviour to directed migration during early PGC development in zebrafish. J Cell Sci *118*, 4027-4038.

Neumann, M and Affolter, M, Remodeling epithelial tubes via cell rearrangements. (submitted)